



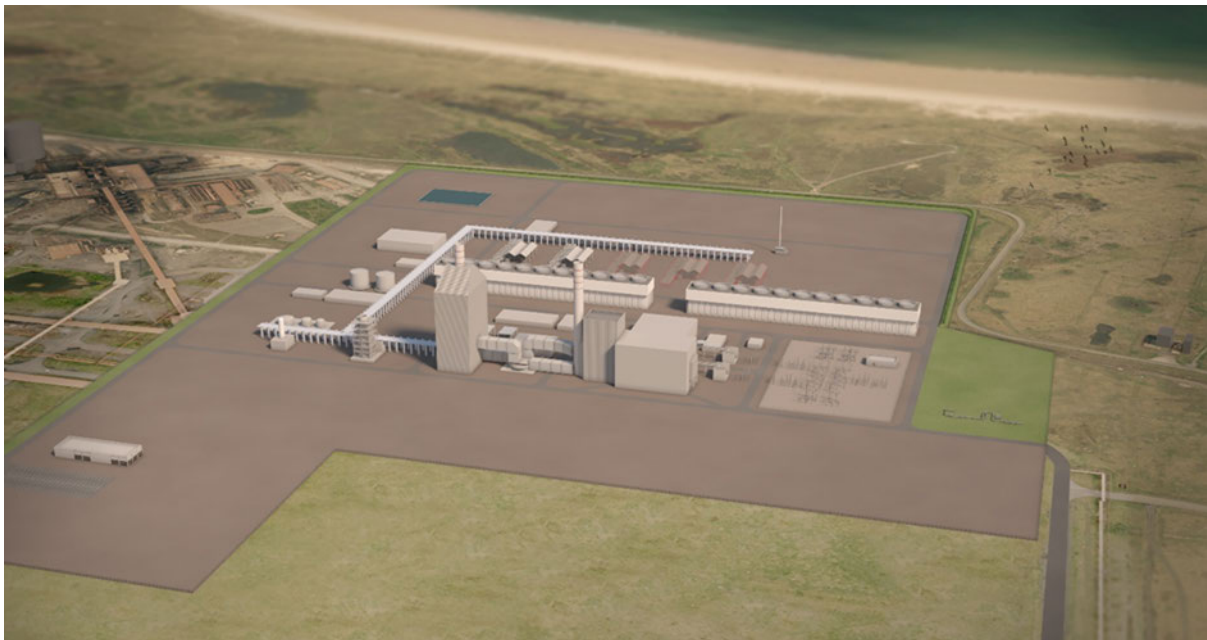
Net Zero Teesside – Environmental Statement

Planning Inspectorate Reference: EN010103

Volume III – Appendices

Appendix 14E: Coastal Modelling Report

The Infrastructure Planning (Environmental Impact Assessment) Regulations 2017 (as amended)



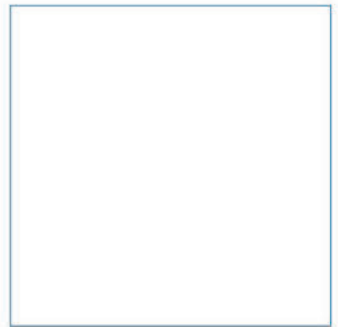
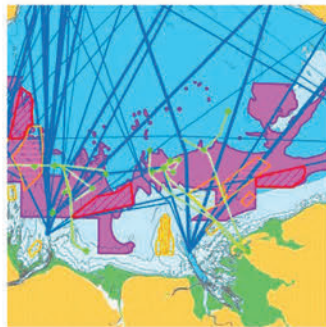
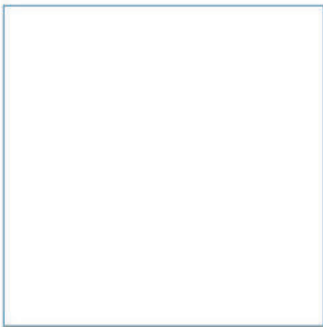
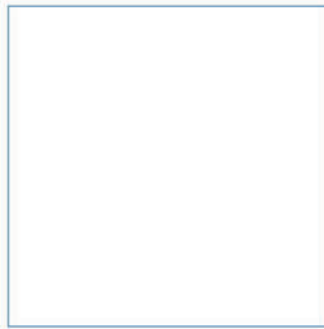
Prepared by: **AECOM**

AECOM

Net Zero Teesside Project

Coastal Modelling – Final Integrated Report

April 2021



Innovative Thinking - Sustainable Solutions



Page intentionally left blank

Net Zero Teesside Project


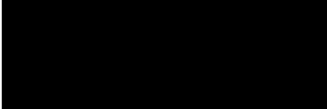

Coastal Modelling – Final Integrated Report

April 2021



Document Information

Document History and Authorisation		
Title	Net Zero Teesside Project	
	Coastal Modelling – Final Integrated Report	
Commissioned by	AECOM	
Issue date	April 2021	
Document ref	R.3393a	
Project no	R/4834/01	
Date	Version	Revision Details
02.03.2021	1	Working Document for Comment - Update to include Outfall 2
17.03.2021	2	Issued for Client Review
14.04.2021	3	Issued for Client Use
19.04.2021	4	Issued for Client Use (Amended)

Prepared (PM)	Approved (QM)	Authorised (PD)
Helen Godwin	Adam Fulford	Gordon Osborn
		

Suggested Citation

ABPmer, (2021). Net Zero Teesside Project, Coastal Modelling – Final Integrated Report, ABPmer Report No. R.3393a. A report produced by ABPmer for AECOM, April 2021.

Contributing Authors

Catherine Merrix, Tom Finch

Notice

ABP Marine Environmental Research Ltd ("ABPmer") has prepared this document in accordance with the client's instructions, for the client's sole purpose and use. No third party may rely upon this document without the prior and express written agreement of ABPmer. ABPmer does not accept liability to any person other than the client. If the client discloses this document to a third party, it shall make them aware that ABPmer shall not be liable to them in relation to this document. The client shall indemnify ABPmer in the event that ABPmer suffers any loss or damage as a result of the client's failure to comply with this requirement.

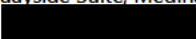
Sections of this document may rely on information supplied by or drawn from third party sources. Unless otherwise expressly stated in this document, ABPmer has not independently checked or verified such information. ABPmer does not accept liability for any loss or damage suffered by any person, including the client, as a result of any error or inaccuracy in any third party information or for any conclusions drawn by ABPmer which are based on such information.

All content in this document should be considered provisional and should not be relied upon until a final version marked '*issued for client use*' is issued.

All images on front cover copyright ABPmer apart from seahorse (A J Pearson).

ABPmer

Quayside Suite, Medina Chambers, Town Quay, Southampton, Hampshire SO14 2AQ

T:  W: <http://www.abpmer.co.uk/>

Executive Summary

Numerical modelling has been undertaken to investigate the extent of thermal discharge resulting from an outfall from a new Carbon Capture, Utilisation and Storage (CCUS) project in the Tees Estuary.

Two potential scenarios for the discharge of treated effluent from the Proposed Development have been considered. The first option is for the re-use of the existing outfall with minor refurbishment; for the remainder of the report, this will be referred to as 'Outfall 1'. The second option is for a replacement outfall along the same corridor as the CO₂ Export Route; for the remainder of the report, this is referred to as 'Outfall 2'. Under no circumstance will both Outfall 1 and Outfall 2 be progressed, however for completeness, both have been assessed as part of this report.

Results of near-field thermal plume modelling undertaken using the CORMIX modelling software show that, for Outfall 1 under spring conditions, the likely extent of a thermal plume (with a 15°C excess temperature at source) would be very localised: a 3°C temperature excess only extends approximately 45 m from the discharge point on the flood and 98 m on the ebb; for a 2°C temperature excess, the ebb extent of the plume increases to 140 m. Considering a further reduced excess temperature shows that a 0.1°C temperature excess is estimated to extend around 750 m from the origin on a spring flood tide, and 720 m on an ebb. In all cases tested, the mixing and plume dispersion appear to occur very rapidly from the origin with very little detectable change (>0.1°C) beyond ~800 m of the outfall location.

At Outfall 2, as a result of lower energy conditions leading to lower/slower rates of dissipation of the outfall plume, the neap tidal phases offer a larger plume, with the 2°C contour extending 600 m and 400 m from the outfall on the flood and ebb respectively, compared to the spring tide which extends 170 m and 270 m on the flood and ebb tide respectively, under normal discharge conditions.

Far field plume dispersion modelling using the Delft3D model shows a small impact of outfall discharge on the ambient water temperature. Depth averaged temperature differences of >0.02°C are detected up to ~9 km from the Outfall 2 site, however greater temperature excesses of up to 0.3°C are localised to within 1.5 km of the outfall in all simulations modelled.

This report has been developed with regular involvement from the Environment Agency, with meetings in March 2020 to discuss the thermal modelling approach and scope, and further meetings to discuss feedback from the initial modelling carried out for the project in January 2021. At the January meeting it was decided that far-field modelling is also required and therefore subsequently included in this re-issued report. The MMO has also been regularly informed at each stage of the project from September 2019 to February 2021.

Contents

1	Introduction.....	1
1.1	Near-field thermal plume modelling	2
1.2	Far-field thermal plume modelling.....	2
2	CORMIX Modelling	3
2.1	Outfall location.....	4
2.2	Model set-up	4
2.3	CORMIX Outfall 1 results	6
3	CORMIX Modelling – Outfall 2	11
3.1	Overview	11
3.2	Outfall 2 location.....	11
3.3	Model set-up	12
3.4	CORMIX Outfall 2 results	13
4	Delft3D Modelling – Far Field Impact.....	16
4.1	Model setup	16
4.2	Scenarios	17
4.3	Results	18
5	Conclusion.....	36
6	References.....	38
7	Acronyms/Abbreviations	39

Appendices

A	Delft Model Setup.....	41
A.1	Model grid.....	41
A.2	Bathymetry.....	43
A.3	Model Setup.....	44
A.4	Model run period	49
B	Delft3D Model Calibration	50
B.1	Flow model calibration	50
C	CORMIX Extreme discharge event	91
C.1	Flood Tide Variation.....	91
C.2	Ebb Tide Variation.....	92
C.3	Temperature Excess Isolines.....	92

Tables

Table 1.	Tidal characteristics for a mean spring tide.....	5
Table 2.	CORMIX Run Summary.....	6
Table 3.	Excess temperature isoline extents from the outfall under peak ebb and flood for a mean spring tide.....	10
Table 4.	Outfall 2 location options.....	12
Table 5.	Input tidal characteristics.....	12
Table 6.	Outfall 2 CORMIX Run Summary.....	13
Table 7.	Isoline extents for all tidal states under normal discharge conditions.....	14
Table 8.	Physical properties of the Delft3D simulations.....	16
Table 9.	Outfall locations for far-field modelling.....	16
Table 10.	Thermal plume properties in Delft3D, summer and winter case.....	17
Table 11.	Delft3D model runs for far-field assessment.....	18
Table 12.	Model grid resolution.....	41
Table 13.	Tidal constituents in the numerical model.....	45
Table 14.	Flow data from the Leven and Tees.....	47
Table 15.	Peak discharge rates at the barrage for flow modelling.....	47
Table 16.	Monthly average wind speeds (m/s) from Durham Tees Valley Airport.....	49
Table 17.	Tide gauge data summary.....	50
Table 18.	Modelled and predicted flows speeds and directions within the offshore coastal region.....	86
Table 19.	Isoline extents for all tidal states under 1-in-30-year discharge conditions.....	92

Figures

Figure 1.	Development site boundary around the outfall locations: Outfall 1 (west) and Outfall 2 (east).....	1
Figure 2.	Net Zero Teesside – Site Boundary for Consultation.....	1
Figure 3.	Location of Outfall 1.....	3
Figure 4.	Tidal characteristics during a mean spring tide.....	5
Figure 5.	Spring flood seasonal variation.....	6
Figure 6.	Summer scenario, flood and ebb sensitivity.....	7
Figure 7.	Spring flood wind sensitivity.....	7
Figure 8.	Spring flood, pipe diameter sensitivity.....	8
Figure 9.	Spring flood, outfall projection sensitivity.....	8
Figure 10.	CORMIX excess temperature isolines (°C) under mean spring, peak flood (SE) and ebb (NW) tidal states.....	9
Figure 11.	Zoomed extent of the CORMIX excess temperature isolines (°C) under mean spring, peak flood (SE) and ebb (NW) tidal states.....	9
Figure 12.	Outfall 2 location indicated by blue circle.....	11
Figure 13.	Location of modelled Outfall 2.....	12
Figure 14.	Spring and neap flood tide plume variations during normal discharge events.....	13
Figure 15.	Spring and neap ebb tide plume variations during normal discharge events.....	14
Figure 16.	Excess temperature isolines during a neap tide under normal discharge conditions.....	15
Figure 17.	Location of Outfalls in far-field (Delft3D) model grid.....	17
Figure 18.	Temperature excess contour plots: Summer spring tide – Outfall 2 location.....	19
Figure 19.	Temperature excess contour plots: Summer neap tide – Outfall 2 location.....	20
Figure 20.	Temperature excess contour plots: Winter spring tide – Outfall 2 location.....	21
Figure 21.	Temperature excess contour plots: Winter neap tide – Outfall 2 location.....	22
Figure 22.	Temperature excess contour plots: Comparison of spring summer conditions with a 230° wind direction (left) vs onshore wind (right).....	24

Figure 23.	Temperature excess contour plots: Comparison of neap summer conditions with a 230° wind direction (left) vs onshore wind (right).....	25
Figure 24.	Temperature excess contour plots: Comparison of spring summer conditions with a 230° wind direction (left) vs 120° wind direction (right).....	26
Figure 25.	Temperature excess contour plots: Comparison of neap summer conditions with a 230° wind direction (left) vs 120° wind direction (right).....	27
Figure 26.	Flow speeds over a spring tide at Outfall 1 and Outfall 2 positions	28
Figure 27.	Flow speeds over a neap tide at Outfall 1 and Outfall 2 positions.....	28
Figure 28.	Temperature contours and Flow Speed Vectors from Run 6: Winter – Outfall 1	29
Figure 29.	Temperature Contours from Run 6: Winter – Outfall 1	29
Figure 30.	Temperature excess contour plots: Comparison of spring summer conditions with a discharge specified at Outfall 2 (left) vs Outfall 1 (right).....	30
Figure 31.	Temperature excess contour plots: Comparison of neap summer conditions with a discharge specified at Outfall 2 (left) vs Outfall 1 (right).....	31
Figure 32.	Temperature excess contour plots: Comparison of spring winter conditions with a discharge specified at Outfall 2 (left) vs Outfall 1 (right).....	32
Figure 33.	Temperature excess contour plots: Comparison of neap winter conditions with a discharge specified at Outfall 2 (left) vs Outfall 1 (right)	33
Figure 34.	Temperature excess contour plots: Comparison of spring summer conditions with normal and extreme flow rates.....	34
Figure 35.	Temperature excess contour plots: Comparison of spring summer conditions with normal and extreme flow rates.....	35
Figure 36.	Delft3D hydrodynamic model grid	42
Figure 37.	Delft3D hydrodynamic model grid – Refinement of nested grid	42
Figure 38.	Scatter plot showing available bathymetry data resolution and coverage. All values are depth positive and referenced to meters below ODN.	44
Figure 39.	HD model domain and boundary positions (shown by yellow lines)	45
Figure 40.	Tees Estuary survey, 1995: Freshwater flow past the barrage.....	46
Figure 41.	Flow data stations assessed for Tees Barrage discharge calculations	47
Figure 42.	Wind rose of Tees Valley Airport wind data (left) and CFSR Hindcast data (right).	48
Figure 43.	Location of model extraction points for tide gauge calibration overlaid onto model grid and underlying bathymetry.....	50
Figure 44.	Water level comparison: Model vs measured data (Tees Dock)	51
Figure 45.	Water level comparison: Model vs measured data (Riverside RORO)	51
Figure 46.	Measured flow speeds, Transect 1, Pass 3: Ebb tide, cross section of speed with depth shown from west (left) to east (right)	53
Figure 47.	Measured flow direction, Transect 1, Pass 3: Ebb tide, cross section of speed with depth shown from west (left) to east (right)	54
Figure 48.	Modelled flow speed, Transect 1: Ebb tide, cross section of speed with depth shown from west (left) to east (right).....	55
Figure 49.	Modelled flow direction, Transect 1: Ebb tide, cross section of direction with depth shown from west (left) to east (right)	56
Figure 50.	Tidal state and transect location extracted from the model for Transect 1 Pass 03: 28/04/2005	57
Figure 51.	Measured flow speeds, Transect 1, Pass 1: Low water, cross section of speed with depth shown from west (left) to east (right)	58
Figure 52.	Measured flow directions, Transect 1, Pass 1: Low water, cross section of speed with depth shown from west (left) to east (right)	59
Figure 53.	Modelled flow speed, Transect 1: Low tide, cross section of speed with depth shown from west (left) to east (right).....	60
Figure 54.	Modelled flow direction, Transect 1: Low tide, cross section of direction with depth shown from west (left) to east (right)	61

Figure 55.	Tidal state and transect location extracted from the model for Transect 1 Pass 01: 28/04/2005	62
Figure 56.	Measured flow speeds, Transect 1, Pass 17: Flood tide, cross section of speed with depth shown from west (left) to east (right)	63
Figure 57.	Measured flow directions, Transect 1, Pass 17: Flood tide, cross section of speed with depth shown from west (left) to east (right)	64
Figure 58.	Modelled flow speed, Transect 1: Flood tide, cross section of speed with depth shown from west (left) to east (right).....	65
Figure 59.	Modelled flow direction, Transect 1: Flood tide, cross section of direction with depth shown from west (left) to east (right)	66
Figure 60.	Tidal state and transect location extracted from the model for Transect 1 Pass 17: 28/04/2005	67
Figure 61.	Measured flow speed, Transect 7, Pass 1: Ebb tide, cross section of speed with depth shown from west (left) to east (right)	68
Figure 62.	Measured flow direction, Transect 7, Pass 1: Ebb tide, cross section of direction with depth shown from west (left) to east (right)	69
Figure 63.	Modelled flow speed, Transect 7: Ebb tide, cross section of speed with depth shown from west (left) to east (right).....	70
Figure 64.	Modelled flow direction, Transect 7: Ebb tide, cross section of direction with depth shown from west (left) to east (right)	71
Figure 65.	Tidal state and transect location extracted from the model for Transect 7 Pass 1: 26/04/2005	72
Figure 66.	Measured flow speed, Transect 7, Pass 14: Low water, cross section of speed with depth shown from west (left) to east (right)	73
Figure 67.	Measured flow direction, Transect 7, Pass 14: Low water, cross section of direction with depth shown from west (left) to east (right).....	74
Figure 68.	Modelled flow speed, Transect 7: Low water, cross section of speed with depth shown from west (left) to east (right).....	75
Figure 69.	Modelled flow direction, Transect 7: Low water, cross section of direction with depth shown from west (left) to east (right)	76
Figure 70.	Tidal state and transect location extracted from the model for Transect 7 Pass 14: 26/04/2005	77
Figure 71.	Measured flow speed, Transect 7, Pass 20: Flood tide, cross section of speed with depth shown from west (left) to east (right)	78
Figure 72.	Measured flow direction, Transect 7, Pass 20: Flood tide, cross section of direction with depth shown from west (left) to east (right)	79
Figure 73.	Modelled flow speed, Transect 7: Flood tide, cross section of speed with depth shown from west (left) to east (right).....	80
Figure 74.	Modelled flow direction, Transect 7: Flood tide, cross section of direction with depth shown from west (left) to east (right)	81
Figure 75.	Tidal state and transect location extracted from the model for Transect 7 Pass 20: 26/04/2005	82
Figure 76.	Fixed current meter location: Buoy 10.....	83
Figure 77.	Measured and modelled flow speed and direction comparison at the top, middle and bottom of the water column. Buoy 10 – Spring tide	84
Figure 78.	Measured and modelled flow speed and direction comparison at the top, middle and bottom of the water column. Buoy 10 – Neap tide.....	85
Figure 79.	Comparison of measured and modelled salinity with depth: Transect 8 (red dot on top water level plot indicates point of the tide).....	88
Figure 80.	Comparison of measured and modelled salinity with depth: Transect 5, closest transect location to the cofferdam (red dot on top water level plot indicates point of the tide).	89

Figure 81.	Comparison of measured and modelled salinity with depth: Transect 3 (red dot on top water level plot indicates point of the tide).....	90
Figure 82.	Spring and neap flood tide plume variations during extreme discharge events.....	91
Figure 83.	Spring and neap ebb tide plume variations during normal discharge events.....	92
Figure 84.	Excess temperature isolines during a neap tide under 1-in-30-year discharge conditions.....	93

1 Introduction

AECOM Ltd. have commissioned ABPmer to undertake hydrodynamic and thermal plume modelling of the Tees Estuary and surrounding region. Numerical modelling is required to provide a description of baseline conditions and investigate potential marine environmental impacts associated with the construction and operation of a new Carbon Capture, Utilisation and Storage (CCUS) project located on the south bank of the Tees Estuary (Figure 1). This report is an update to the ABPmer (2020) report to include Outfall 2.

The purpose of the numerical modelling is to assess the near-field and far-field impact of thermal discharge at the location of Outfall 1 and Outfall 2. Locations are shown in Figure 1 below and Figure 2 on the following page.



Source: AECOM, 26/03/21

Figure 1. Development site boundary around the outfall locations: Outfall 1 (west) and Outfall 2 (east)

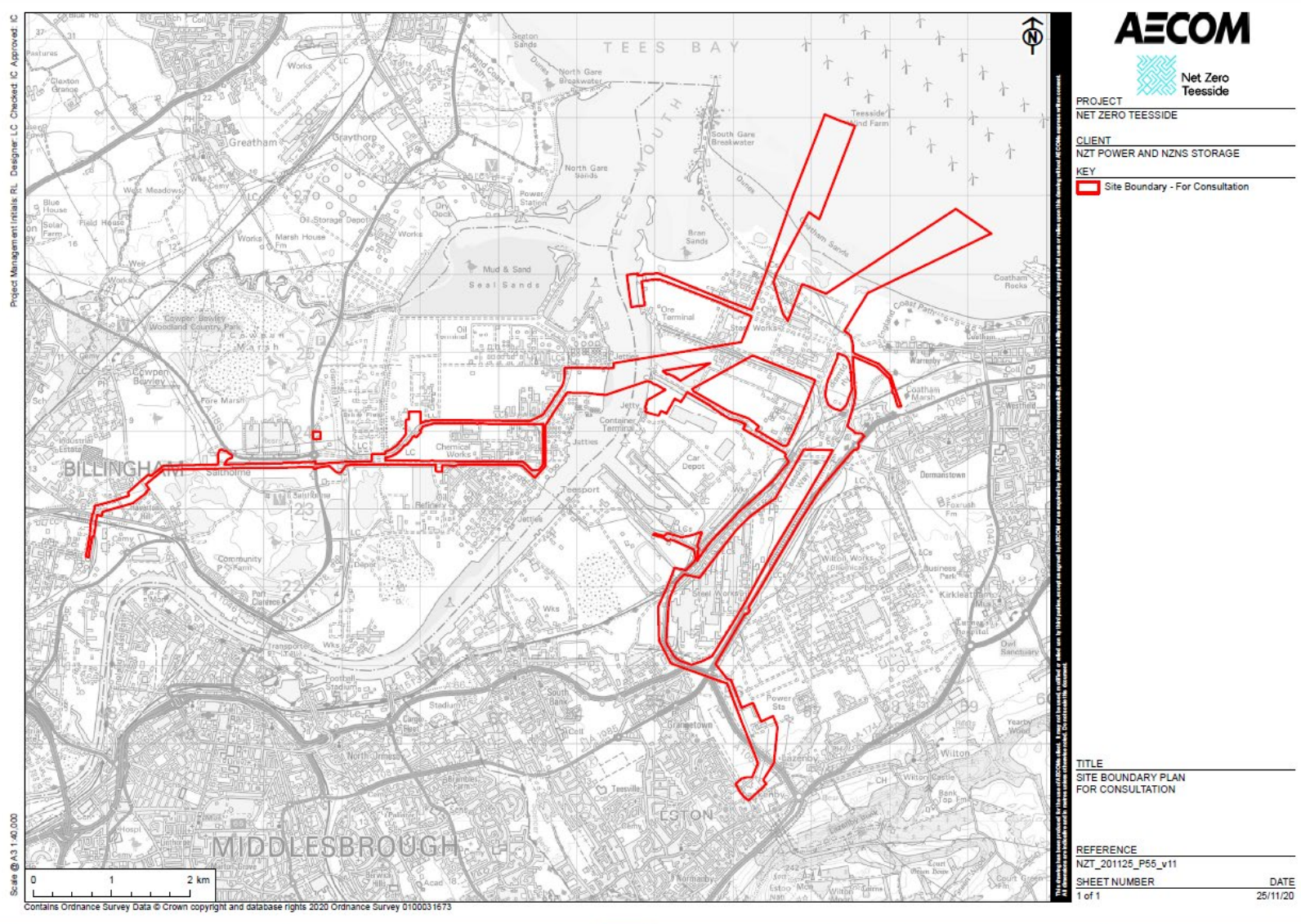


Figure 2. Net Zero Teesside – Site Boundary for Consultation

The site boundary outlining the outfall locations is shown in the previous figures. The positions of both outfall options are defined more accurately in Section 2 (Outfall 1) and Section 3 (Outfall 2)

Two stages of modelling have been undertaken for this phase of the work, which comprise the following:

- Near-field thermal plume modelling at two different outfall locations; and
- Far-field 3D thermal plume modelling.

1.1 Near-field thermal plume modelling

The first stage of the work uses the baseline outfall conditions established from the hydrodynamic model to construct thermal plume simulations using the MixZon Inc. CORMIX modelling software. Sensitivity to a range of environmental variables has been considered in order to better assess and quantify the possible extent of a plume from both outfall locations with particular thermal properties.

1.2 Far-field thermal plume modelling

The second stage of work makes use of a Delft3D hydrodynamic model constructed to establish the flow conditions within the Tees estuary and offshore. The model extends approximately 10 km offshore and 30 km along the Hartlepool, Redcar and Cleveland coastline. This model has been updated to include temperature in the physical properties being modelled and to simulate a discharge with fixed thermal and saline properties at the outfall locations.

This report details the numerical modelling set up, calibration, and model results in the following report sections:

- Section 2:** CORMIX Modelling – Outfall 1: Provides details of the thermal plume model setup and presentation of results.
- Section 3:** CORMIX Modelling – Outfall 2: Provides details of the updated thermal plume modelling and presentation of results.
- Section 4:** Far-field modelling provides details of the Delft3D model setup, scenarios run and results of the modelling
- Appendix A:** Delft Model Setup
- Appendix B:** Delft 3D Model Calibration
- Appendix C:** CORMIX Extreme Discharge Modelling

2 CORMIX Modelling

The CCUS project uses a hybrid cooling system which results in a thermally uplifted effluent being discharged from the generating station through the planned outfall location (Figure 3). An investigation of 'near-field' mixing processes is required to establish the scale of the mixing zone for the thermal discharge. Thermal plume modelling for this study has been undertaken using the CORMIX modelling software. The methods and results from this thermal plume modelling are presented in the following report sections.



Figure 3. Location of Outfall 1

The CORMIX modelling software, produced by MixZon Inc., has been designed for the prediction and analysis of aqueous toxic or conventional pollutant discharges into diverse water bodies, with the latter being addressed in this study. The user-interface requires singular values to represent specific controlling parameters of geometries (e.g. discharge port) and water body characteristics (e.g. densities). The model uses these parameters to create the predicted plume, which is represented as an instantaneous snap-shot in time of the dispersion and dilution of the two specified water bodies.

CORMIX modelling, assessing the near-field impact of the of thermal plume, has been undertaken in two stages during this project. This first section considers a selection of discharge scenarios and sensitivity tests that were undertaken based upon an initial outfall location provided by AECOM (Outfall 1. Location detailed in Section 2.1). Results from these assessments are documented in Section 2.3.

2.1 Outfall location

An initial planned location of a thermal outfall has been provided to ABPmer via a technical drawing specifying chainage values from fixed onshore landmarks. The orientation of the planned outfall pipe has been estimated by determining the existing outfall orientation to shore from Admiralty Charts and measuring the appropriate distance from shore along the same bearing. Using this approach, the estimated location for the outfall is: 54.64°N, 1.117°W. The water depth in the model at this location is 7.75 m (ODN). Hydrodynamic conditions for this location have been extracted from the Delft3D model, for depth averaged conditions at the time of a mean spring and mean neap range to input into the CORMIX thermal plume modelling, as described in the following sections.

2.2 Model set-up

The CORMIX model set-up is composed of 3 main areas or tabs that require the input of specific parameters to represent geometries and aqueous characteristics within the model. The three tabs are individually outlined below, with the used input parameters stated. All parameters were chosen in consultation with AECOM and are representative of real world conditions.

2.2.1 Effluent

The software allows specification of the key characteristics of the effluent water body that will be discharged from the outfall into the marine environment. Consideration is given to the type of effluent i.e. non/ conservative in which growth and decay rates can be applied. Additionally; heated, saline and sediment discharges can be simulated.

For this study, the effluent was characterised as a heated, conservative (no growth/ decay processes) effluent, which required the following input parameters:

- Temperature Excess: 15°C;
- Flow rate: 1.37 m³/s; and
- Density: 1,018/ 1,020 kg/m³ (summer/ winter representations).

It should be noted that the raw water intake is no longer required as the supply will be provided via a separate private supply, and therefore the higher densities modelled in this study represent a worst-case scenario.

2.2.2 Ambient

To represent the ambient ocean conditions that the outfall will disperse into, hydrodynamic conditions at the proposed outfall location (457108.31 E, 527562.69 N (OSGB)) were extracted from an existing Delft3D hydrodynamic model (See Appendix A and B) and analysed to determine key tidal characteristics; water levels (WL), current speed (CurSpd) and current direction (CurDir).

Following a series of sensitivity testing under mean spring and neap conditions, a mean spring tidal range (approximately 4.6 m) was isolated from the spring-neap cycle of the model output since a worse-case (spring tide) scenario will represent the greatest tidal excursion from the origin. Within this mean spring tide, the WL and CurDir that coincided with the peak CurSpd, for both the flood and ebb phases were obtained. Figure 4 highlights the tidal signal and its key characteristics, which have been isolated to represent the mean spring tide, with the value tabulated in Table 1. Additionally, seasonal wind speeds (m/s) were extracted from the analysis of Durham Tees Valley Airport measured data described in Appendix A.3.5 Wind speeds of 4.08 and 5.32 m/s were selected to represent summer and winter, respectively.

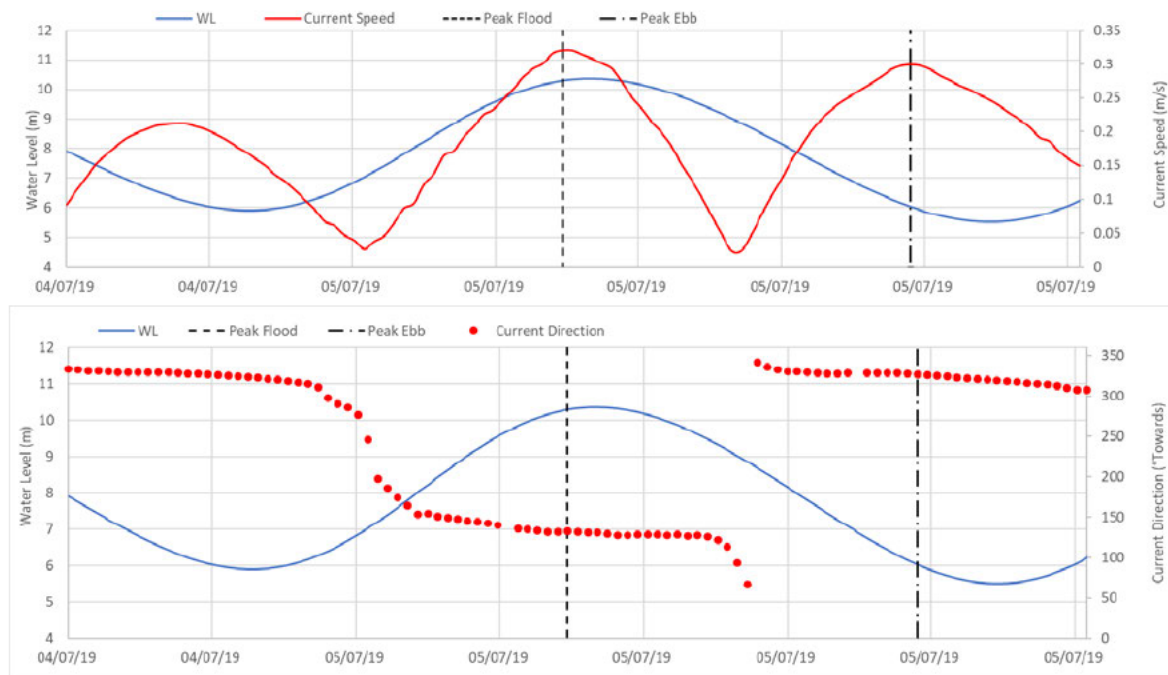


Figure 4. Tidal characteristics during a mean spring tide

Table 1. Tidal characteristics for a mean spring tide.

Tidal Characteristic	Peak Flood	Peak Ebb
Water Level (m)	10.3	6.0
Current Speed (m/s)	0.32	0.30
Current Direction (°N)	132	327

To conclude this tab, the ambient density of the receiving water (1,026 kg/m³) and bed roughness (default of 0.04) parameters were also applied. Furthermore, the enabling of the model environment to be classified as 'Unbounded' is possible, which indicates that there is only one 'bank' in the model (consistent with outfalls into the open sea). This is opposed to a riverine environment, which would be classed as 'Bounded', in which the distance between banks would be required.

2.2.3 Discharge

For this study, the discharge has been represented as standard 'simple port' that is 860 m from the nearest bank, with a 90° (vertical) projection. The Current Direction (CurDir) is considered by determining the direction of the nearest bank – right or left, based on flood or ebb flow direction. The software assumes the user is looking downstream of the flow to determine this. By using the flood and ebb CurDir (132° and 327° as in Table 1), under ebb conditions the nearest bank is defined on the left and on the right under flood phases.

The specific port geometries are also specified within this tab which include:

- Port diameter: 0.8 m; and
- Port height above bed: 1 m.

2.3 CORMIX Outfall 1 results

Following a range of sensitivity tests under mean spring and neap conditions, it was concluded that the spring tidal range under summer conditions offered the largest plume extent, which included the following seasonal parameters;

- Effluent density of 1,018 kg/m³; and
- A mean wind speed of 4.08 m/s.

This model setup has been used as a ‘baseline’ scenario to use as a comparison for a range of sensitivity tests. The tests completed to reach this conclusion are outlined below. A summary of the sensitivity tests presented in this report section are provided in Table 2.

Table 2. CORMIX Run Summary

Run no	Description
01	Spring flood tide (summer season) baseline case, this includes: <ul style="list-style-type: none"> ▪ Seasonal wind speeds ▪ 0.8 m pipe diameter ▪ Pipe orientation vertical
02	Spring flood tide (winter season)
03	Spring flood tide (summer season) no winds applied
04	Spring flood tide (winter season) no winds applied
05	Spring flood tide (summer season) 0.6 m pipe diameter
06	Spring flood tide (summer season) 1 m pipe diameter
10	Spring ebb tide (summer season)
16	Spring flood tide (summer season) 15 m/s wind speed
17	Spring flood tide (summer season) horizontal pipe orientation, directed offshore

2.3.1 Spring flood - Seasonal variation

Shown in Figure 5 is the spring flood tide, demonstrating the seasonal variation (summer/ winter). The winter variation is distinguished by applying different wind speeds (4.08 and 5.23 m/s) and effluent densities (1,018 and 1,020 kg/m³) in separate runs. The seasonal variation is negligible with the summer plume extending very slightly further than the winter, highlighted at around 150 m and the red (summer) 2 and 3°C flags extending slightly further from the origin than the blue (winter).

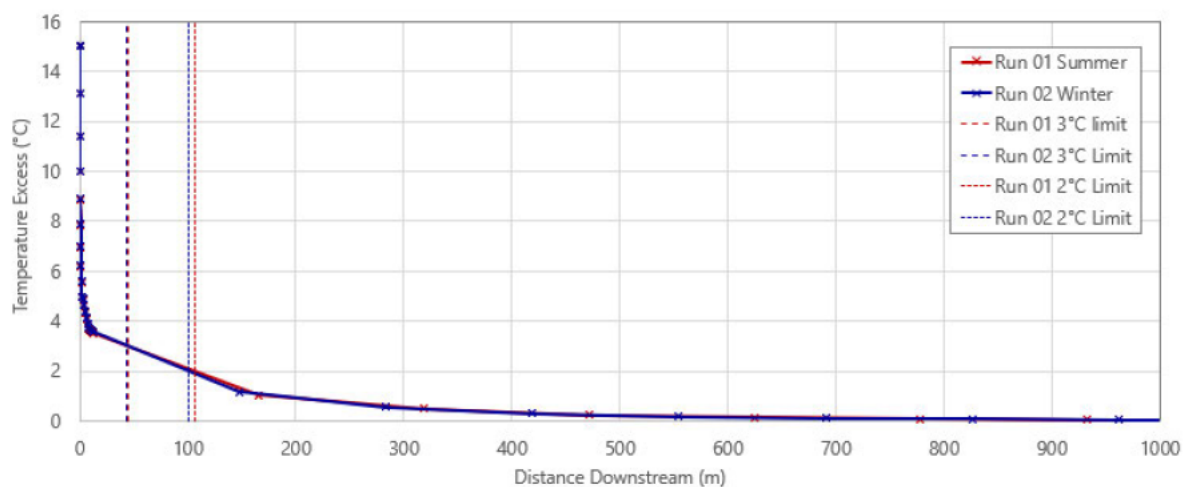


Figure 5. Spring flood seasonal variation

2.3.2 Summer season – Tidal variation

In Figure 6 the summer season has the ebb and flood phases compared against each other (variable for flood and ebb conditions as in Table 1) and shows the ebb plume (Run 10) to better maintain its excess temperature, especially within the first 100 m, which is also shown by the 2 and 3°C flags (blue) extending further than that of the flood (red). However, outside of the near-field region, around 300 m, the two runs converge.

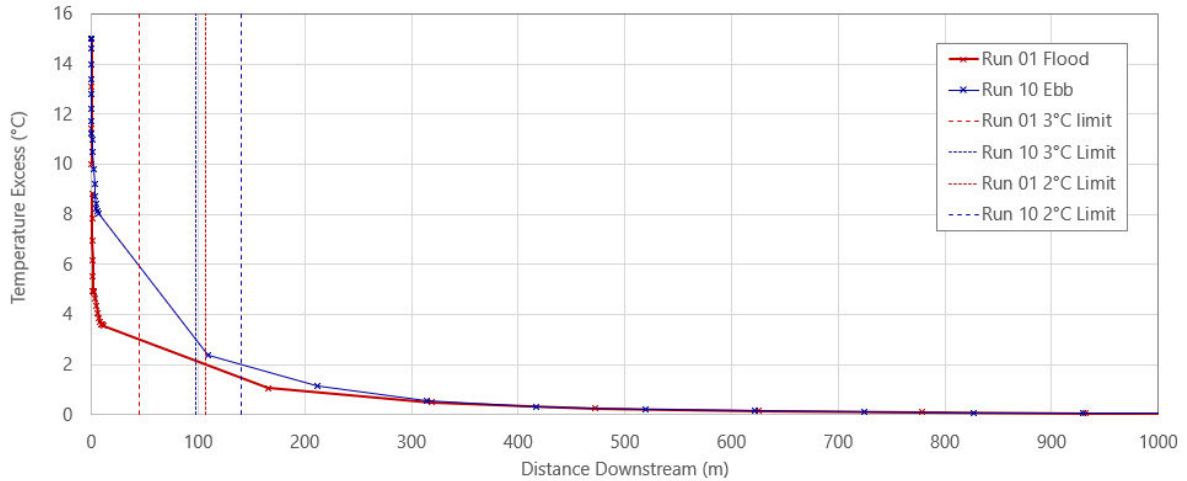


Figure 6. Summer scenario, flood and ebb sensitivity

2.3.3 Spring flood – Wind sensitivity

Shown in Figure 7 is the plume sensitivity to winds. The summer wind value of 4.08 m/s is a light wind and doesn't appear to have any influence on the plume when comparing runs 01 and 03. When a significantly stronger wind of 15 m/s is applied (Run 16), the plume is slightly affected causing the excess temperature to drop slightly quicker around the 100 m mark, also shown by the difference in the 2 and 3°C flags. However, it's to be noted that this wind speed of 15 m/s is approximately triple the speed of the faster mean winter wind speed of 5.32 m/s, and is considered here for sensitivity testing purposes only.

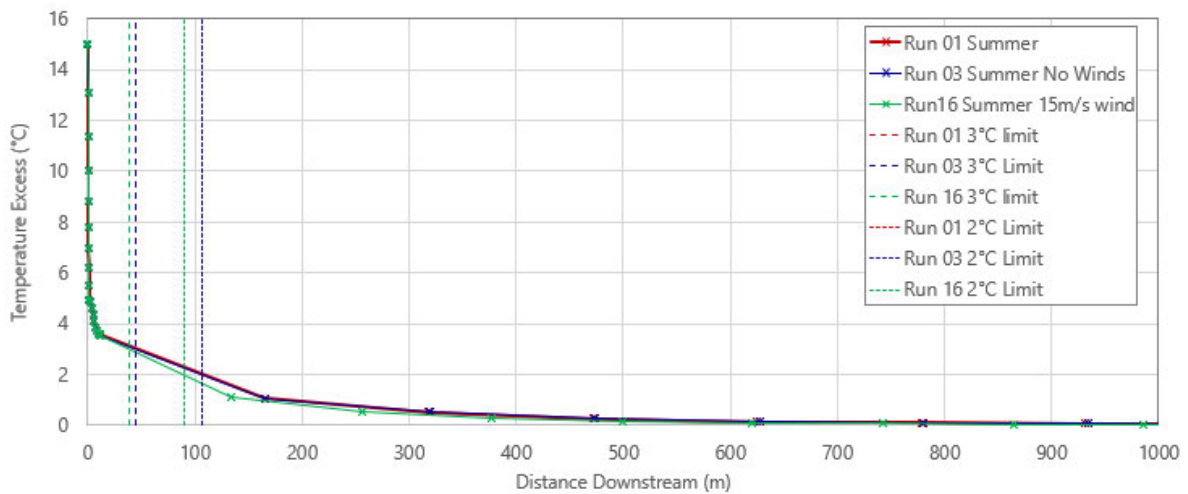


Figure 7. Spring flood wind sensitivity

2.3.4 Spring flood – Pipe diameter

Figure 8 shows the tests addressing the plume sensitivity to the discharge port diameter. The baseline run (Run 01 Summer) has a diameter of 0.8 m, with ± 0.2 m applied in sensitivity runs; Run05 (0.6 m) and Run06 (1.0 m). The larger port diameter (Run 06) shows the excess temperature dilutes notably faster than the two smaller diameters in the near-field region, after which, at around 160 m all the runs converge.

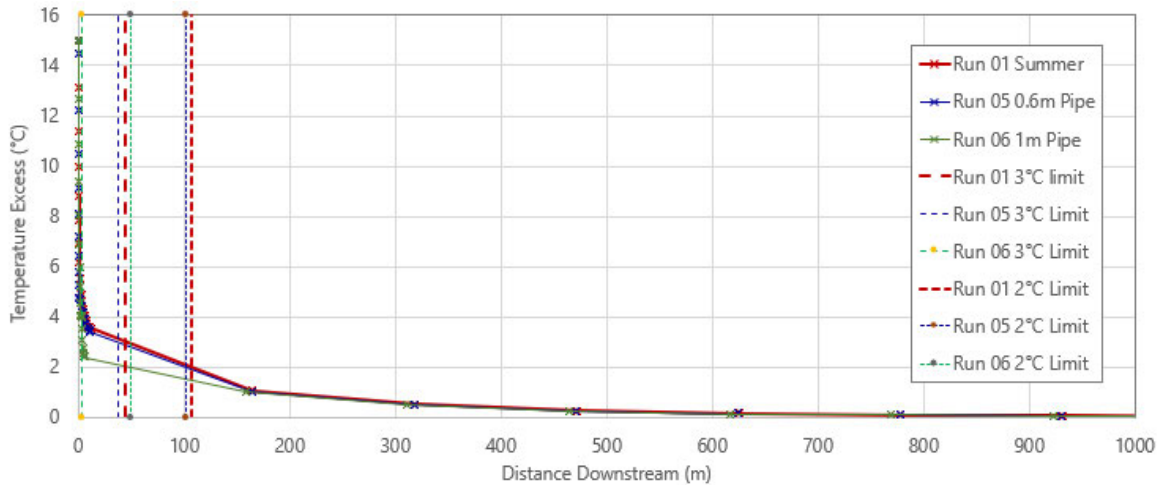


Figure 8. Spring flood, pipe diameter sensitivity

2.3.5 Spring flood – Pipe projection

Figure 9 shows the plume sensitivity to projection of the outfall port. Run 01 has a vertical projection off the seabed, contrasted by Run 17 having an offshore-aligned, horizontal projection, which shows dispersion of the excess temperature far more efficiently, with the 2°C being exceeded at around 15 m, compared to approximately 105 m for the vertical projection in Run 01.

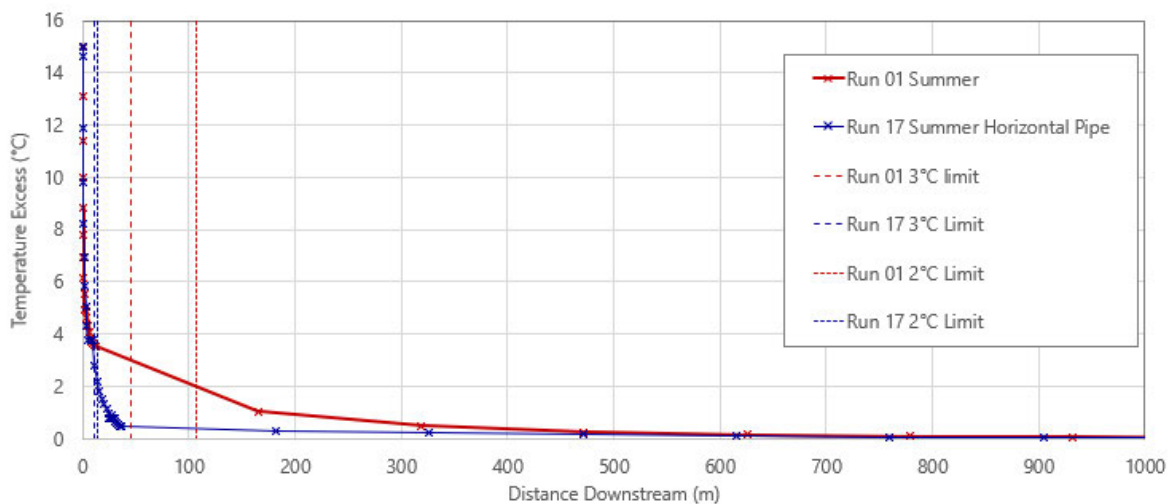


Figure 9. Spring flood, outfall projection sensitivity

2.3.6 Temperature excess isolines

The spring tidal range under summer conditions has also been utilised to demonstrate the plume extent for both the peak flood and ebb flow conditions (tidal characteristics as in Table 1). The plume shown in Figure 10 represents the extents of the excess temperatures isolines from +5°C to +0.1°C and have been overlaid on a map view to indicate the plume extent in relation to the site. A zoomed extent is also shown in Figure 11.



Figure 10. CORMIX excess temperature isolines (°C) under mean spring, peak flood (SE) and ebb (NW) tidal states



Figure 11. Zoomed extent of the CORMIX excess temperature isolines (°C) under mean spring, peak flood (SE) and ebb (NW) tidal states

Additionally, each isoline extent from the outfall is tabulated for both flood and ebb conditions in Table 3.

Table 3. Excess temperature isoline extents from the outfall under peak ebb and flood for a mean spring tide

Excess Temperature Isoline (°C)	Peak Flood (Run 01)		Peak Ebb (Run 10)	
	Isoline Extent from Outfall (m)	Area of Excess Temperature (m ²)	Isoline Extent from Outfall (m)	Area of Excess Temperature (m ²)
5.0	1.6	32	61.3	2
4.0	6.6	49	79.4	3
3.0	44.7	71	97.6	21
2.0	106.5	1,673	140.0	76
1.0	179.3	7,500	235.4	1,455
0.1	754.2	81,256	718.1	74,578

3 CORMIX Modelling – Outfall 2

3.1 Overview

As stated in Section 2, CORMIX modelling, assessing the near-field impact of the of thermal plume has been undertaken in two stages during this project. This section considers key scenarios that have been reproduced based upon a new outfall location and including an alternative ‘extreme’ flow scenario.

For this investigation, spring and neap tidal states have been compared during peak ebb and flood phases. In addition to this, a further case has been considered, in which the pipe diameter is increased to 2.4 m. This change in diameter is to account for a 1-in-30-year worst-case storm event to accommodate for the run off from the site. This scenario is considered across the same tidal states and phases as the initial scenarios and is representative of an extreme and anticipated to be a highly infrequent scenario. The setup and results of this scenario are presented separately in Appendix A.

3.2 Outfall 2 location

In February 2021 AECOM provided an update to the planned outfall location. Easting and Northings have been provided for three possible locations, in close proximity, named East, Mid and West. These sites are listed in Table 4 and the corresponding locations shown in the technical drawing provided by AECOM in Figure 12.

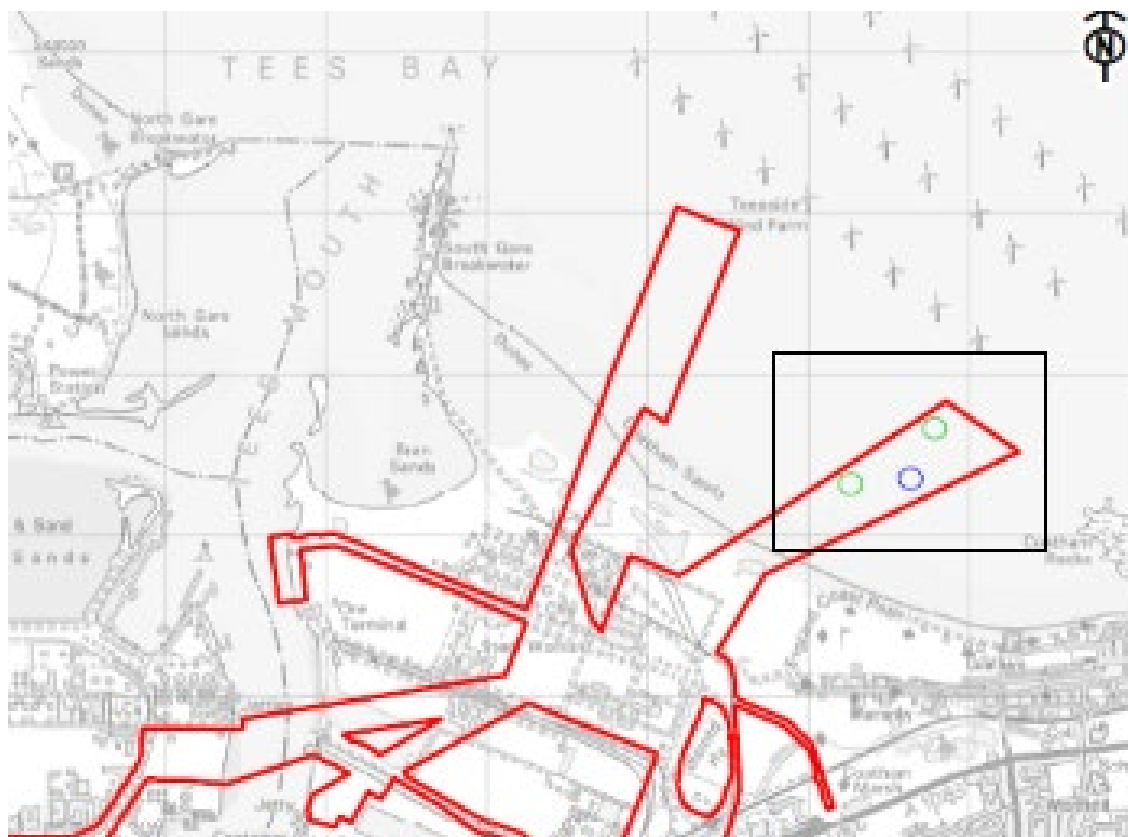


Figure 12. Outfall 2 location indicated by blue circle

Table 4. Outfall 2 location options

Location	Easting (m)	Northing (m)
Eastern-most	458737	526655
Mid (blue circle)	458622	526308
Western-most	458143	526315

3.3 Model set-up

The summer density of the effluent (1,018 kg/m³) was carried over from the initial sensitivity tests since this offered a slightly greater plume compared to a winter equivalent. Tidal data at three locations provided by AECOM as potential sites for the outfall location were compared to determine any differences in tidal conditions. Differences were negligible and so the middle location was used. The site-specific tidal characteristics for Outfall 2 are presented in Table 5. All the runs (normal and extreme discharge events) completed and analysed for Outfall 2 (position shown in Figure 13) are outlined in Table 6.



Figure 13. Location of modelled Outfall 2

Table 5. Input tidal characteristics.

Tidal State	Tidal Characteristic	Peak Flood	Peak Ebb
Spring	Water Depth (m)	8.1	5.0
	Current Speed (m/s)	0.24	0.17
	Current Direction (°N)	119	306
Neap	Water Depth (m)	4.7	6.5
	Current Speed (m/s)	0.07	0.11
	Current Direction (°N)	111	292

Table 6. Outfall 2 CORMIX Run Summary.

Run no.	Description
18	Spring flood tide
19	Neap flood tide
26	Spring flood tide (extreme 1-in-30-year) *
28	Neap flood tide (extreme 1-in-30-year) *
22	Spring ebb tide
23	Neap ebb tide
27	Spring ebb tide (extreme 1-in-30-year) *
29	Neap ebb tide (extreme 1-in-30-year) *

*results presented in Appendix A.

3.4 CORMIX Outfall 2 results

Since the tests at this outfall focus on the variability across tidal states, the runs are presented by flood and ebb phases during both spring and neap tides.

3.4.1 Flood tide variation

Figure 14 shows the downstream temperature excess of the resultant plume during a spring (run 18) and neap (run 19) flood tide under normal discharge conditions, at Outfall 2. The neap tidal characteristics result in a larger, more extensive plume. The excess temperature is dispersed at a slower rate due to the slower tidal velocities when compared to spring equivalent as shown in Table 5. This is highlighted by the offset of the 2 and 3°C flag limits.

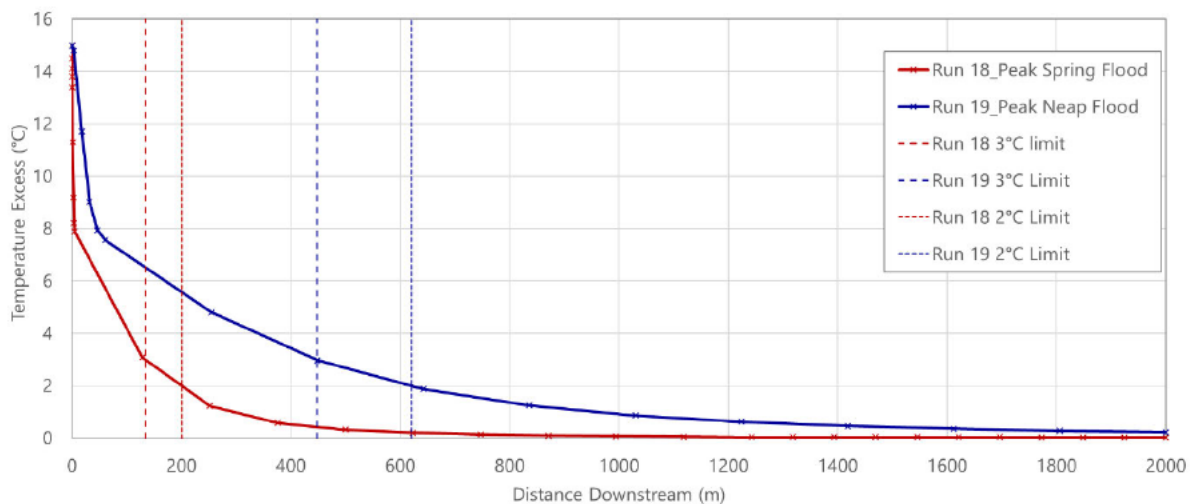


Figure 14. Spring and neap flood tide plume variations during normal discharge events.

3.4.2 Ebb tide variation

Figure 15 shows the downstream temperature excess of the resultant plume during a spring (run 22) and neap (run 23) ebb tide under normal discharge conditions, at Outfall 2. As with the flood tide, the neap plume is shown to have a larger extent under ebb conditions due to the slower tidal velocities resulting in a slower dispersion of the excess temperature, but both spring and neap plumes are dispersed by 1,200 m downstream of the origin.

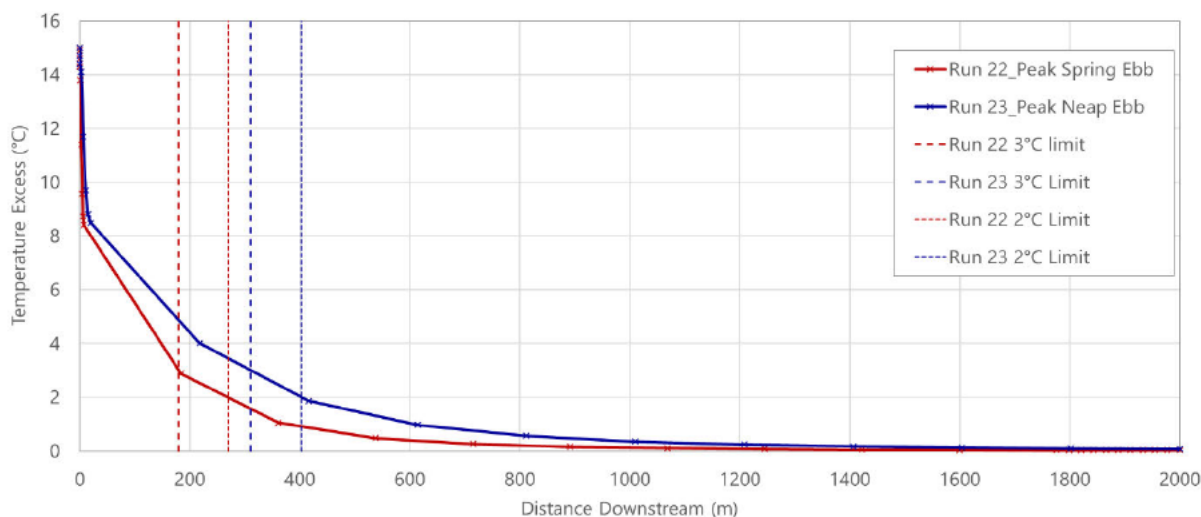


Figure 15. Spring and neap ebb tide plume variations during normal discharge events.

3.4.3 Temperature excess isolines

The tidal velocities that occur during the neap tide reduce the rate of dispersion of the excess temperature and therefore result in a larger plume. The extents of the 1-5 °C isolines for the neap tide are outlined in Table 7, with the isolines from the neap tidal states geo-referenced in Figure 16 which represent the ‘worst-case’ under normal discharge conditions. It should be noted that the CORMIX assessments assume constant ambient flow conditions and provide a prediction of the fully developed plume. In the tidal coastal waters at the Outfall locations, flow speeds and directions are constantly shifting with tidal phase, meaning that a fully developed plume will not experience the assumed constant flow regime. The results of the far-field thermal assessment (detailed in Section 4) take account of the changing tidal conditions and, as a result, are likely to give a more realistic representation of the thermal plume under the assessed conditions.

Table 7. Isoline extents for all tidal states under normal discharge conditions.

	Spring Flood Tide (Run 18)	Spring Ebb Tide (Run 22)	Neap Flood Tide (Run 19)	Neap Ebb Tide (Run 23)
Excess Temperature Isoline (°C)	Isoline Extent from Outfall (m)	Isoline Extent from Outfall (m)	Isoline Extent from Outfall (m)	Isoline Extent from Outfall (m)
1	308	381	913	609
2	170	266	599	398
3	114	184	431	293
4	57	146	329	203
5	5	117	237	149



Figure 16. Excess temperature isolines during a neap tide under normal discharge conditions.

4 Delft3D Modelling – Far Field Impact

AECOM wish to assess the potential far-field impact of a thermal discharge produced by cooling water from the CCUS into the sea off the Teesside coastline. Far-field thermal plume modelling has been requested to satisfy the requirements of the Development Consent Order for the CCUS project.

The following section describe the Delft Far Field modelling undertaken to assess the impact of the thermal plume discharge through a simulated outfall and present the results from the scenarios which have been tested. A summary of observations from the far-field modelling is provided in each subsection of the results presentations (Section 4.3) and summary statements are provided in the modelling conclusions in Section 5.

4.1 Model setup

The far-field thermal plume modelling makes use of the existing Delft3D model, as described earlier in the report, constructed to assess the hydrodynamic conditions in the estuary. Details of the model setup are provided in Appendix A

This model has been updated to include temperature in the physical properties being modelled and to simulate a discharge with fixed thermal and saline properties at the outfall location.

A summary of the physical parameters applied in the Delft3D model is provided in Table 8. These parameters have been kept consistent with the hydrodynamic and near field thermal plume modelling undertaken in previous report sections. Their derivation is described earlier in this report.

Table 8. Physical properties of the Delft3D simulations

Parameter	Summer value	Winter value
Wind Speed (m/s)	4.08	5.32
Wind Direction (° from)	230	230
Ambient water temperature (°C)	14	5.8
Ambient salinity (ppt)	33.9	33.9

4.1.1 Outfall location

Two possible outfall locations have been (separately) simulated in this far-field assessment. The first is the original outfall location (Outfall 1) provided by AECOM during the original modelling scope (2020), the second is a revised location (Outfall 2) slightly further to the east of the original. Three possible 'updated' locations for the outfall were provided by AECOM in February 2021, the central location of the three has been used in the far field assessment. Further details for Outfall 1 and Outfall 2 have been provided in Section 2.1 and 3.2 of this report. For convenience the two locations modelled in the far field simulations are listed in Table 9 and their position in the Delft3D grid shown in Figure 17.

Table 9. Outfall locations for far-field modelling

Location	Easting (m)	Northing (m)
Outfall 1 (Original)	457088	527565
Outfall 2 (Updated - Mid)	458622	526308

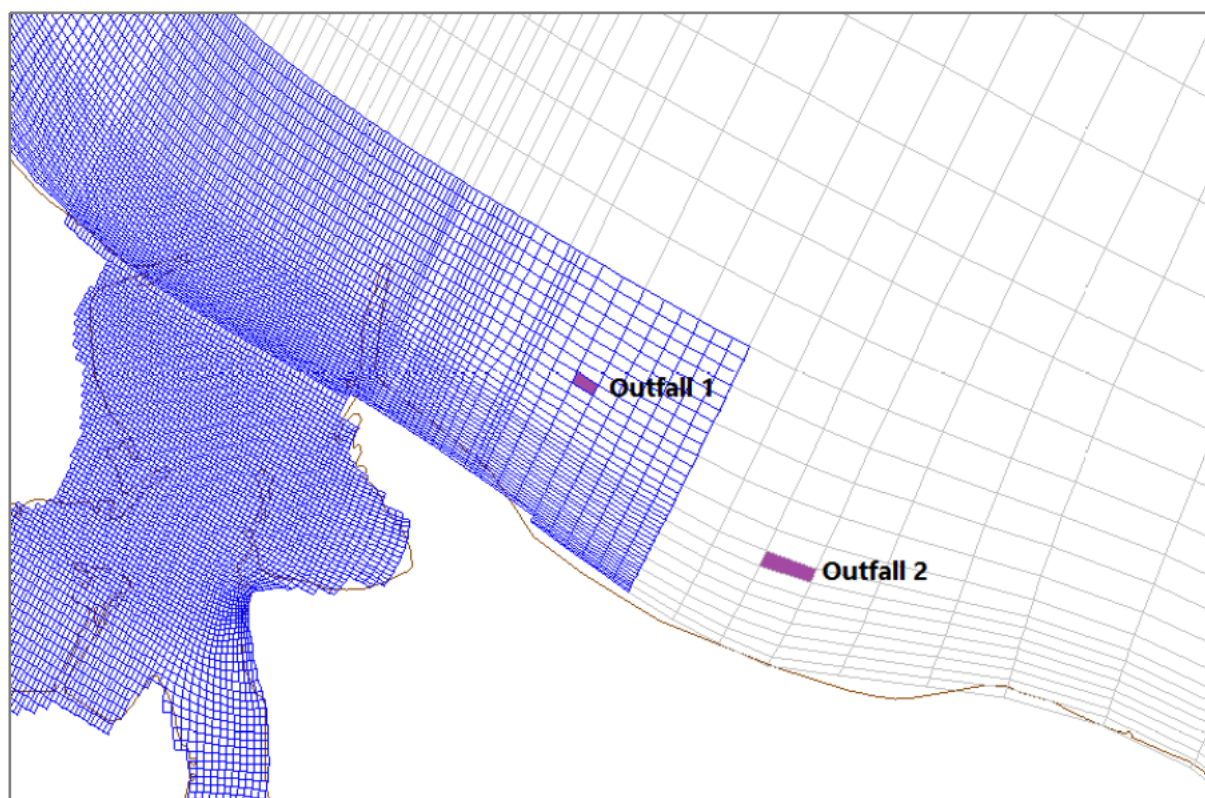


Figure 17. Location of Outfalls in far-field (Delft3D) model grid

4.1.2 Definition of the Outfall in Delft3D

Delft3D provides the option to include a ‘discharge’ in the flow model grid. In order to simulate the outfall a discharge has been defined in the applicable model grid cell (see Figure 17) in vertical layer 8 (nearest to the sea bed). The thermal and saline properties of the ambient and effluent water are shown in Table 10 below. A continuous flow rate of 1.37 m³/s is specified for the thermal discharge.

Table 10. Thermal plume properties in Delft3D, summer and winter case

Input/Parameter	Summer		Winter	
	Ambient	Effluent	Ambient	Effluent
Salinity (ppt)	33.9	29.3	33.9	29.3
Temperature (°C)	14	29	5.8	20.8

4.2 Scenarios

Summer and winter scenarios have been simulated for a 14-day duration in 2019 covering a spring and neap period. These have been produced for both the outfall locations. The simulation time is the same as that modelled in the assessment of hydrodynamic conditions in Appendix A.

Sensitivity tests assessing the impact of wind direction and flow rate have been undertaken using the Outfall 2 location – this being the best current estimate of the likely discharge site.

A summary of model runs undertaken to assess the far-field thermal plume impact is provided in Table 11.

Table 11. Delft3D model runs for far-field assessment

Run	Description
Run 1	Summer conditions for a spring-neap period: Outfall 2
Run 2	Winter conditions for a spring-neap period: Outfall 2
Run 3	Summer conditions for a spring-neap period – Onshore wind: Outfall 2
Run 4	Summer conditions for a spring-neap period – Wind from south east: Outfall 2
Run 5	Summer conditions for a spring-neap period: Outfall 1
Run 6	Winter conditions for a spring-neap period: Outfall 1
Run 7	Summer conditions for a spring neap period – high flow rate scenario: Outfall 2

4.3 Results

Contour plots of excess temperature are presented in Figure 18 to Figure 35 showing the impact of the thermal discharge on the sea water temperature. Excess temperature is shown as a positive difference relative to the ambient temperature (14°C for the summer condition and 5.8°C in winter). Temperatures shown are depth averaged across all vertical layers in the model.

For the initial summer and winter model runs, contour plots are presented for four stages of the tide: a peak flood, peak ebb and the slack waters in between. For later sensitivity comparisons, the times of peak flow are sufficient to provide comparisons.

The times of peak flood and ebb have been selected from representative periods of mean spring and neap tidal range. These selected times also correspond to those used in the identification of CORMIX input parameters in the nearfield assessments.

For reference in the excess temperature contours:

- Temperature excess less than 0.02°C is not shaded in these plots;
- The first grey band of colour shows a temperature excess of between 0.02°C and 0.04°C; and
- The next light blue band shows a temperature excess of between 0.04°C and 0.06°C;

4.3.1 Runs 1 and 2: Summer and Winter Spring/Neap conditions using the Outfall 2 location

Figure 18 to Figure 21 on the following pages show the contour plots of excess temperature produced from simulating the thermal discharge at the updated outfall site for the summer and winter conditions.

Four stages of the tide are shown for each of the summer/winter spring/neap combinations.

For both the summer and winter scenarios the same spring vs neap observations are made:

- The thermal discharge over a spring tide tends to stay closer to the shore and extend further along the coastline in comparison to the neaps.
- The neap simulations show a higher temperature excess close to the point of discharge and a plume which extends further offshore than seen in the spring cases.
- Overall the distance from source over which a difference in temperature is observed is greater in the spring simulations than the neaps.
- In a spring scenario, the extent of the temperature excess between 0.02 and 0.04°C extends approximately 9 km to the south east of the outfall location.
- No temperature excess >0.02 degrees extends into the estuary mouth in these scenarios.

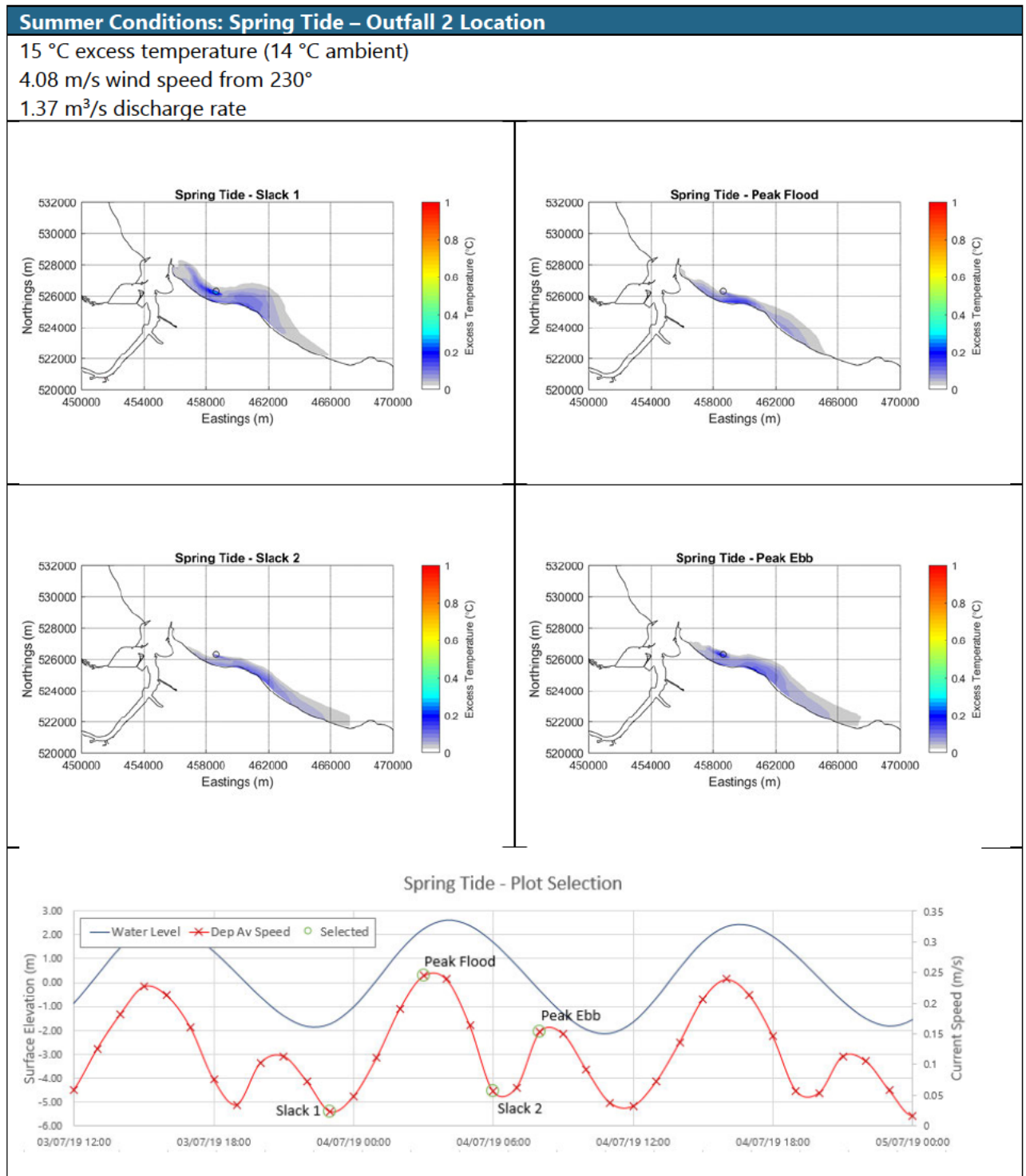


Figure 18. Temperature excess contour plots: Summer spring tide – Outfall 2 location

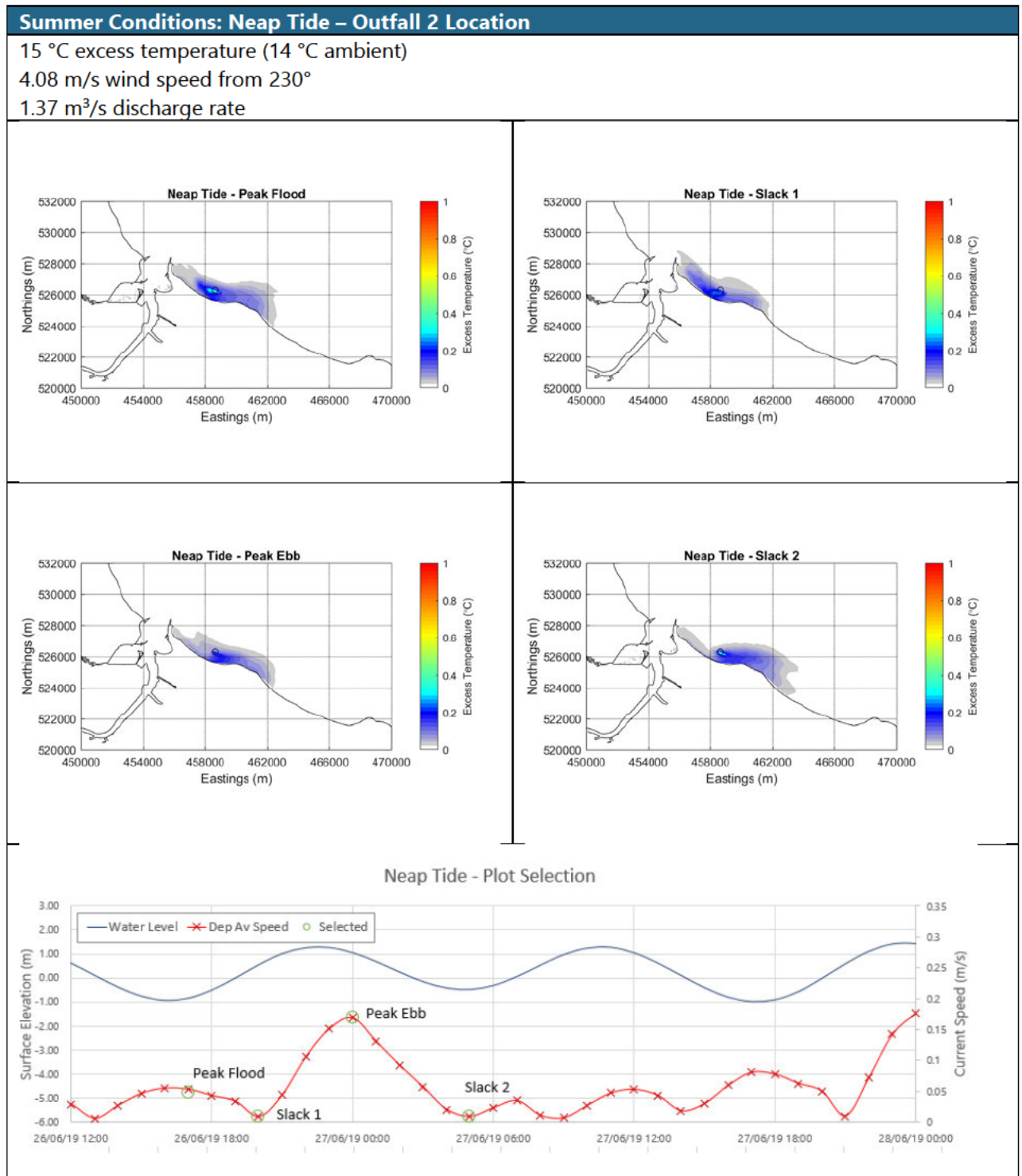


Figure 19. Temperature excess contour plots: Summer neap tide – Outfall 2 location

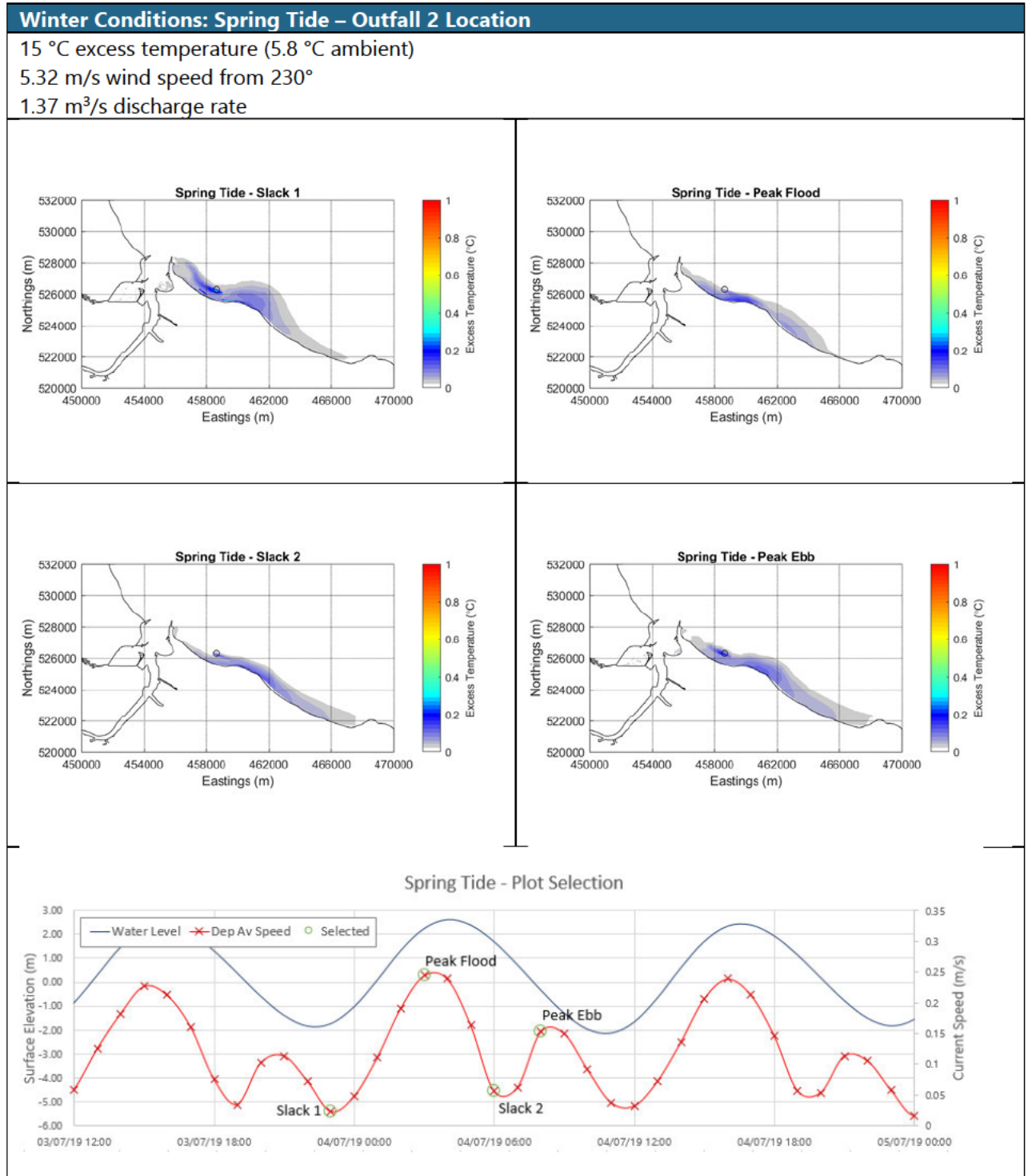


Figure 20. Temperature excess contour plots: Winter spring tide – Outfall 2 location

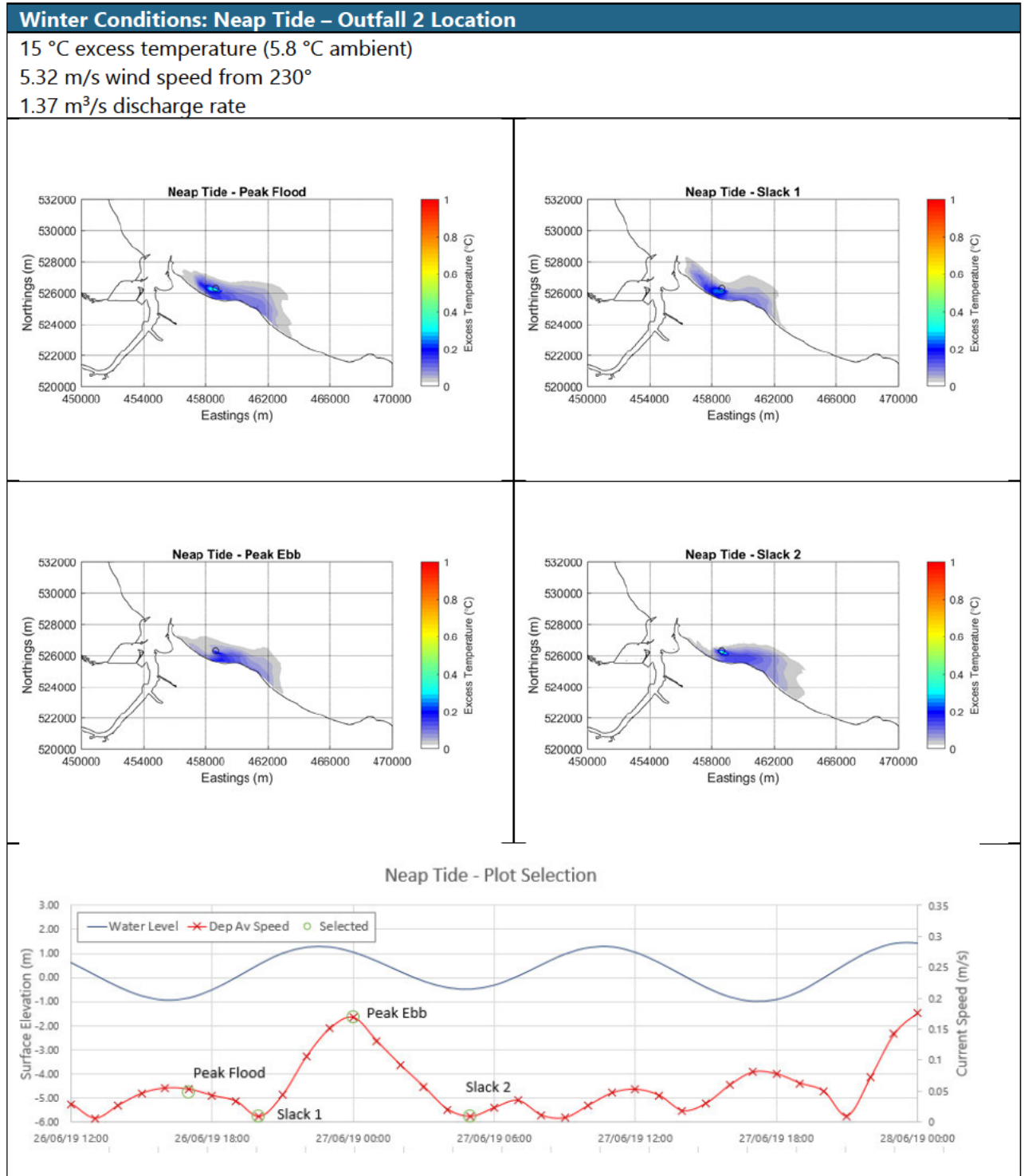


Figure 21. Temperature excess contour plots: Winter neap tide – Outfall 2 location

4.3.2 Runs 3 and 4: Sensitivity to Wind conditions

The Run 1 and 2 simulations applied the average seasonal wind conditions (derived during model calibration (Appendix A)), of 4.08 m/s for the summer and 5.32 m/s in the winter, both applied with a continuous direction of 230° from.

In order to test the sensitivity of the plume discharge to wind directions, two further simulations have been run. These both use the baseline summer condition: ambient temperature of 14° and wind speed of 4.08 m/s, but with altered wind directions as follows:

- Run 3: Onshore wind. A forcing direction of 30° (from) has been applied to simulate a continuous wind perpendicular to the coast (onshore).
- Run 4: South East. A forcing direction of 120° (from) has been applied to simulate a continuous wind running parallel to the coastline from approximately a south east direction.

Results from these simulations have been compared with the summer scenario with a 230° wind in Figure 22 to Figure 25. The following observations are made:

- Comparison of the south westerly (230°) vs the onshore (30°) wind direction show small differences in the distribution of the thermal plume:
 - During the spring tides, when flows are relatively higher, very little change in the excess temperature plots is seen as a result of the change in wind direction.
 - During the neap tide a more discernible difference is seen, with the discharge being held closer to the coast in the presence of an onshore wind.
- When a south easterly (120°) wind is applied to the summer thermal plume discharge scenario the effect is to reduce the eastern extent of the thermal plume. This is more pronounced in the neap comparisons where flow speeds are lower and the along-coast extent of the plume is already smaller compared with the spring case.

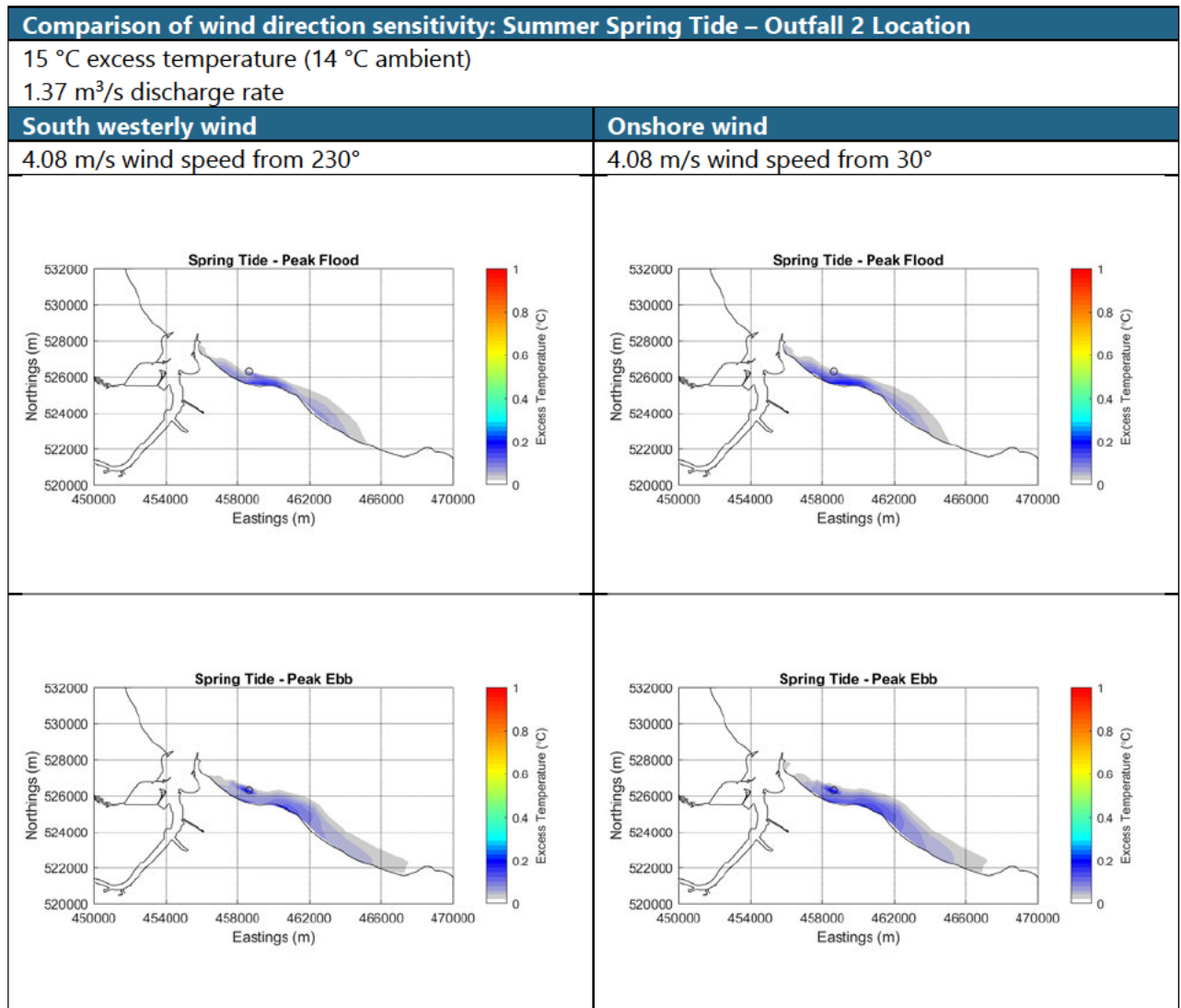


Figure 22. Temperature excess contour plots: Comparison of spring summer conditions with a 230° wind direction (left) vs onshore wind (right)

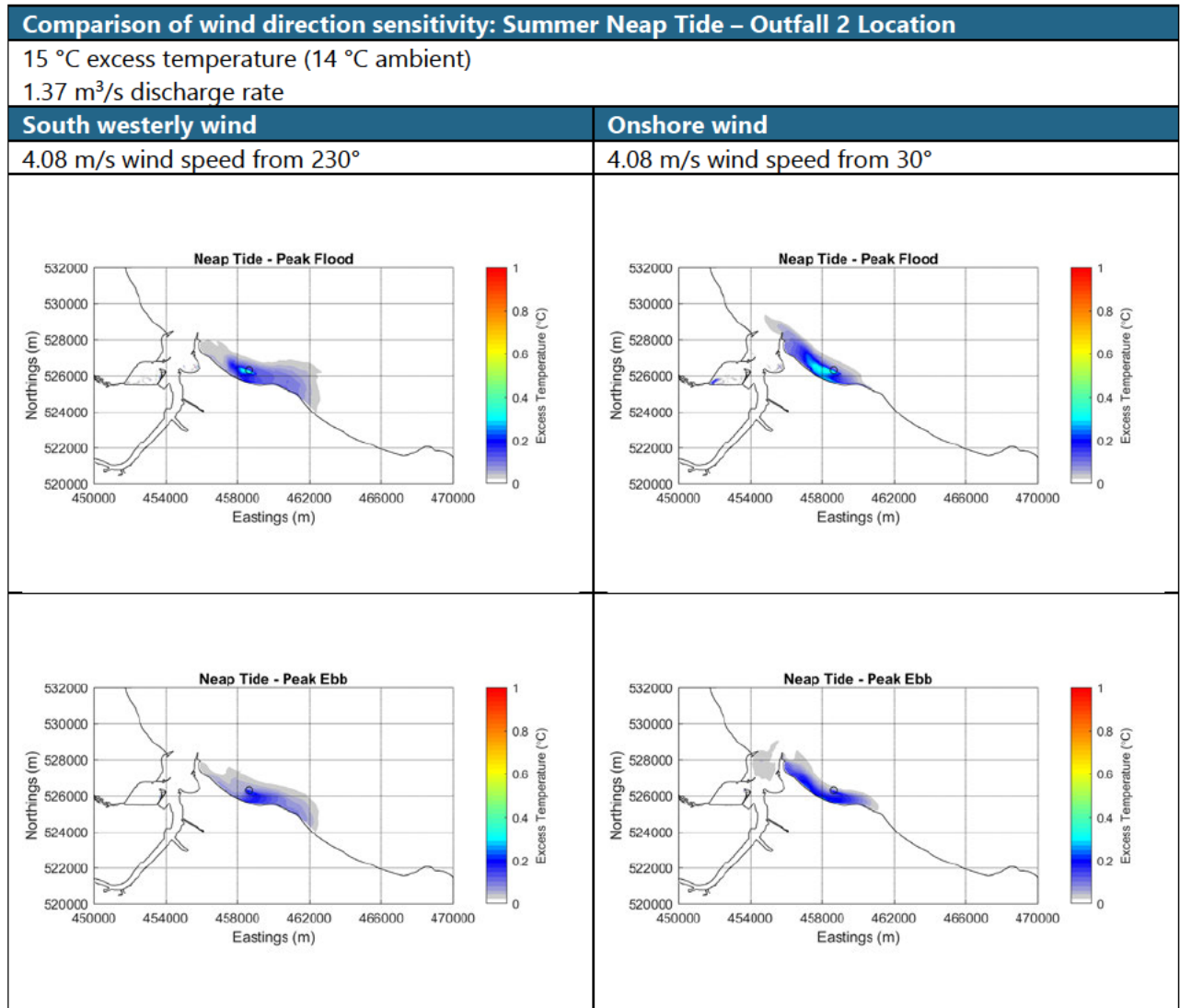


Figure 23. Temperature excess contour plots: Comparison of neap summer conditions with a 230° wind direction (left) vs onshore wind (right)

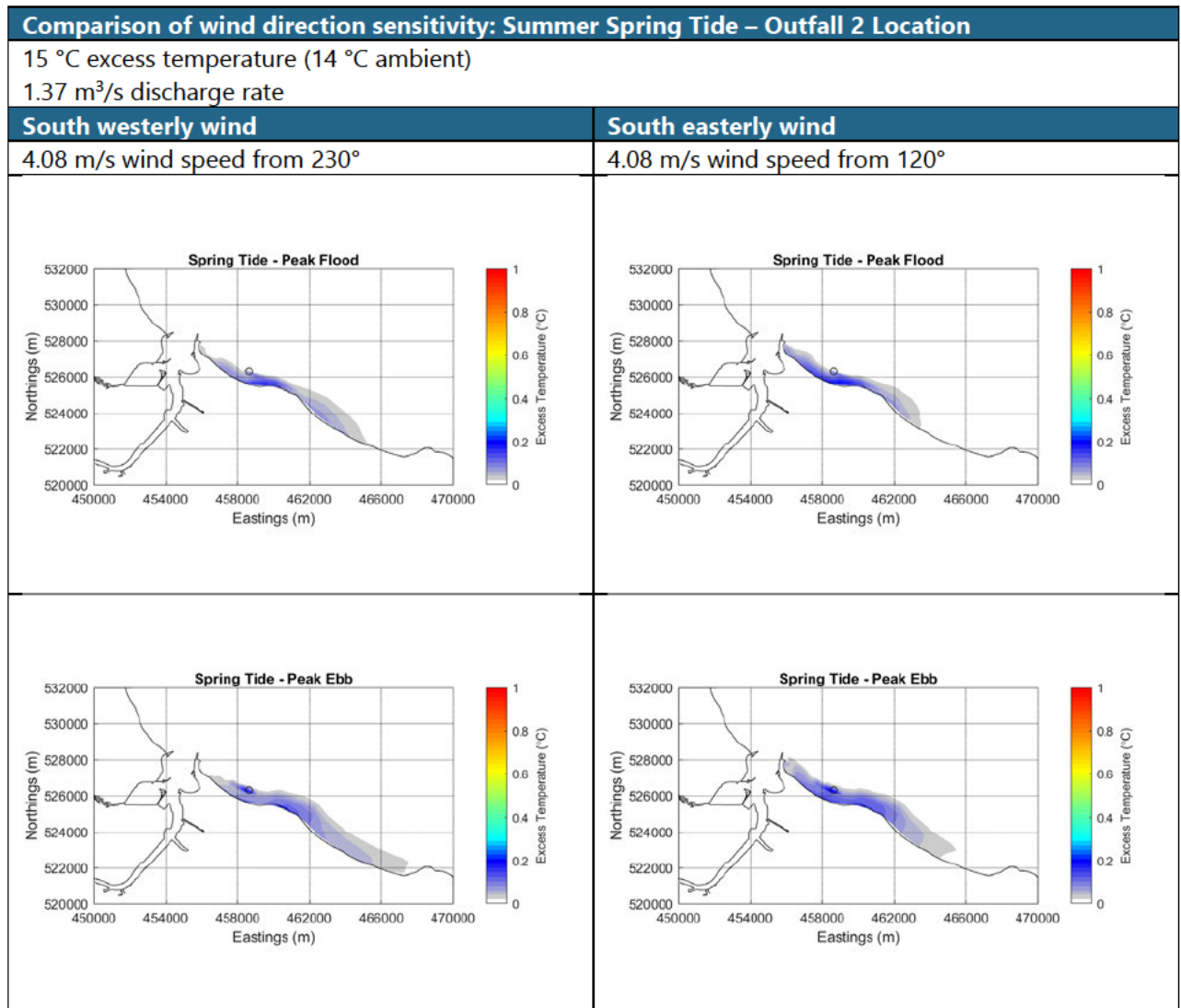


Figure 24. Temperature excess contour plots: Comparison of spring summer conditions with a 230° wind direction (left) vs 120° wind direction (right)

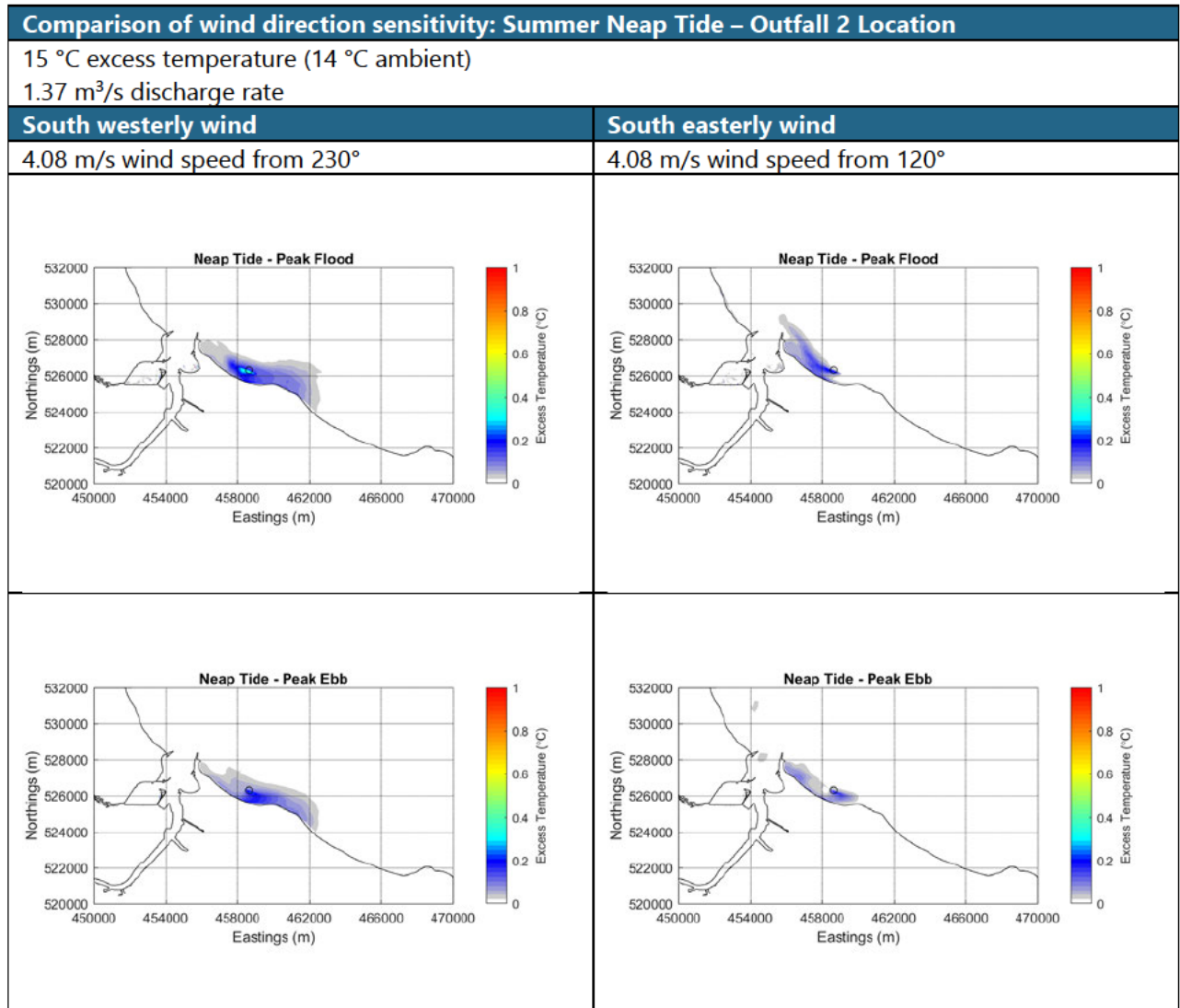


Figure 25. Temperature excess contour plots: Comparison of neap summer conditions with a 230° wind direction (left) vs 120° wind direction (right)

4.3.3 Runs 5 and 6: Outfall location assessment

Runs 5 and 6 simulate the summer and winter conditions over a spring/neap cycle with the discharge specified at the Outfall 1 site (Figure 17). These are compared for selected tidal conditions with the discharge modelled from the Outfall 2 location. The following observations are made:

- During the summer cases, the extent of the thermal discharge (up to 0.04°C) from the updated location is greater than that simulated in the original location.
- Using the Outfall 1 location: during the summer some of the temperature impact is seen inside the estuary in the neap simulations. This temperature excess does not exceed 0.06°C within the estuary mouth.
- During the winter period a temperature difference is seen extending into the Tees Estuary, particularly noticeable in the spring tide scenarios. It should be noted that the excess temperatures seen are very small (< 0.04°C excess) compared with the background of 5.8°C.

These scenarios have been examined in more detail in order to explain the differences seen between the two different outfall scenarios. It should be noted that the flow speeds vary between the two sites despite their close proximity. This has been illustrated in Figure 26 and Figure 27 below for a representative spring and neap flow. The selected times peak ebb and flood tide for the Outfall 2 assessment are shown on these plots (the timings of these will vary slightly from those selected for the Outfall 1 flow data. The flow differences seen between the two sites, particularly on the neap tide, are relatively large compared with the magnitude of the flow speed. It can be seen that the flow speeds at the Outfall 1 site are consistently higher which may be contributing to faster dispersion of the plume as well as the widened extent in some cases.

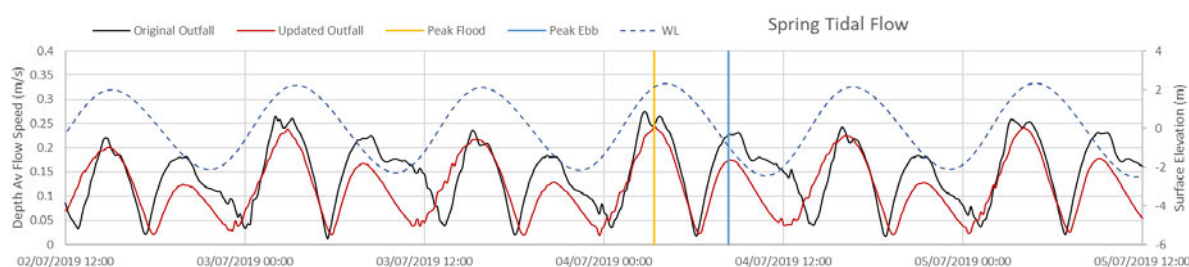


Figure 26. Flow speeds over a spring tide at Outfall 1 and Outfall 2 positions

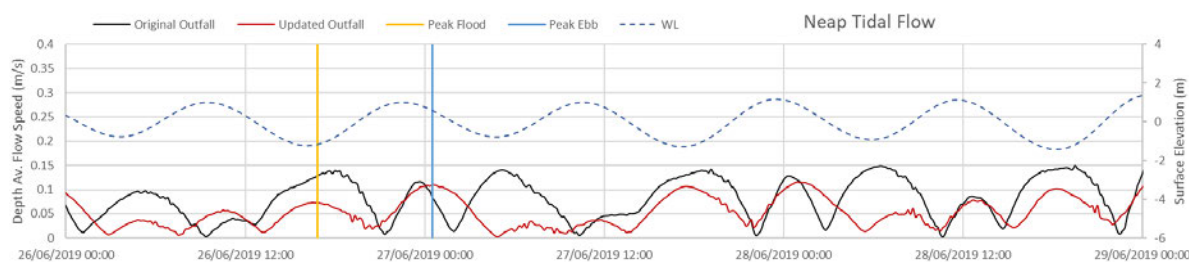


Figure 27. Flow speeds over a neap tide at Outfall 1 and Outfall 2 positions

Figure 28 below shows flow vectors during a spring period where flow direction is towards the north west. The underlying colour contours show the sea temperature, in which the outfall impact is evident. This plot shows the along shore flow directing the plume discharge into the estuary. Plot Figure 29 shows the same time with the vectors removed to better illustrate the temperatures within the estuary. It should be emphasised that the colour scales on these plots have been stretched to illustrate this effect (showing a range of 0.4°C) and that the temperature differences observed are very small.

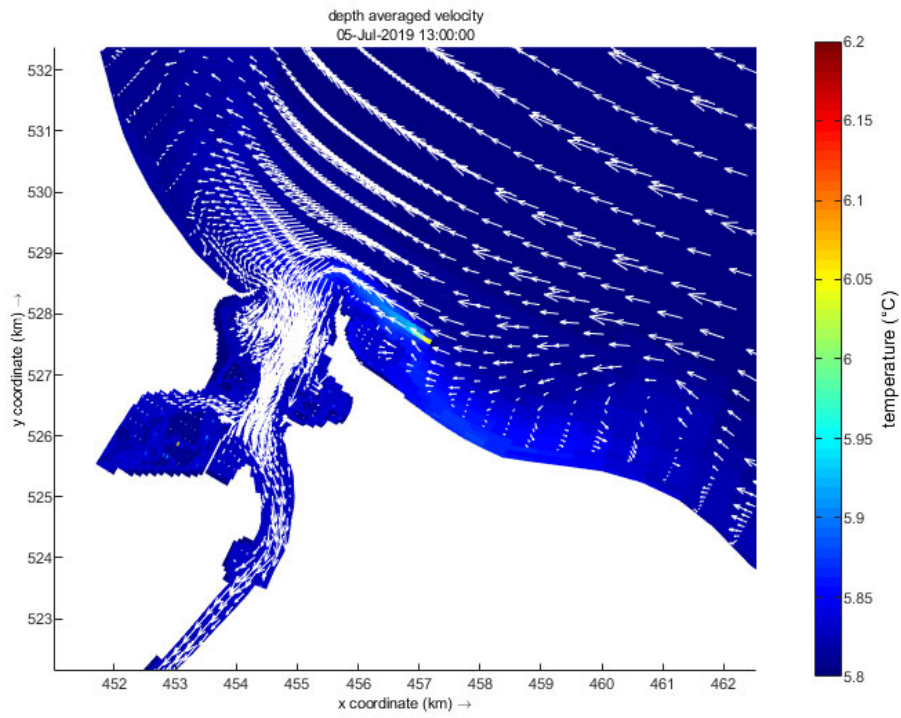


Figure 28. Temperature contours and Flow Speed Vectors from Run 6: Winter – Outfall 1

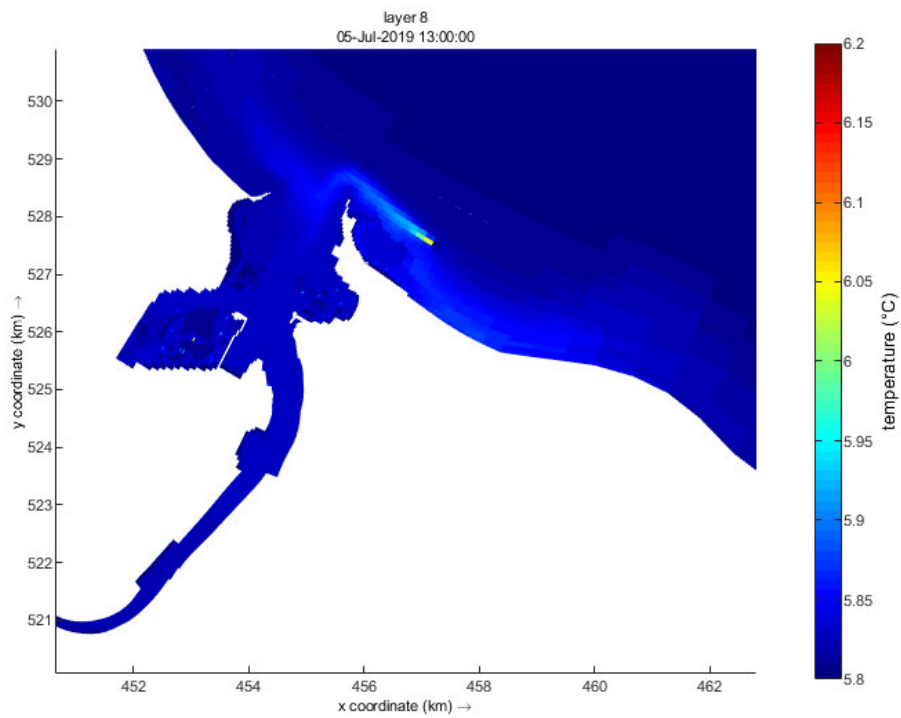


Figure 29. Temperature Contours from Run 6: Winter – Outfall 1

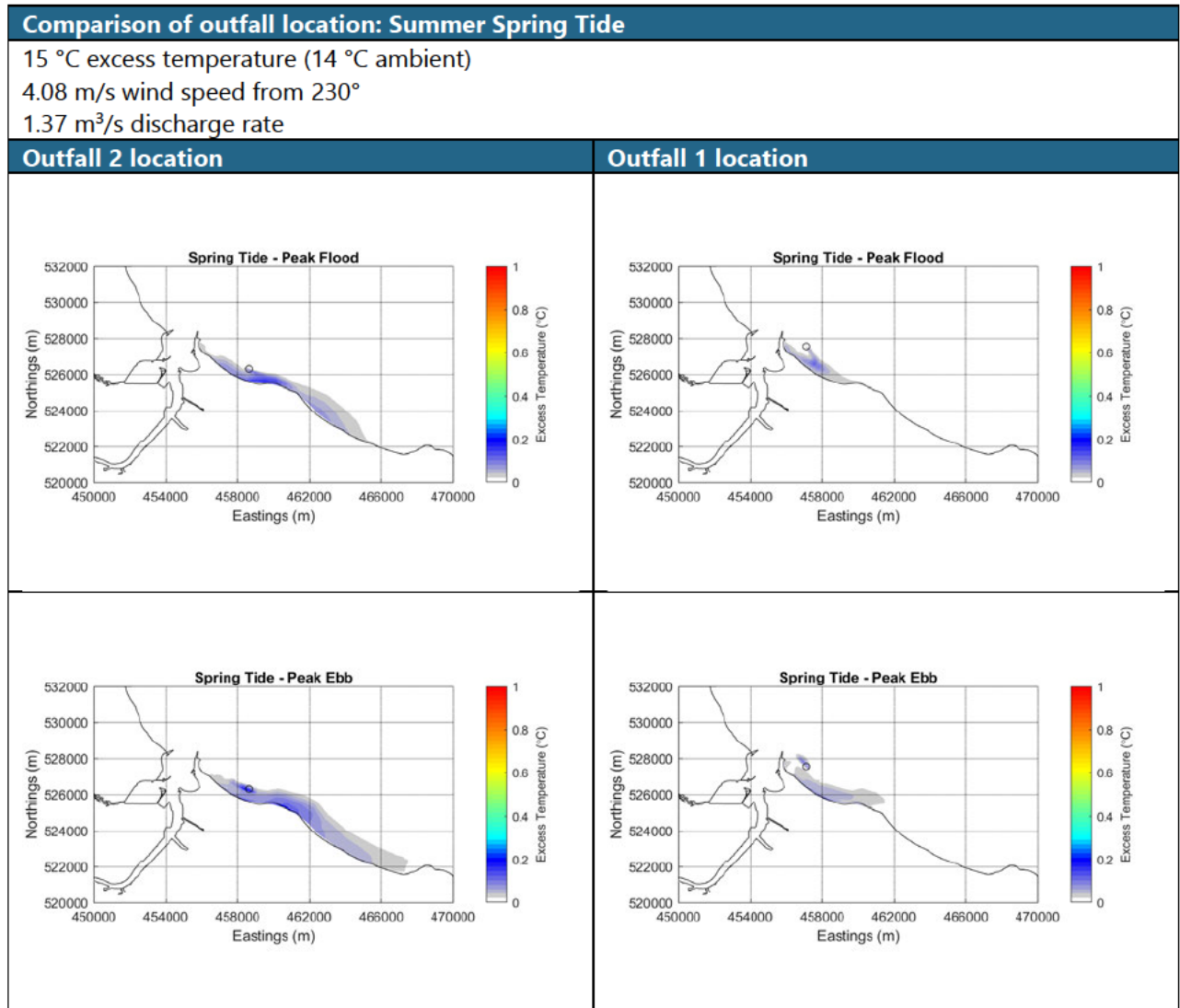


Figure 30. Temperature excess contour plots: Comparison of spring summer conditions with a discharge specified at Outfall 2 (left) vs Outfall 1 (right)

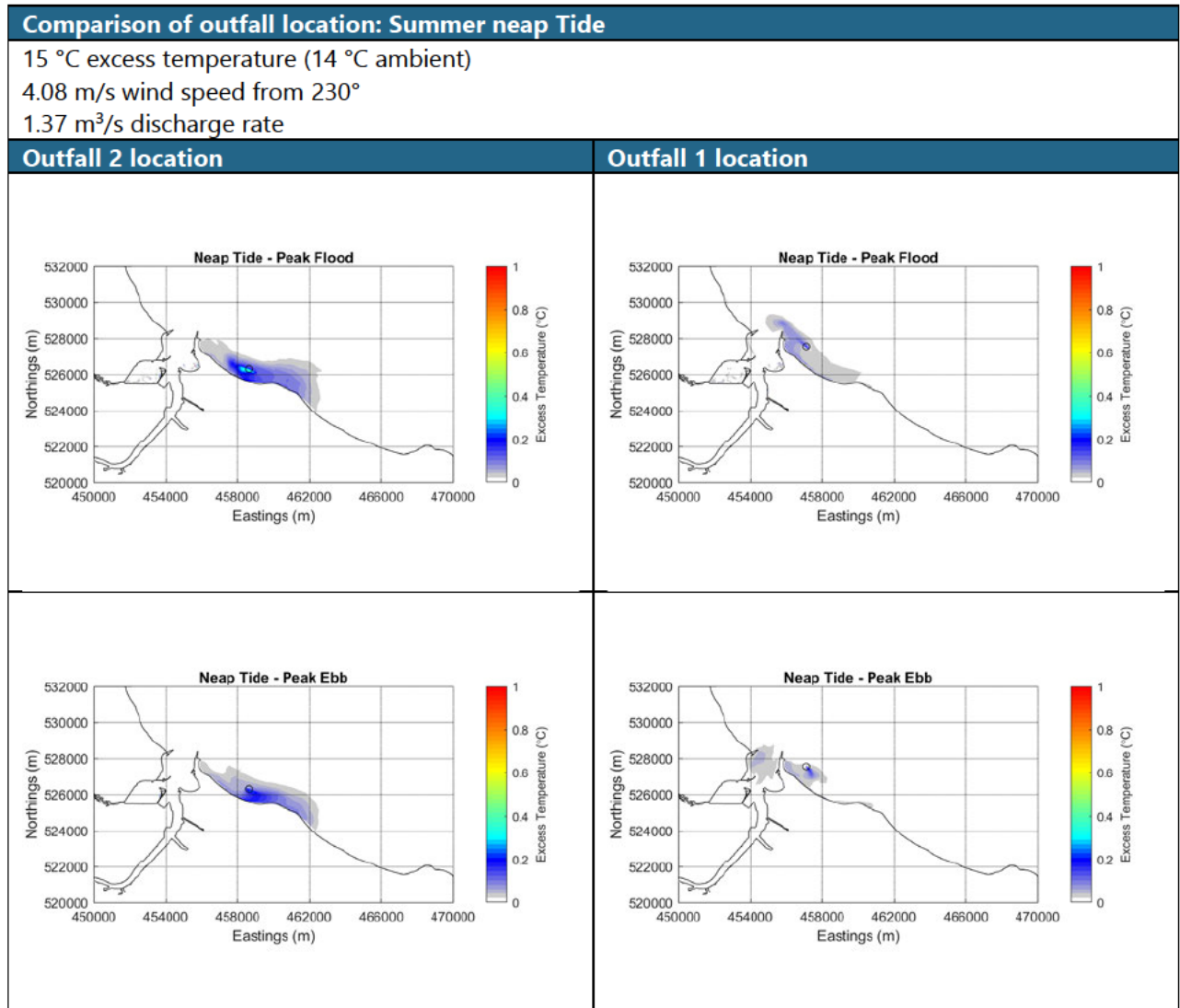


Figure 31. Temperature excess contour plots: Comparison of neap summer conditions with a discharge specified at Outfall 2 (left) vs Outfall 1 (right)

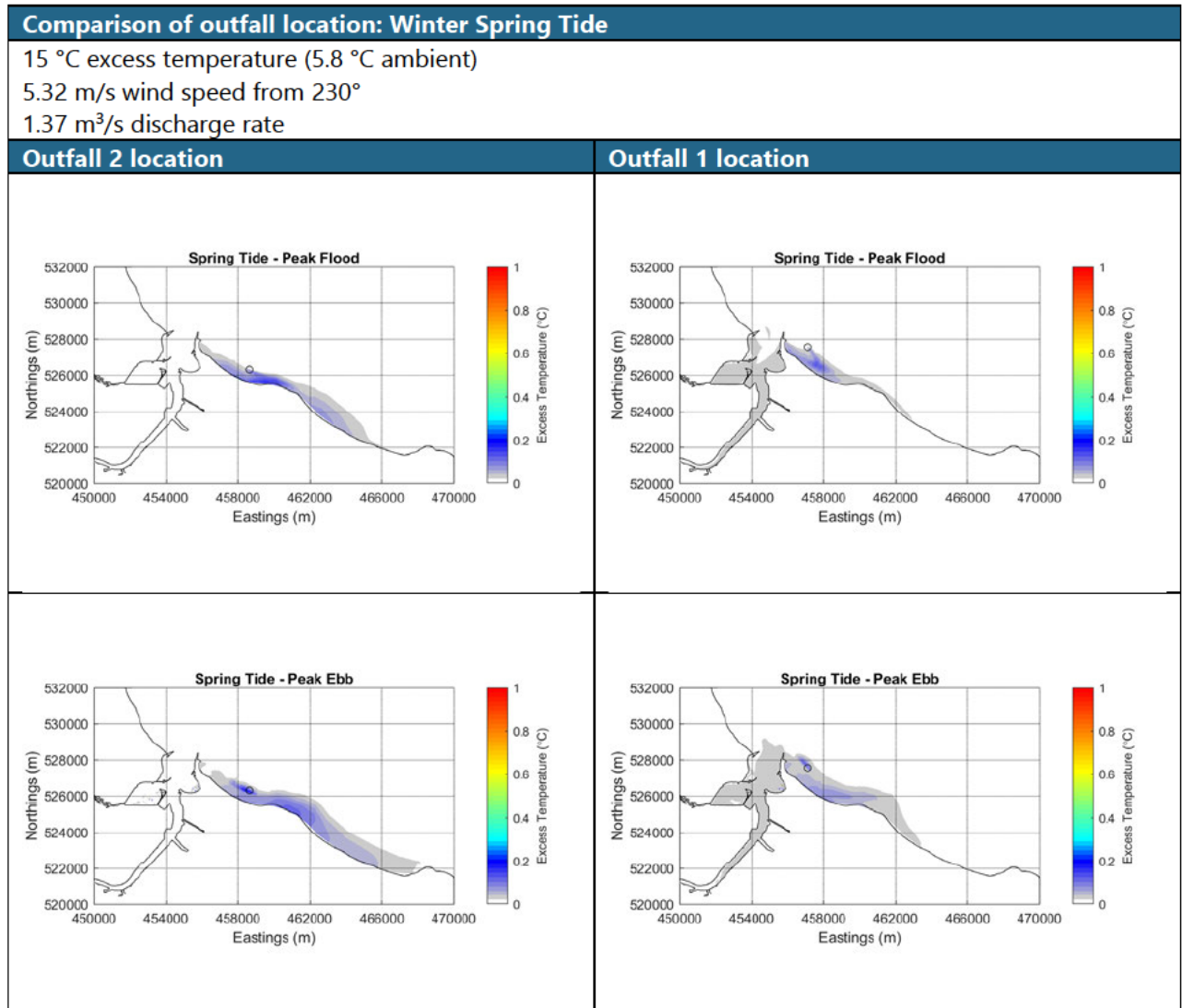


Figure 32. Temperature excess contour plots: Comparison of spring winter conditions with a discharge specified at Outfall 2 (left) vs Outfall 1 (right)

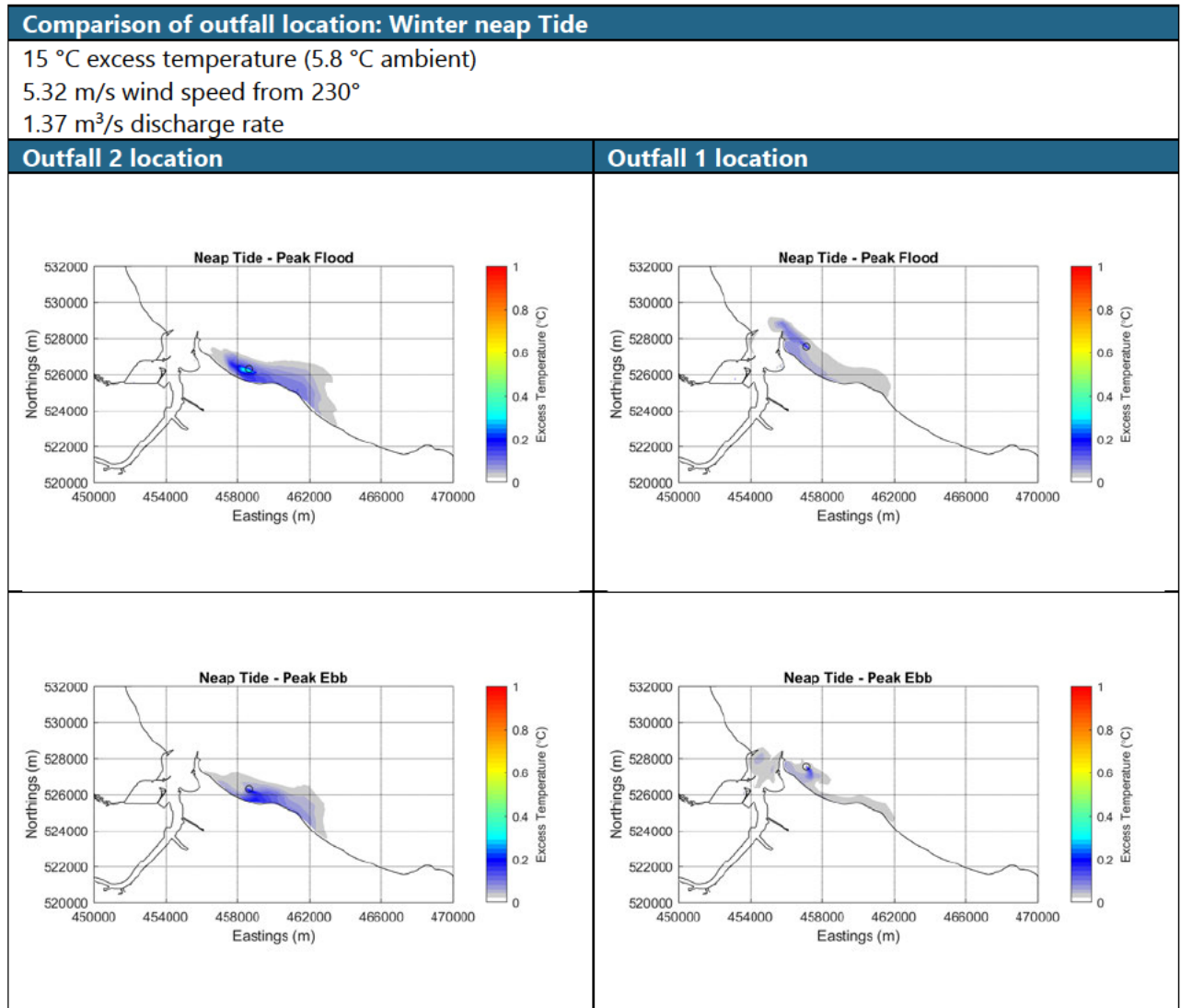


Figure 33. Temperature excess contour plots: Comparison of neap winter conditions with a discharge specified at Outfall 2 (left) vs Outfall 1 (right)

4.3.4 Run 7: Comparison of high flow scenario

The nearfield thermal plume modelling considered an extreme 1 in 30-year flow rate discharge through the pipe, with a specified rate of 5.75 m³/s. This discharge would consist of a portion of heated water combined with land run-off water at ambient temperature. Information provided by AECOM anticipates an approximate ratio of 31% warm and 69% ambient water would be discharged during this type of extreme event resulting in a combined temperature excess of approximately 5°C. Effluent salinity has also been calculated to reflect the mixture of warmed and ambient water.

This 1 in 30-year high flow event has been simulated in the Deflt3D far field model and compared over summer spring and neap conditions in this section.

Comparisons in Figure 34 and Figure 35 show that the thermal plume distribution over both the normal and extreme discharge case are largely similar. A slightly larger area of excess temperature is seen in the high flow case compared with the normal case in both the spring and neap tide conditions. A greater temperature excess is seen at the point of the plume discharge in the neap scenarios.

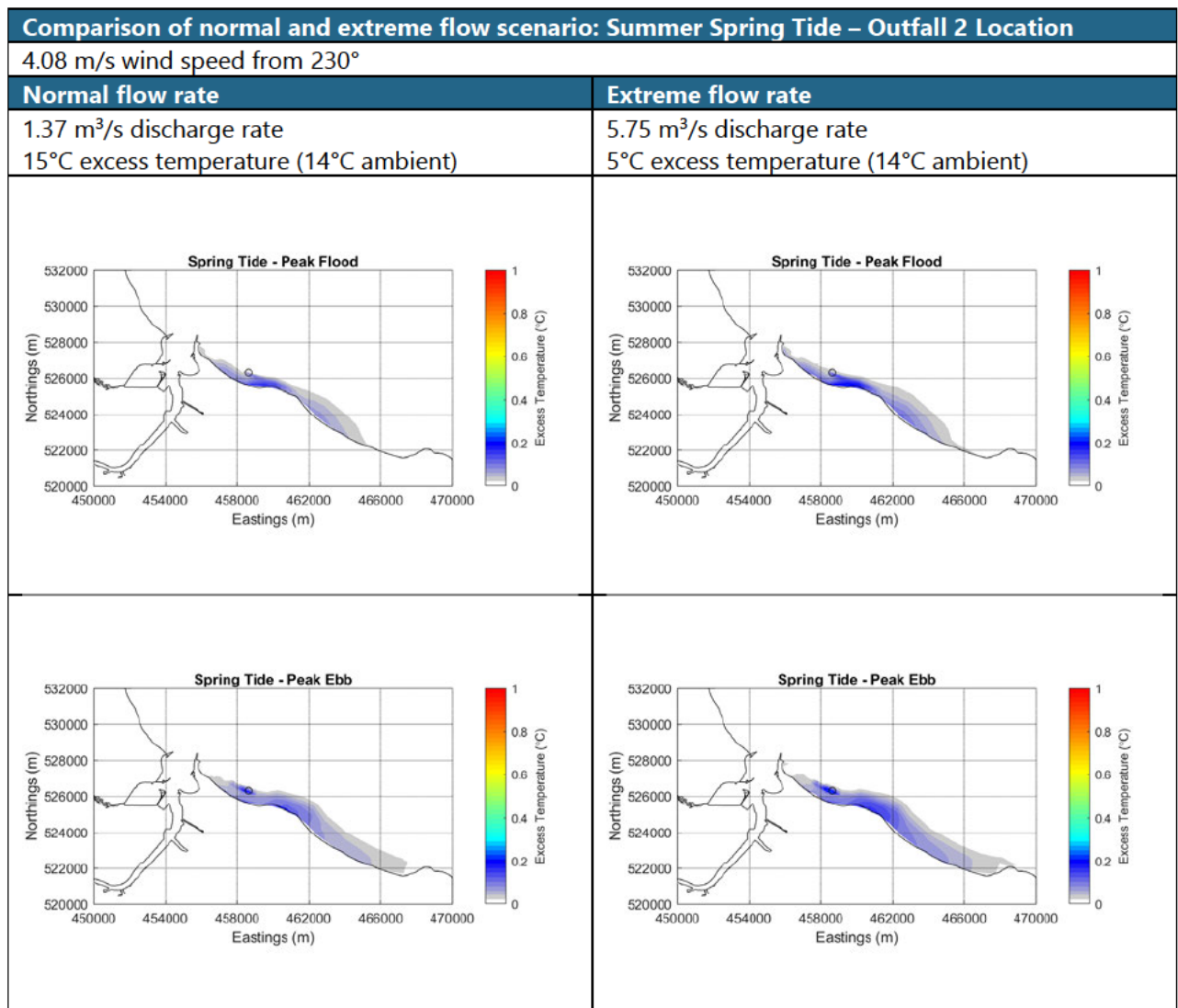


Figure 34. Temperature excess contour plots: Comparison of spring summer conditions with normal and extreme flow rates

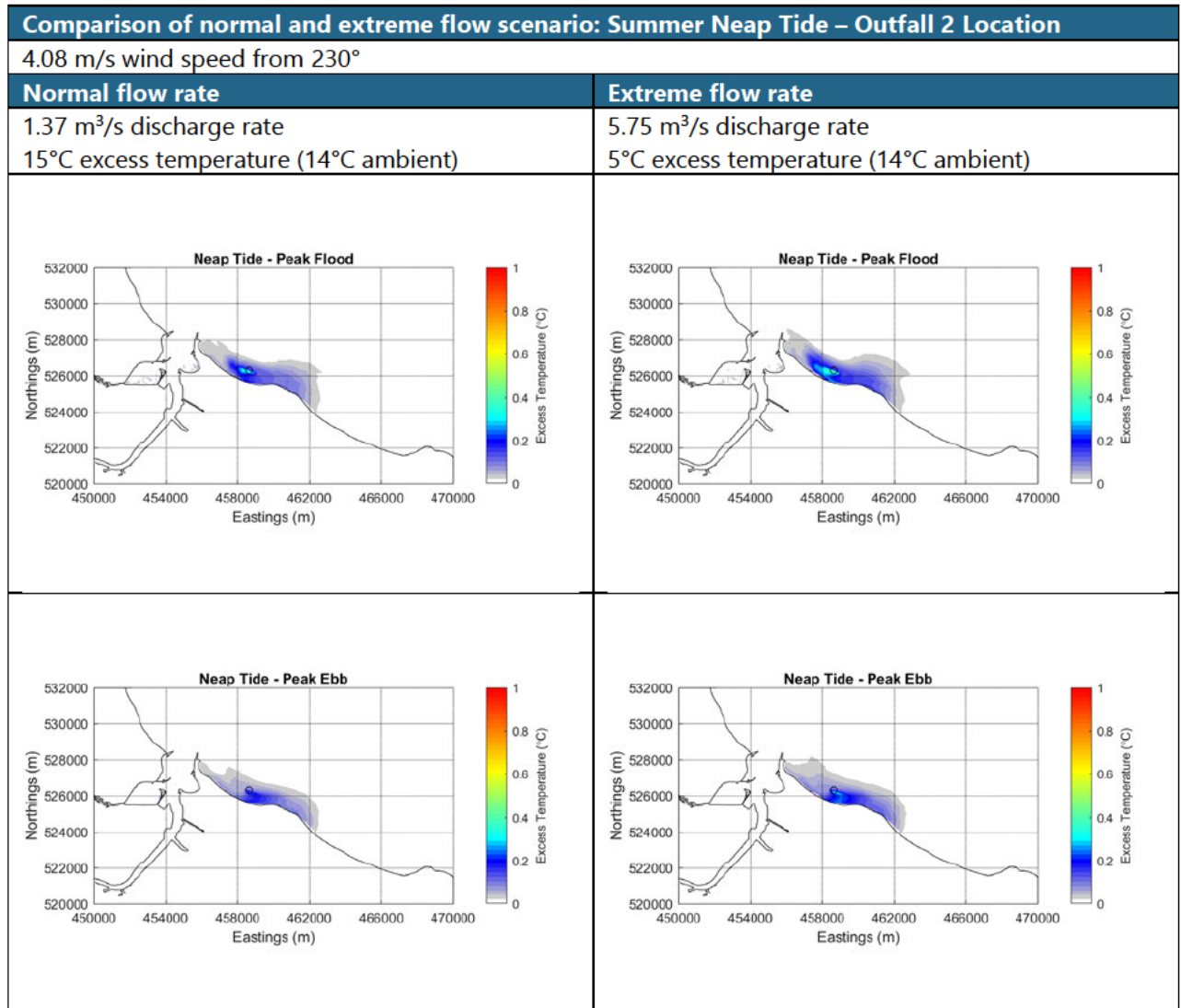


Figure 35. Temperature excess contour plots: Comparison of spring summer conditions with normal and extreme flow rates

5 Conclusion

Hydrodynamic modelling has been undertaken using the Delft3D flow modelling software to create a representative baseline condition of the Tees Estuary which produces a good comparison of flow, water level and vertical water column structure in the estuary in comparison with available measurements. Implementing the proposed cofferdam within the model run suggests that the impacts on flow speeds around the construction site will be very limited and restricted to within approximately 150 m of the structure when considering flow speed differences of >0.05 m/s. Changes in flow will be felt mostly in the faster flowing surface and mid water layers and less so nearer to the bed where flow speeds are lower. Flow directions will alter as flows are redirected around the new structure, extending further from the coastline than the original infrastructure. The proposed cofferdam structure is only temporary whilst enabling works are completed. Once finished, the cofferdam will be removed, and the orientation of the coastline will revert to the existing (baseline) condition.

Near-field thermal plume modelling has been undertaken using the CORMIX modelling software to trace the likely extent of thermal discharge at two proposed outfall locations. At Outfall 1, under spring conditions, the likely extent of a thermal plume (of the properties modelled) would be very localised: a 3°C temperature excess only extends approximately 45 m from the discharge point on the flood and 98 m on the ebb. Considering a 2°C temperature excess the ebb extent of the plume increases to 140 m, and then 235 m to the 1°C excess temperature contour, which still represents a very limited excursion from the original discharge point.

To examine the wider plume dispersion a 0.1°C temperature excess contour was exported from CORMIX. This shows that a 0.1°C temperature excess is estimated to extend around 750 m from the origin on a spring flood tide, and 720 m on an ebb. At lower speeds (e.g. near slack water), reduced mixing could allow the plume to stay buoyant for longer, however the excursion from the plume would be limited by the speeds and mixing with subsequent dispersion occurring as speeds increase through the tidal cycle. Sensitivity testing showed only a small influence on plume extent due to wind and seasonal variations, while the outfall orientation (horizontal or vertical) has a relatively larger impact on the dispersion of the plume.

At Outfall 2, as a result of lower energy conditions leading to lower/slower rates of dissipation of the outfall plume, the neap tidal phases offer a larger plume, when compared to the spring tide, under normal discharge conditions. In particular, the neap flood tide offers the largest plume extent as highlighted in Table 7 (run 19).

However, it is to be noted that the CORMIX model assumes full plume development under the given conditions and, in reality, the ambient flows (defined as constant in the model) will not persist long enough for a fully developed plume (as defined) to form. As the flows reduce, either side of the peak conditions modelled, and turn with the tidal phase, further dissipation of the plume is expected before it can fully develop to the state portrayed by the CORMIX outputs. The results of the far-field thermal modelling (using the Delft3D model) better represents the influence of the shifting tidal conditions on the discharge.

Far field plume dispersion modelling has been undertaken using the Delft3D modelling software using both the original and updated planned outfall locations for a range of environmental conditions. Temperature excess plots of the plume impact have shown a small impact of the outfall discharge on the ambient water temperature. Depth averaged temperature differences of $>0.02^{\circ}\text{C}$ are predicted up to ~ 9 km of the Outfall 2 site, however greater temperature excesses of up to 0.3° are localised to within 1.5 km of the outfall in all simulations modelled.

In order to ensure a robust assessment of the likely significance of the environmental effects of the Proposed Development, the Environmental Impact Assessment (EIA) for NZT is being undertaken adopting the principles of the 'Rochdale Envelope' approach, where appropriate. This involves assessing the maximum (or where relevant, minimum) parameters for the elements where flexibility needs to be retained (such as the building dimensions or operational modes for example).

Justification for the need to retain flexibility in certain parameters is also outlined in Chapter 4: The Proposed Development and Chapter 6: Alternatives and Design Evolution (ES Volume I (Document Ref. 6.2)). As such, the NZT ES represents a reasonable worst-case assessment of the potential impacts of the Proposed Development at its current stage of design.

In terms of coastal modelling, the reporting is highly precautionary for several specific reasons. For example, the parameters defined at the start of the modelling process were based on three CCGT trains; as the Proposed Development is now only for a single CCGT train, the modelling assumptions are highly precautionary. Furthermore, any performance benefits from the presence of a terrestrial mixing zone (i.e. surge pit / outfall retention pool) before discharge of treated effluent to the outfall have not been factored in. For this reason, no losses of heat to the atmosphere or through mixing with other water sources (i.e. surface water) were factored in (again, highly precautionary).

6 References

ABPmer. (2003). Tees Entrance Channel Study, Part II: Numerical Modelling of Deepening of Seaton Channel. ABP Marine Environmental Research Ltd, Report No. 991.

ABPmer, (2020). Net Zero Teesside Project, Coastal modelling, ABPmer Report No. R.3393, for AECOM, 2020.

GOV.UK: <https://environment.data.gov.uk/DefraDataDownload/?Mode=survey>

JBA. (2011). Tidal Tees Integrated Flood Risk Modelling Study. JBA Consulting, September 2011.

NFRA: <https://nrfa.ceh.ac.uk/data/search>

UKHO (2020) Admiralty Tide Tables, United Kingdom and Ireland, NP201B, Volume 1B. UK Hydrographic Office 2020.

Wood (2020). Gas Power – Cooling System Analysis Report 13430-01-8110-RP-3001 REV F1 DRAFT report. Selected data shared by AECOM, access to full report not provided to ABPmer.

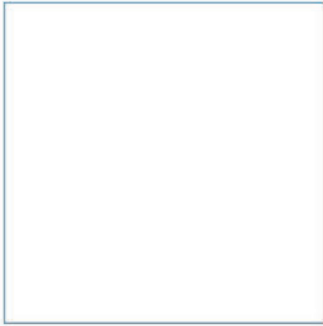
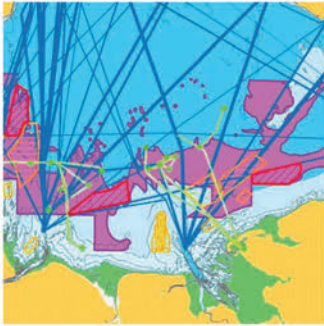
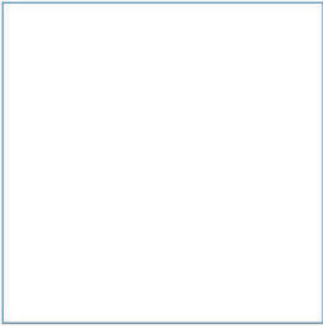
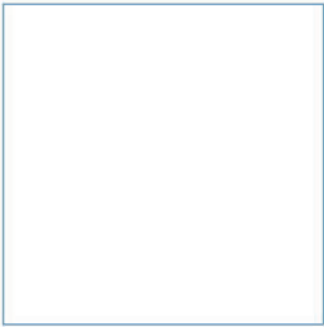
7 Acronyms/Abbreviations

2D	Two Dimension(al)
3D	Three Dimension(al)
ADCP	Acoustic Doppler Current Profiler
AECOM	AECOM Ltd
CCGT	Combined Cycle Gas Turbines
CCUS	Carbon Capture, Utilisation and Storage
CD	Chart Datum
CFSR	Climate Forecast System Reanalysis
CTD	Conductivity-Temperature-Depth
CurDir	Current Direction
CurSpd	Current Speed
dd	Domain Decomposition
DHI	Danish Hydraulic Institute
Dir	Direction
EIA	Environmental Impact Assessment
ES	Environmental Statement
HD	Hydrodynamic
HW	High Water
ITT	Invitation to Tender
JBA	JBA Consulting
LAT	Lowest Astronomical Tide
LiDAR	Light Detection and Ranging
MMO	Marine Management Organisation
NFRA	National River Flow Archive
NRFA	National River Flow Archive
NZT	Net Zero Teesside
ODN	Ordnance Datum Newlyn
OSGB	Ordnance Survey Great Britain
Q	Quartile
RORO	Roll-on/Roll-Off
THPA	Tees and Hartlepool Port Authority
UK	United Kingdom
UKHO	United Kingdom Hydrographic Office
WL	Water Levels
WS	Wind Speed

Cardinal points/directions are used unless otherwise stated.

SI units are used unless otherwise stated.

Appendices



Innovative Thinking - Sustainable Solutions

A Delft Model Setup

For the present study a three-dimensional hydrodynamic model has been run using the Delft3D software package developed by Deltares. The version of the software used for this study is version 4.03.01. The software is designed for complex applications within oceanographic, coastal and estuarine environments. The Delft3D-FLOW module has been used to simulate the tidal water variation and flows in the area of interest.

ABPmer holds an existing Delft3D model of the Tees Estuary, calibrated and validated against various datasets within the area (ABPmer 2003). This existing model forms the basis for the current study: The original model has been refined across the region of interest and updated with recent bathymetric data with high resolution coverage across key areas. The model performance has been cross checked against previous simulations and the calibration re-assessed against measured data available for this study. The setup of the Delft3D model is detailed in this section; the performance of the model is then demonstrated in Appendix B of this report.

A.1 Model grid

The Delft3D model uses a curvilinear computational grid, which allows a grid composed of various sizes to be used throughout a model domain. In addition to this, the original hydrodynamic model has been further refined using a 'domain decomposition' (dd) approach. This approach allows the creation of higher resolution grids which can be nested within the wider area domain, and dynamically coupled using defined dd boundaries. Two domains have been created in the Tees Estuary hydrodynamic model.

These are shown in Figure 36, with the outer grid shown in blue, and the nested (finer resolution) inner grid in black. A refinement factor of 1:3 was applied in the nested grid, in line with Deltares guidance, illustrated in Figure 37.

Beyond the Tees barrage the river section of the HD model does not align with the Tees River Channel. This part of the model was altered during the calibration phase of the previous modelling work (ABPmer 2003) to accurately represent the correct water volumes up to the tidal limit of the estuary when simulating pre-barrage conditions in the Tees. For the present study the barrage is included in all simulations as a barrier which does not allow the movement of saline water upstream, and the flow across the barrage is represented as a time varying discharge (details of these are provided in Section A.3.2). The upstream part of the Delft3D model is therefore effectively excluded from the hydrodynamic computations beyond the Tees Barrage.

Table 12. Model grid resolution

Area	Average Dimensions (m)
Offshore boundary	1,000 x 1,000
Outfall location	160 x 80
Central Estuary	30 x 30
Upper Tees	12 x 150

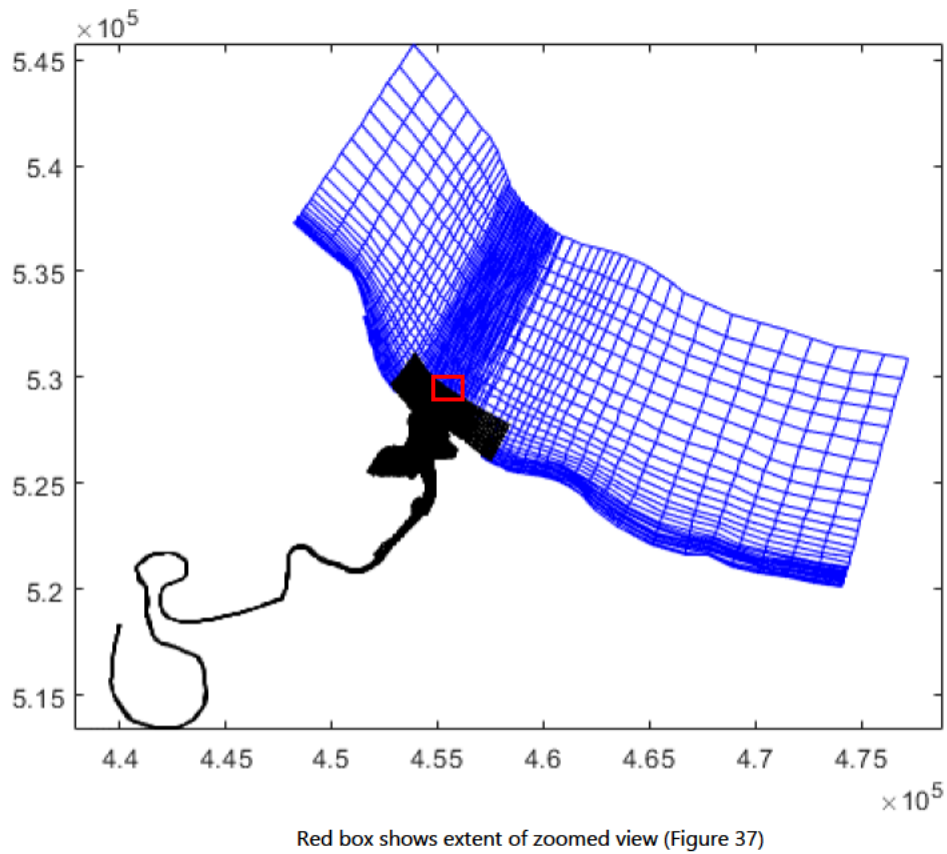


Figure 36. Delft3D hydrodynamic model grid

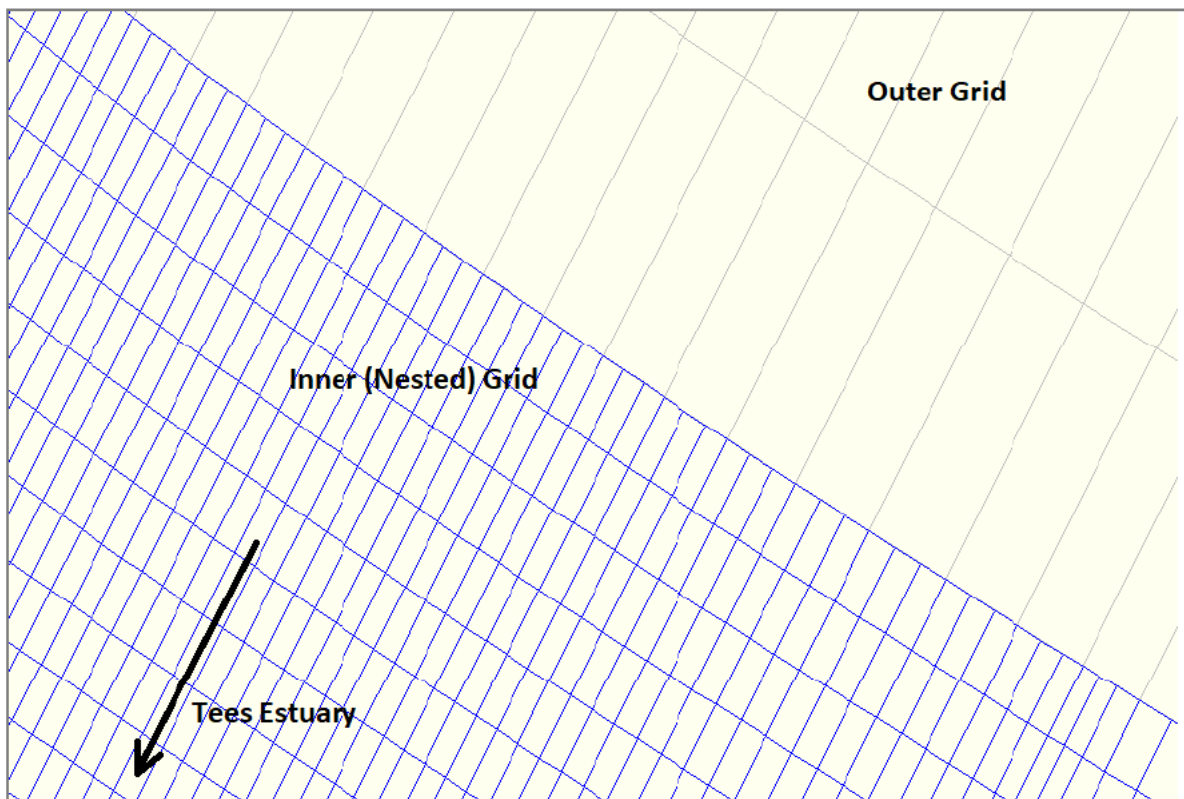


Figure 37. Delft3D hydrodynamic model grid – Refinement of nested grid

A.1.1 Vertical structure

The hydrodynamic model is three-dimensional (3D) with eight layers through the vertical representing 2, 3, 5, 7, 10, 15, 23 and 35% of the water column, respectively, from surface to bed. This configuration gives enhanced focus in the upper part of the water column, making the model suitable for any ongoing thermal plume or contamination modelling.

A.2 Bathymetry

The bathymetric data for the model grid construction has been compiled from the following sources:

PD Teesport Redcar Bulk Terminal Survey Data: Provided by AECOM as a digital .pdf drawing. This provides surveyed depths around the Redcar Bulk Terminal from soundings taken on 29/01/2020. Depths are provided to LAT.

PD Teesport Survey Data: xyz bathymetry data were provided by AECOM from PD Teesport surveys dating from 2019. Depth information has been provided relative to chart datum. These data cover the main channel to approximately 3.5 km beyond the estuary mouth and upstream to 2 km beyond the Tees Dock Tide Gauge.

LiDAR Contours: LiDAR data have been downloaded from the Defra survey download portal¹, to provide coverage of the intertidal areas within the Tees Estuary and outer coastline. Data have been downloaded from the available composite catalogue of the Tees area which means that sampling dates from the data may not be coincident across the spatial extent. However, the data is considered adequate for the purpose of model construction to achieve the correct volumes of water movement across the intertidal zones. The data have been cleaned to remove the water surface from the measurements and the data imported in 0.5 m depth contours up to the +3 m ODN level.

CMap: AECOM have provided bathymetry data for Tees Mouth and Tees Bay from the CMap database. Data were provided relative to chart datum and ODN. CMap is an electronic chart database managed by the Danish Hydraulic Institute (DHI) as part of their Mike software modelling provision. Spatial coverage provided by this database is adequate in the offshore region of the model but sparse within the estuary relative to the spatial resolution of the model grid.

Admiralty Charts: Admiralty charts of the Tees Estuary² have been used to inform the water depth in areas where alternative data were sparse. Chart depths were manually digitised for the areas of interest which included the Philips Inset Dock and dredged areas of the Tees river channel.

River Data: Beyond the region of the Teesport survey the depths in the Tees river have been extracted from previous ABPmer models of the Tees (ABPmer 2003). These originated from Tees and Hartlepool Port Authority surveys and Admiralty chart depths.

¹ <https://environment.data.gov.uk/DefraDataDownload/?Mode=survey>

² Admiralty Chart 2566 Tees and Hartlepool Bays

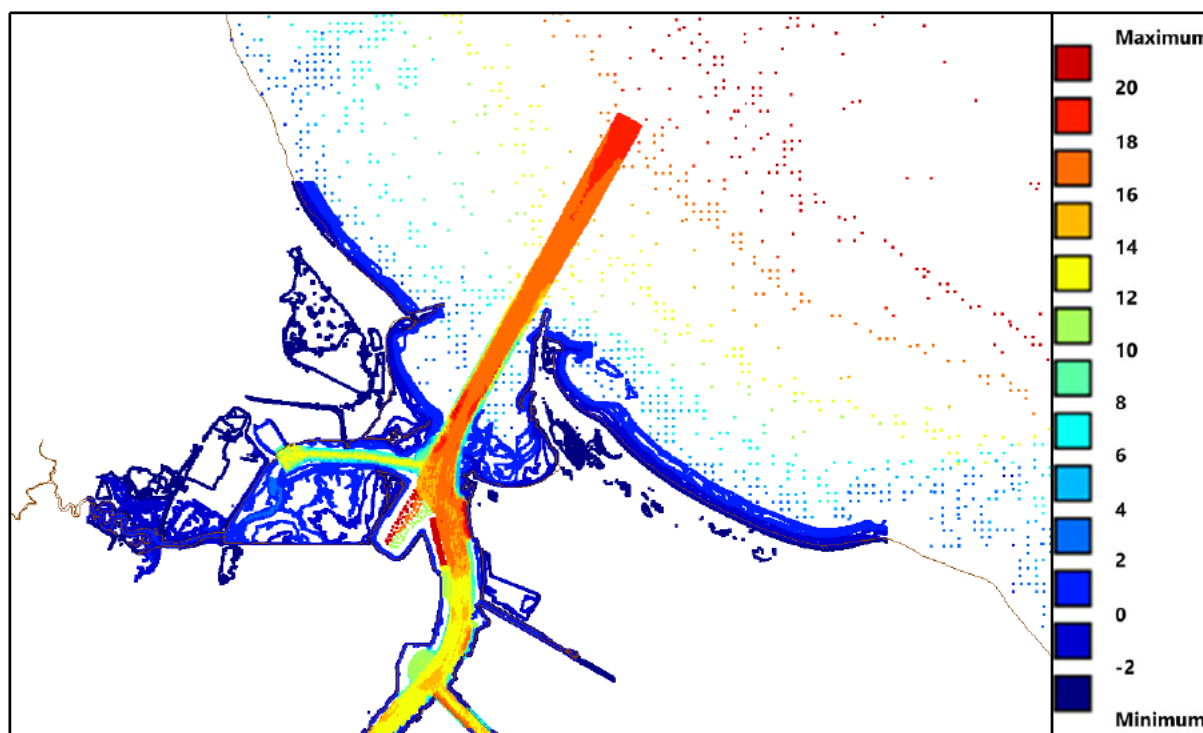


Figure 38. Scatter plot showing available bathymetry data resolution and coverage. All values are depth positive and referenced to meters below ODN.

A.2.1 Bathymetry data processing

All bathymetry datasets were converted to Ordnance Datum Newlyn (ODN) using the values stated on the Admiralty Tide Tables for the Tees: $ODN = CD + 2.85 \text{ m}$. This relationship is consistent with the CMap conversions already supplied by AECOM.

Where bathymetry data from different sources overlapped, these datasets were cropped to consider only a single dataset for any spatial area and allow smooth interpolation of bathymetry through the model: prioritising the best quality datasets. In order of priority these were:

- PD Teesport Survey;
- LiDAR Contours;
- CMap;
- Admiralty Chart; and
- Previous model depths in the upper section for rivers.

The bathymetry interpolation across the model grid was visually assessed to ensure contours appeared smooth and consistent, particularly across the interface between the nested grids and in key areas of interest.

A.3 Model Setup

A.3.1 Offshore tidal boundaries

The hydrodynamic model is defined by three offshore boundaries driven by tidal harmonics, shown in Figure 39.

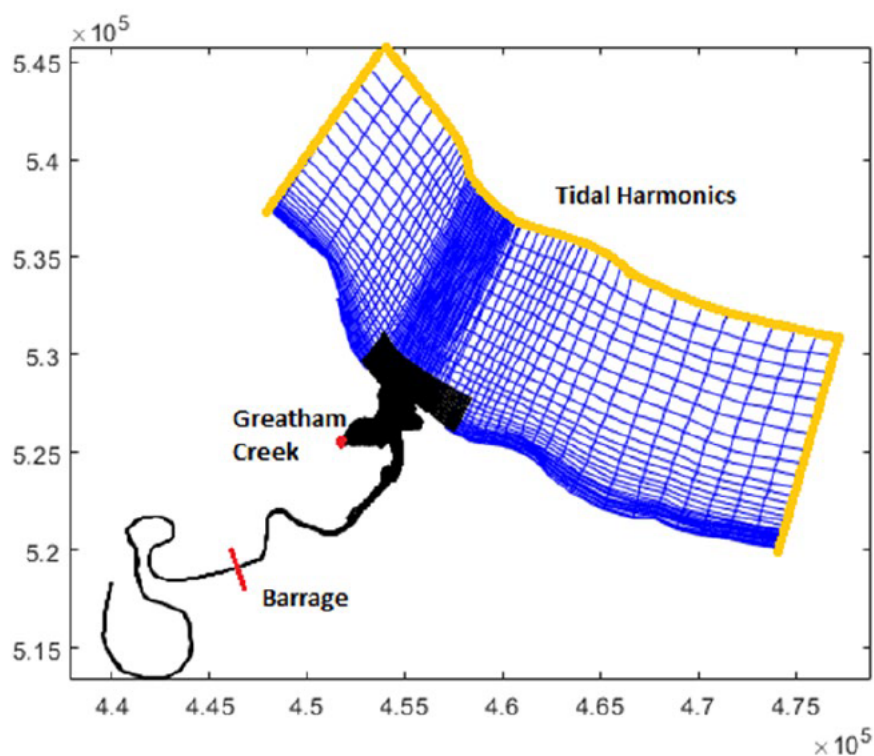


Figure 39. HD model domain and boundary positions (shown by yellow lines)

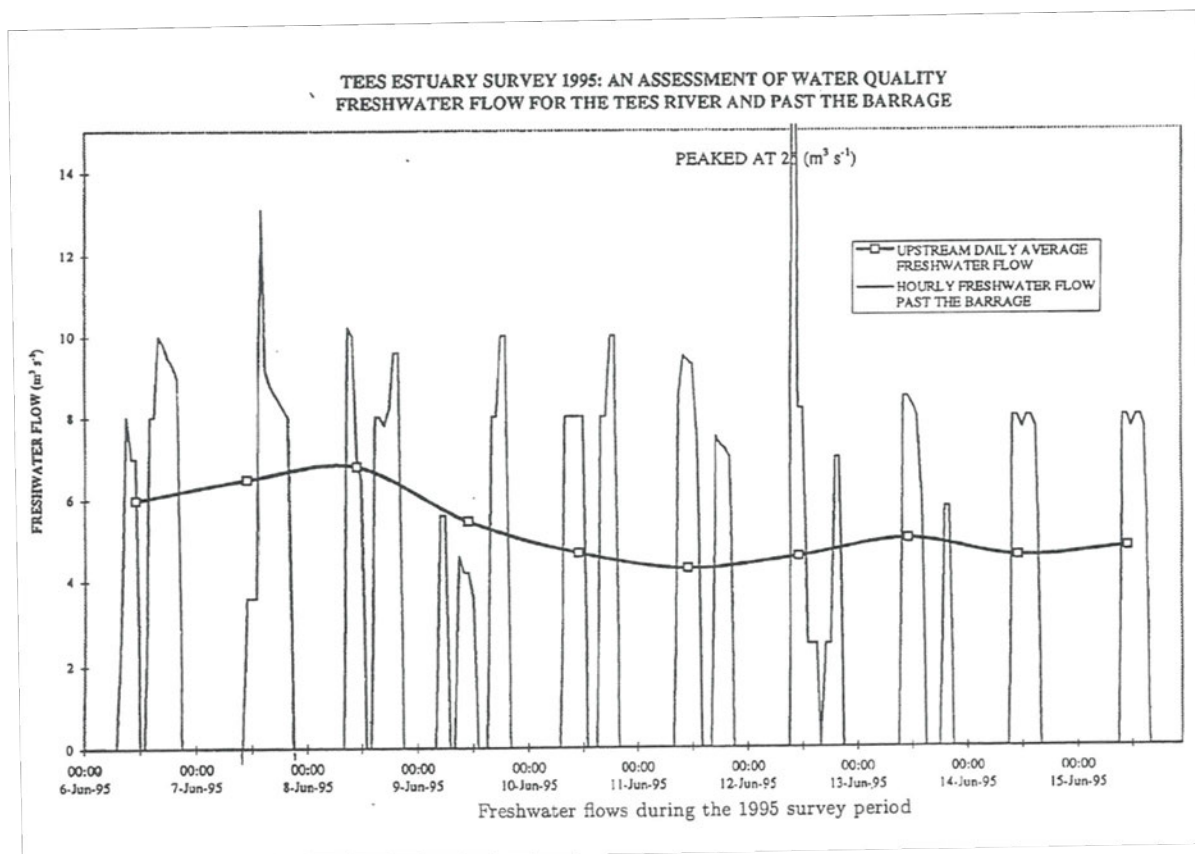
The harmonic constituents defined at these boundaries have been extracted from a wider area model (ABPmer 2003) previously constructed by ABPmer which has previously been calibrated and verified against three data sets. This data has been derived from TIDECALC (a programme for generating tidal predictions for and time period), Admiralty charts and THPA fixed current meter observations. The tidal constituents included in each boundary are given in Table 13. The amplitude and phase of each constituent is defined along the model boundaries. Each boundary is described using more than one set of tidal harmonics to allow any gradient in surface elevation along the boundary to be replicated.

Table 13. Tidal constituents in the numerical model

Harmonic	Brief Description
A0	Initial constituent
M2	Main lunar semidiurnal constituent
S2	Main solar semi-diurnal constituent
N2	Lunar constituent due to monthly variation in the Moons distance
K2	Solar-lunar constituent due to changes in declination of the sun and the moon throughout their orbital cycle
O1	Main lunar diurnal constituent
K1	Solar-lunar constituent
L2	Elliptical lunar semi-diurnal constituent
Q1	Elliptical lunar diurnal constituent
P1	Main solar diurnal constituent
EPSILON2	Lunar semi-diurnal constituent
NU2	Lunar semi-diurnal constituent
LABDA2	Evectional semi-diurnal constituent
M4	Shallow water component
MS4	Shallow water component

A.3.2 Inclusion of the Tees Barrage

At the upstream boundary of the model the Tees barrage is included in the model as a 'thin dam' structure, which acts as a barrier to saline water to extend upstream of this point. In addition, a freshwater discharge was added at the section of the barrage. The setup of the discharge takes into consideration that the barrage acts as a barrier to the upstream movement of the tide. The freshwater release from the barrage is not continuous. Survey data available from previous studies indicates that the release of water typically occurs at mid-day, regardless of tidal state (Figure 40). Whilst the survey data is for a period of time in 1995, it is not expected that this will have changed considerably over the years and is therefore suitable for this type of assessment.



Extracted from: ABPmer 2003

Figure 40. Tees Estuary survey, 1995: Freshwater flow past the barrage

Freshwater discharges from the barrage have been calculated from flow data available from the National River Flow Archive (NRFA)³. Data from gauging stations at Leven Bridge and Low Moor have been assessed to derive the annual mean flow for the combined stations as well as the 5% and 95% exceedance values which have been extracted to represent the winter and summer conditions, respectively. These have been chosen to provide the highest and lowest discharges of the year. Data from the measurement stations (Figure 41) are presented in Table 14, and the derived mean, summer and winter flows across the barrage in Table 15. The discharge from the barrage is defined in the model as a time varying input of fresh water, peaking at each mid-day in the simulation at the values calculated in Table 15.

³ <https://nrfa.ceh.ac.uk/data/search>

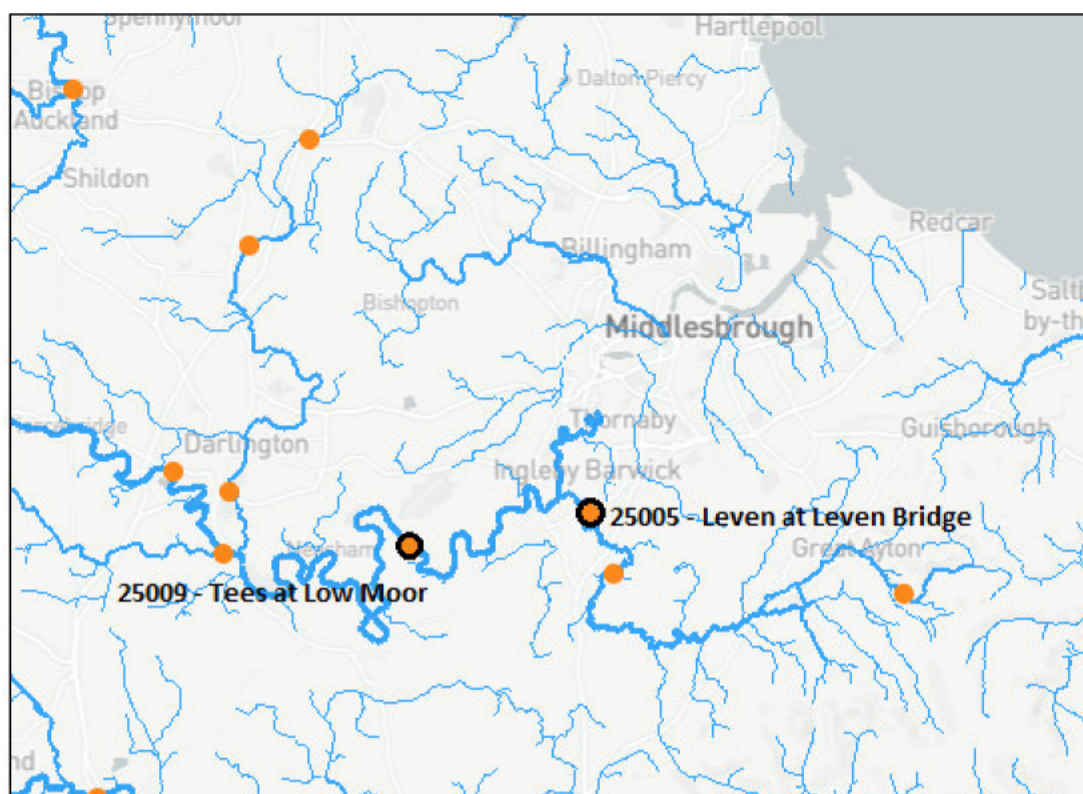


Figure 41. Flow data stations assessed for Tees Barrage discharge calculations

Table 14. Flow data from the Leven and Tees

	25005 - Leven at Leven Bridge	25009 - Tees at Low Moor
Period of Record:	1959 - 2008	1969 - 2018
Percent Complete:	>99 %	0.98
Base Flow Index:	0.42	0.39
Mean Flow:	1.892 m³/s	20.528 m³/s
95% Exceedance (Q95):	0.249 m³/s	3.07 m³/s
70% Exceedance (Q70):	0.517 m ³ /s	6.15 m ³ /s
50% Exceedance (Q50):	0.873 m ³ /s	10.9 m ³ /s
10% Exceedance (Q10):	4.248 m ³ /s	46.5 m ³ /s
5% Exceedance (Q5):	6.78 m³/s	67.7 m³/s

Source: National River Flow Archive, March 2020

Table 15. Peak discharge rates at the barrage for flow modelling

Parameter	Flow rate (m ³ /s)
Mean Flow	22
Summer	3
Winter	74

A.3.3 Greatham Creek

A discharge has been defined in the model where freshwater enters the estuary at Greatham Creek. No local flow data has been forthcoming in the project, discharges have therefore been based on values adopted by JBA Consulting in previous modelling work (JBA, 2011) and set at a constant 1.8 m³/s freshwater input for all modelled scenarios.

A.3.4 Salinity

Salinity was included in the hydrodynamic model because the Tees has both a vertical and lateral salinity distribution.

Salinity values have been defined at all existing boundaries and discharge locations: The seaward boundary salinities were set to 35 ppt whilst at Greatham Creek and the Tees Barrage the discharges were defined as completely fresh (0 ppt).

An initial salinity value of 33.9 ppt was defined across the whole model domain based on values provided by AECOM from the Wood Draft Report (Wood, 2020) for seawater properties.

A.3.5 Wind speed

Wind speed data have been provided by AECOM to ABPmer from the location of the Durham Tees Valley airport anemometer. Data are available between 01/01/2015 and 31/12/2019 at hourly intervals, providing wind speed and direction.

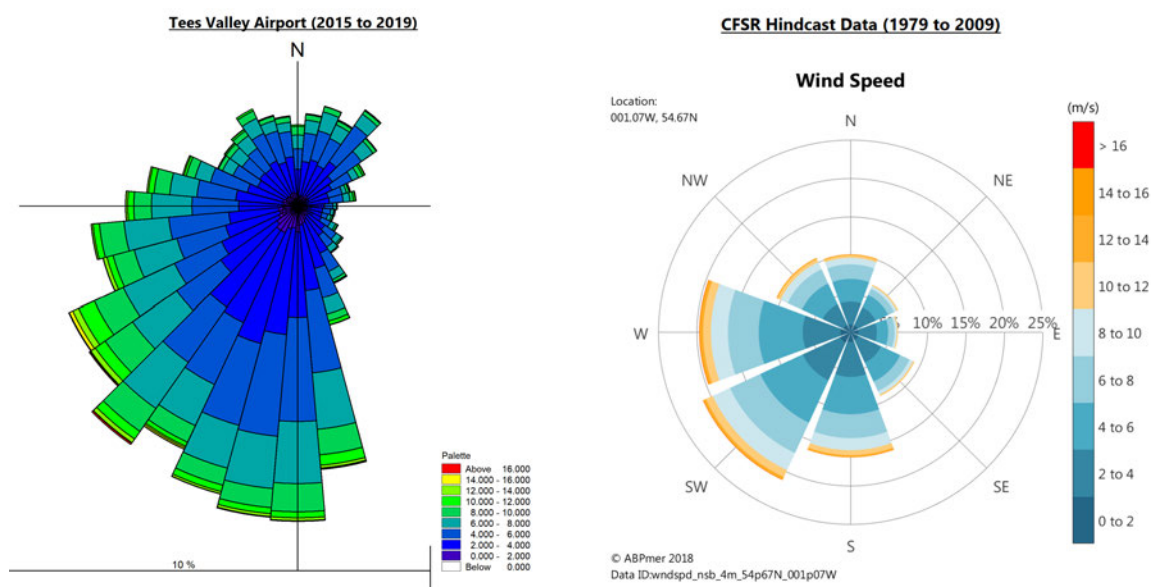


Figure 42. Wind rose of Tees Valley Airport wind data (left) and CFSR Hindcast data (right).

The wind speed and direction data have been analysed to calculate the monthly average wind speeds and direction across the five-year record (Table 16).

From these averages, the highest and lowest average speeds were taken as the winter and summer peak values and the annual average used for the mean condition runs. The direction was sufficiently consistent that a value of 230°N was selected for all model runs. This was checked against the wind rose created from the data, along with data from CFSR Hindcast data obtained from ABPmer’s database.

The measurement height of the records is 10 m above ground level and therefore require no further adjustment before being applied in the model.

The wind field was applied as a constant speed and direction across the model domain throughout each model simulation

Table 16. Monthly average wind speeds (m/s) from Durham Tees Valley Airport

	Jan	Feb	Mar	Apr	May	Jun	Jul	Aug	Sep	Oct	Nov	Dec	Annual
Average WS	5.14	5.16	5.32	4.50	4.55	4.42	4.08	4.64	4.35	4.47	4.91	5.05	4.72
Average Dir	228	217	236	262	271	253	234	218	221	230	231	210	227

A.3.6 Bed roughness

The sediment type in the Tees Estuary varies between silt and gravel in the upper estuary, to sands at the estuary mouth. The majority of material moving at the bed is sand sized (ABPmer, 2003), and the bed roughness in the Delft3D HD model has, therefore, been set to a constant value throughout the model. The roughness formulation has been changed from Chezy to Manning (n) as the latter is designed for use in an environment where depths are shallow. A constant value of 0.025 ($m^{-1/3}s$) has been defined in both the U and V direction.

A.4 Model run period

The Delft3D hydrodynamic model was run for three simulation periods, described in the following paragraphs. The model takes approximately 24 hours of simulated time to 'warm up': where the flows and water levels stabilise to allow the hydrodynamic processes in the estuary to be simulated in a realistic way.

Calibration period: 20/04/2005 to 01/05/2005: The model was run for a 12-day period, including one day of warm up time, to coincide with the ADCP and CTD data available from PD Teesport (see Appendix B). The model duration is centred on a spring tide, with a maximum tidal range of 4.80 m (mid estuary). This is slightly larger than the mean spring range of 4.6 m for the River Tees Entrance reported in the Admiralty tide tables (UKHO, 2020).

Validation period: 13/10/2001 to 27/10/2001: This model period was selected to duplicate the run period of the previous hydrodynamic model (ABPmer 2003). This 14-day run period includes a period of mean spring and mean neap range. The tidal range also reaches a 5.5 m at the peak of the spring tide. Repeating this model run time also allows flow speed and direction comparisons to be made against the previous project model runs and measured data available from the previous project.

2019 Seasonal Runs: 23/06/2019 to 08/07/2019: Following calibration and validation the model was simulated for a period in 2019 to generate outputs for summer, winter and average conditions, described in the model setup paragraphs in A.3. These model runs were used to extract flow conditions for the CORMIX thermal plume modelling (Section 2) The model was run for a 14-day simulation period, which was selected to ensure that mean spring and mean neap tidal conditions were captured within the model run time.

B Delft3D Model Calibration

A calibration and validation exercise are required to provide a measure of confidence in the numerical model performance. Model data from the three run periods (Section A.4) were used to undertake calibration and validation of the model, selected to coincide with the available calibration datasets, details of which are provided in the following sections.

B.1 Flow model calibration

B.1.1 Water levels

Measured water level data are available from two tide gauges in the Tees Estuary; Tees Dock and Riverside RORO, detailed in Table 17. All water level measurements were transformed to mODN using the 2.85 m adjustment sourced from the Admiralty tide tables for the Tees.

Table 17. Tide gauge data summary

Name	Dates	Location (OSGB)	Description
Riverside RORO	20/11/2018 to 21/01/2020	454922 524424	Water level measurements relative to Chart Datum
Tees Dock	08/06/2009 to 14/08/2019	454311 523508	Water Level measurements relative to Ordnance Datum

Time series data of water levels were extracted from the numerical models for the nearest appropriate model grid cell to the measured locations (shown in Figure 43).

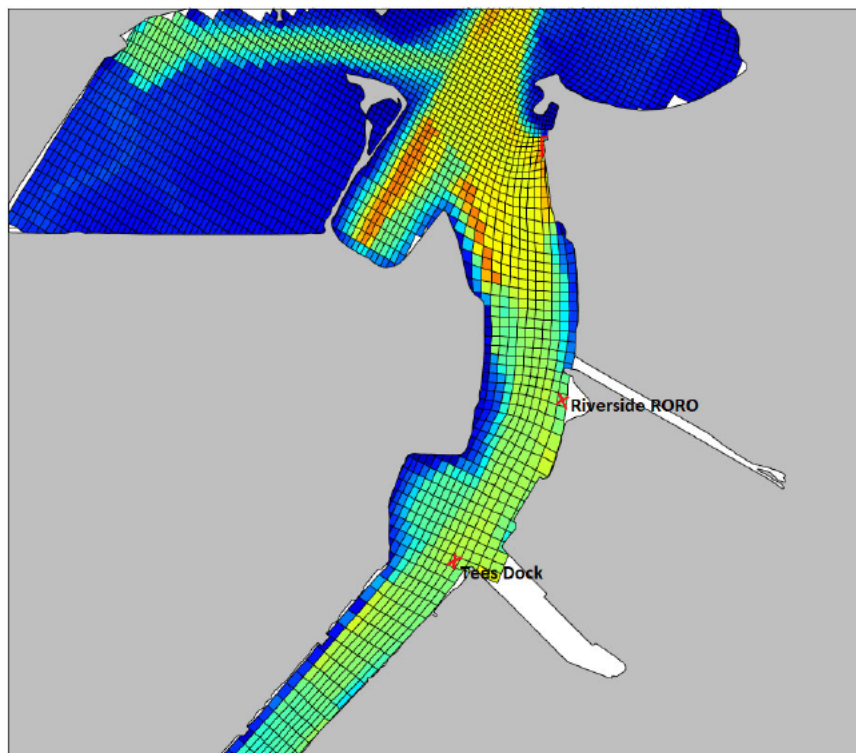


Figure 43. Location of model extraction points for tide gauge calibration overlaid onto model grid and underlying bathymetry.

Time series comparisons of the measured and modelled datasets are shown in Figure 44 and Figure 45.

It can be seen that there is good agreement in the phasing and amplitude between the two datasets at both locations. It is worth noting that the measured gauge data will also include any residual water variations driven by meteorological forcing at the time of measurements, while the modelled data represent only the tidal component of water level.

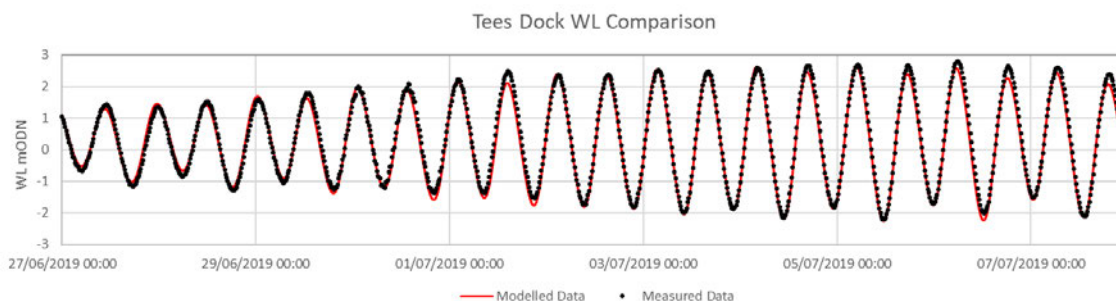


Figure 44. Water level comparison: Model vs measured data (Tees Dock)

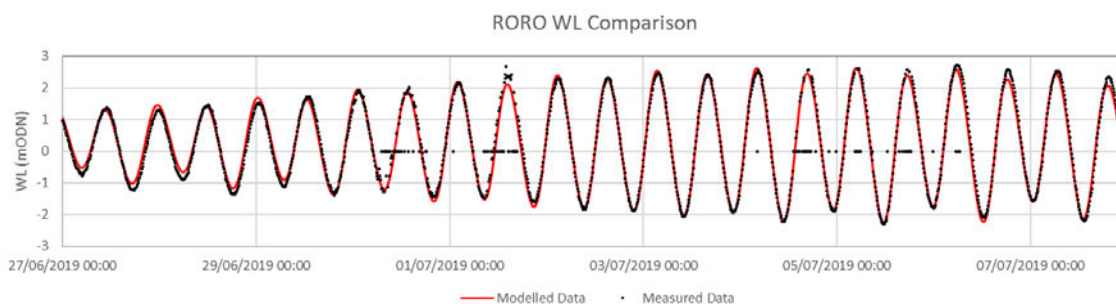


Figure 45. Water level comparison: Model vs measured data (Riverside RORO)

B.1.2 Flow speeds and direction

ADCP flow data 2005

ADCP survey data has been provided by AECOM from PD Teesport. These consist of field data and plots from a measurement campaign undertaken between 21/04/2005 and 30/04/2005. Flow data have been measured across 11 transects between the entrance to Philips Inset Dock and the bend in the Tees at Middlesbrough. For the purposes of model assessment, visual comparisons have been made between the transect plots provided by AECOM in the data files, and flow cross section data extracted from the model presented in a similar way for comparison. These comparisons are shown in Figure 46 to Figure 75. The following points should be considered when viewing these comparisons:

- Colour maps of speed and direction in the modelled outputs have been matched, visually, as closely as possible to the PD Teesport plots, however some small variation may exist between the two.
- The horizontal axis of the modelled transects represent model grid cells. These are plotted as being of equal width across the channel. This is a reasonable approximation across the transects considered – however it does mean that the X axis of the plots are not directly comparable and transect start and end points may not exactly align with the model cells.

- The vertical structure in the model is split into 8 layers, each representing a fixed percentage of the water column (see Section A.1.1). The absolute depth of each of these layers will vary with position in the estuary (depending on water depth) as well as through time as the water level rises and falls. The model data layers have been plotted to visualise this variation.
- Modelled flow data across the transects are exported from the model at hourly intervals. When comparing against available measurements the nearest hourly record has been identified and plotted. The tidal state relative to high water has also been checked against the notes in the ADCP data files.
- Flow data comparisons have been presented for two transects at different stages of the tide to provide a selection of visual assessments within this report.

Throughout the comparison of flow speeds and direction in Figure 46 to Figure 75, there appears to be good visual agreement between the measured ADCP transects and the modelled outputs. The variation in surface flows and the main water column at various stages of the tide appears to be well simulated in the model and in agreement with the measured data. Variations in flow direction with depth also appear to correlate between the measurements and modelled data which lends confidence in the model's ability to simulate the flow through the vertical water structure.

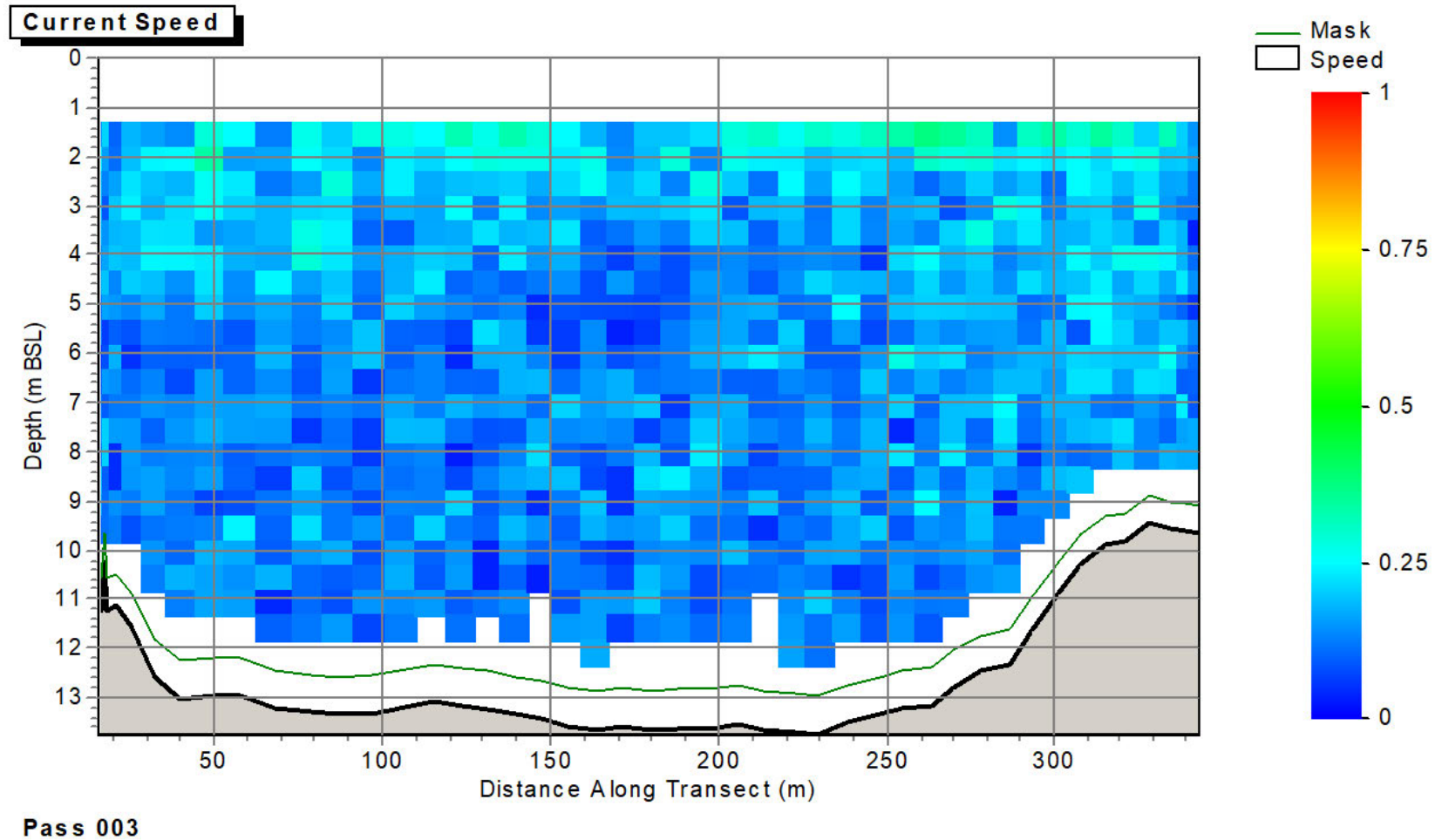


Figure provided by PD Teesport

Figure 46. Measured flow speeds, Transect 1, Pass 3: Ebb tide, cross section of speed with depth shown from west (left) to east (right)

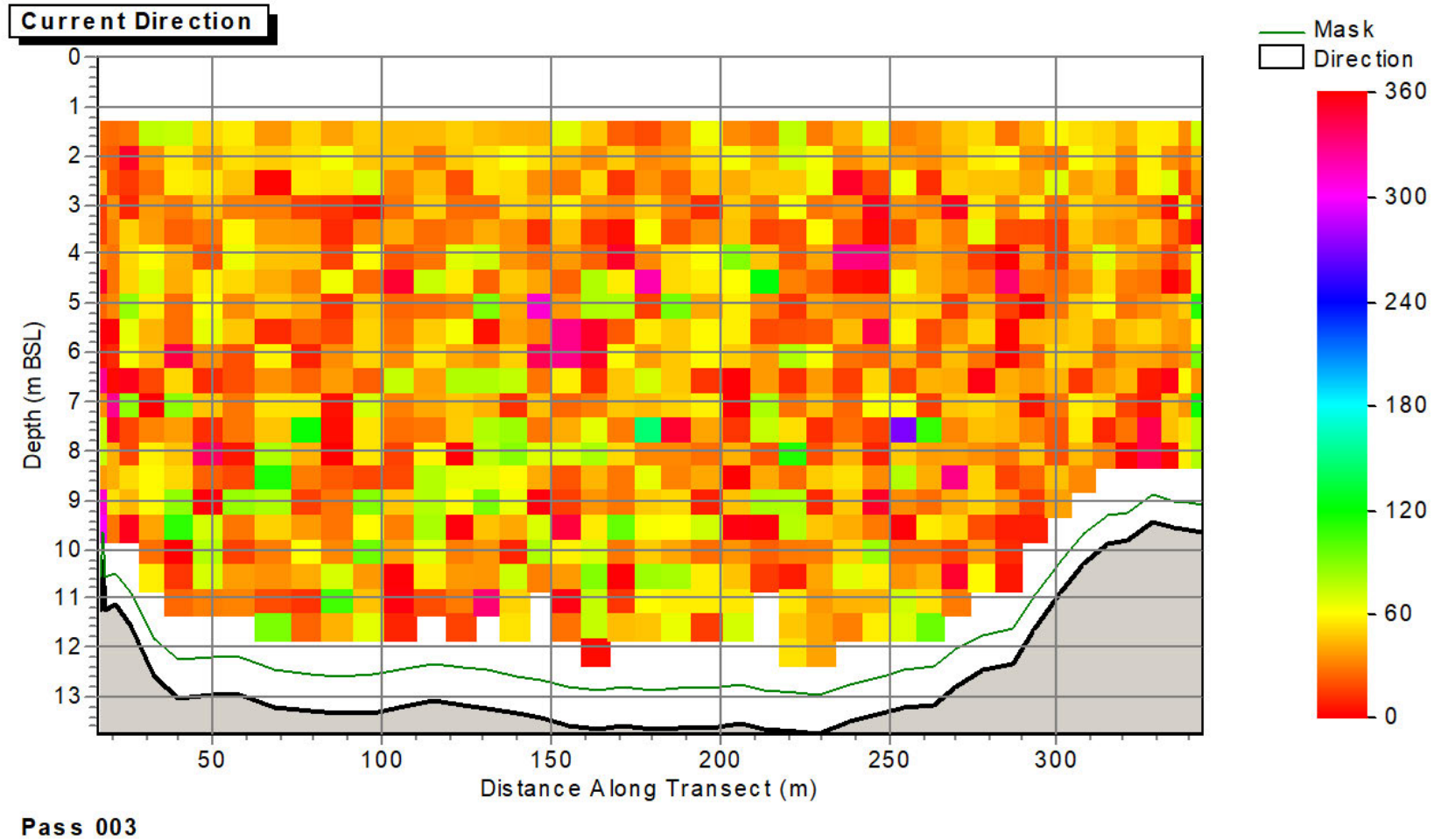


Figure provided by PD Teesport

Figure 47. Measured flow direction, Transect 1, Pass 3: Ebb tide, cross section of speed with depth shown from west (left) to east (right)

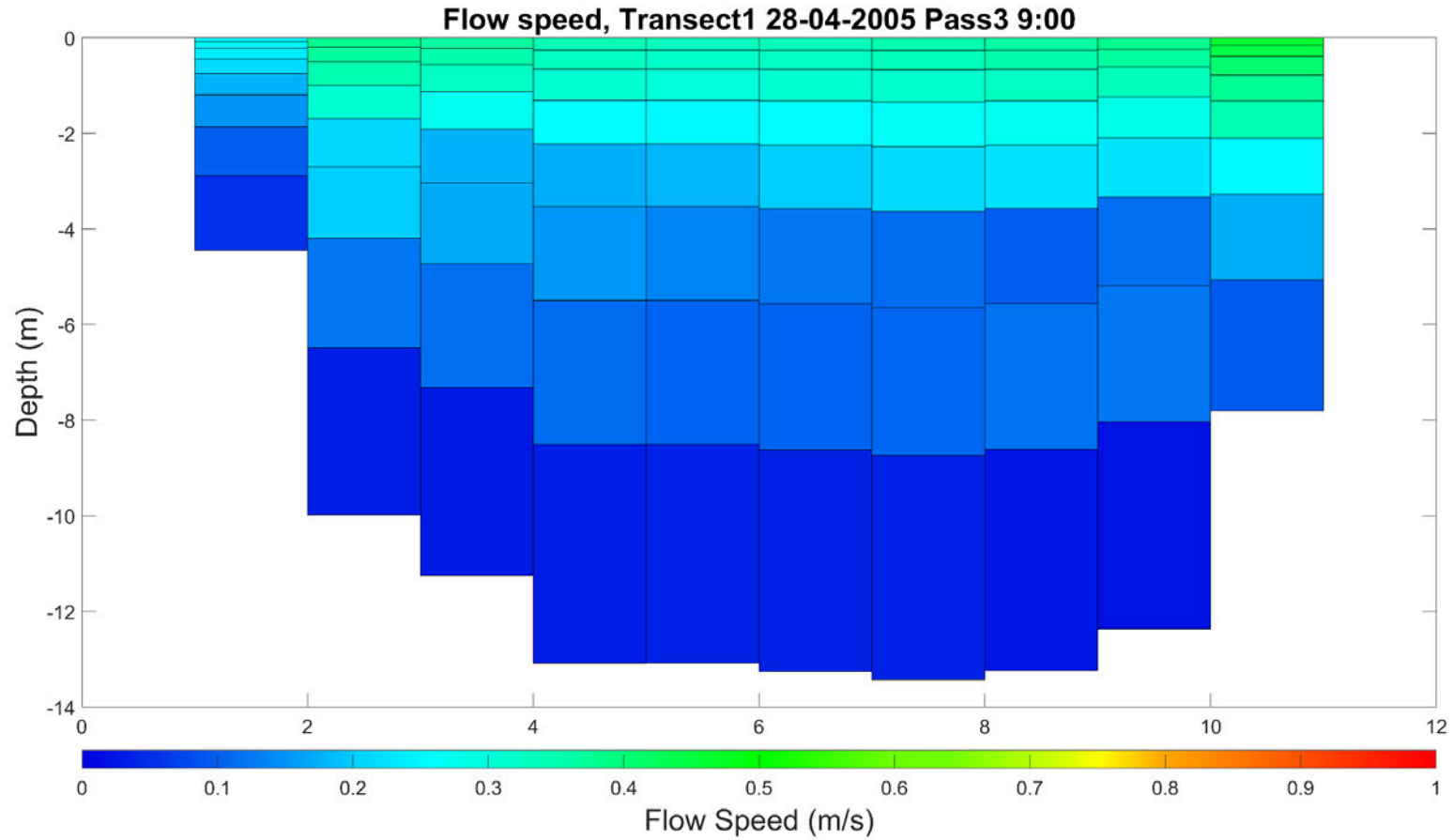


Figure 48. Modelled flow speed, Transect 1: Ebb tide, cross section of speed with depth shown from west (left) to east (right)

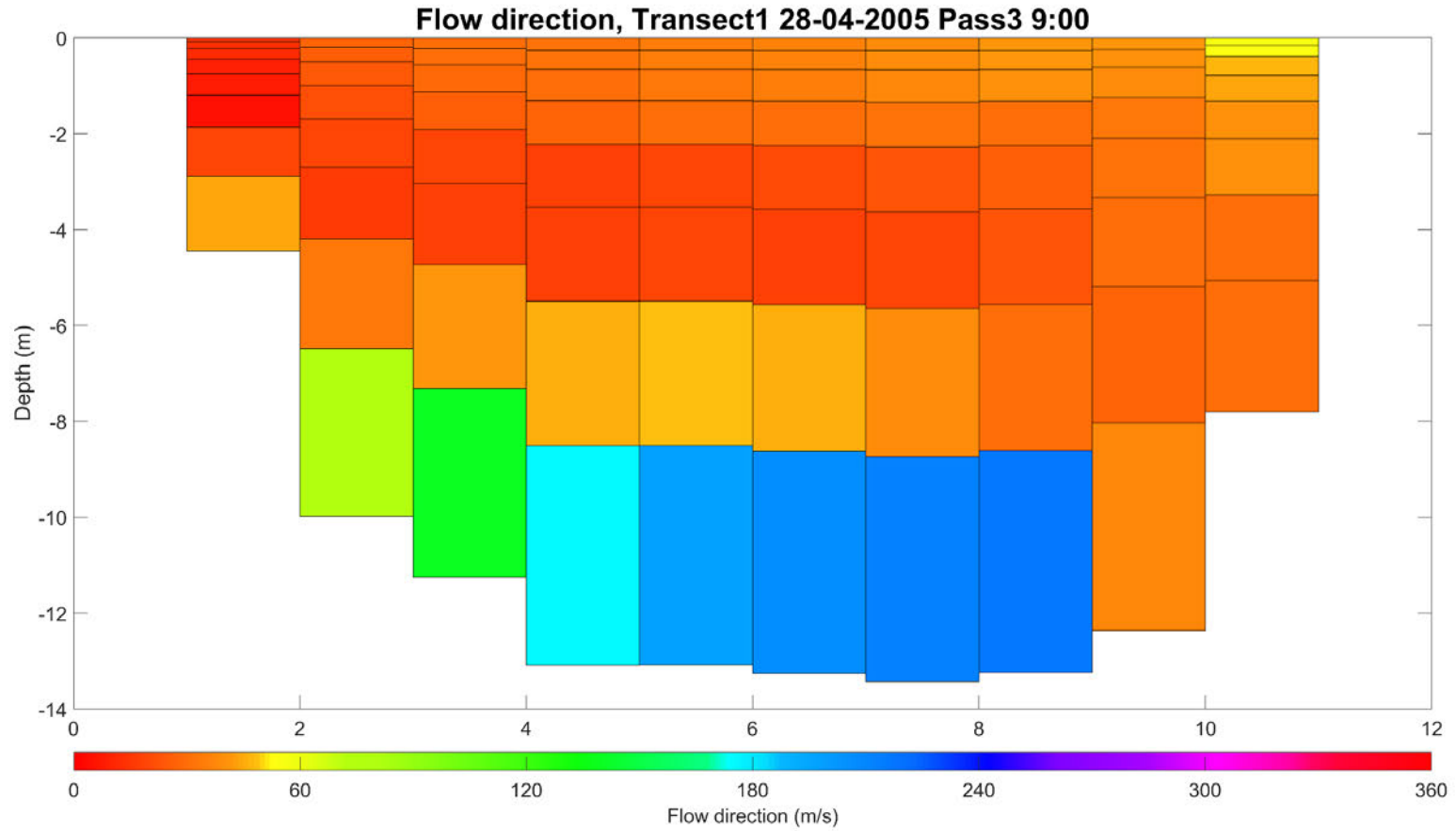


Figure 49. Modelled flow direction, Transect 1: Ebb tide, cross section of direction with depth shown from west (left) to east (right)

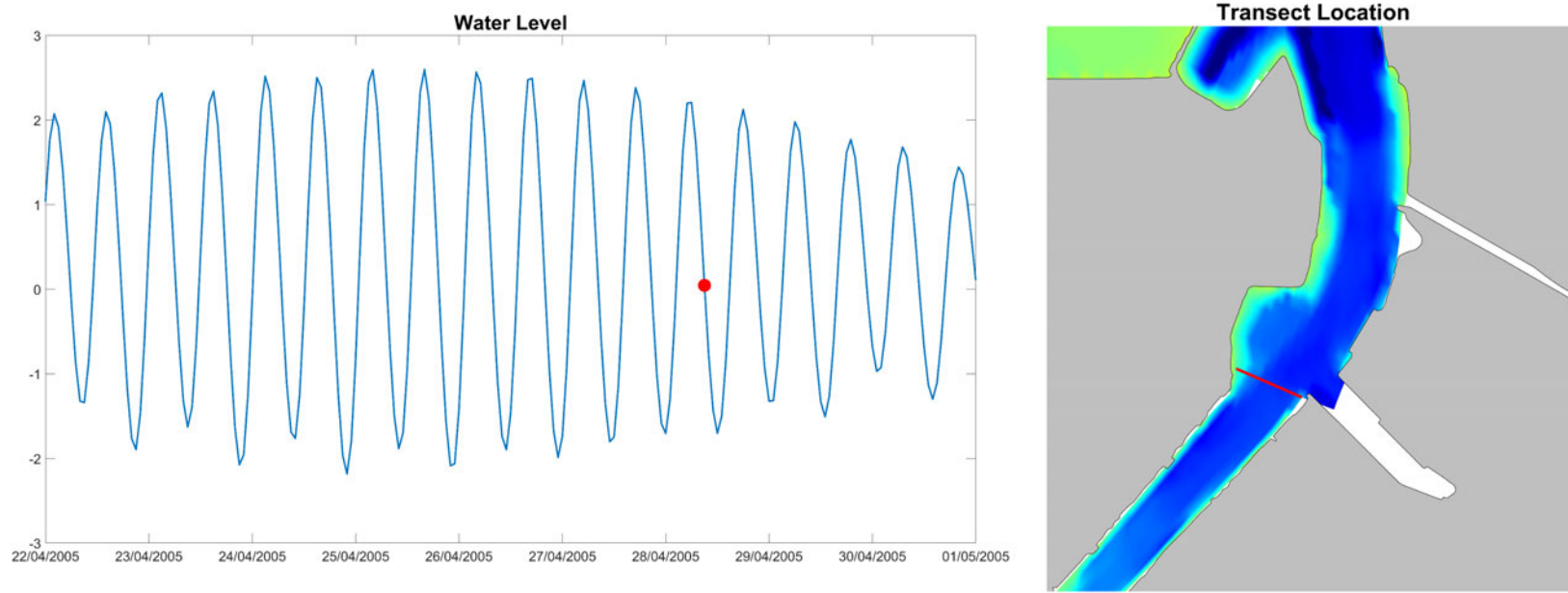


Figure 50. Tidal state and transect location extracted from the model for Transect 1 Pass 03: 28/04/2005

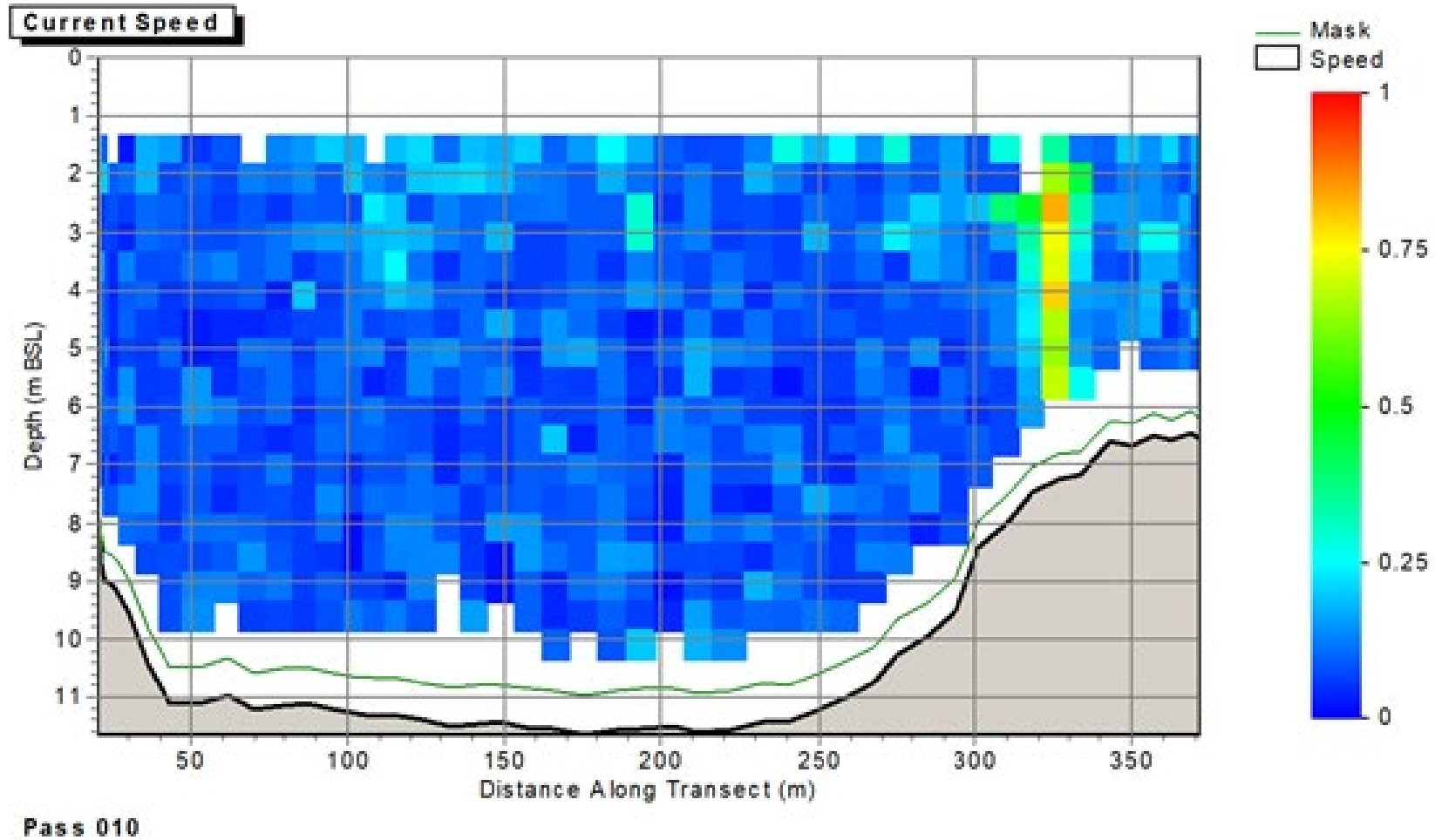


Figure provided by PD Teesport

Figure 51. Measured flow speeds, Transect 1, Pass 1: Low water, cross section of speed with depth shown from west (left) to east (right)

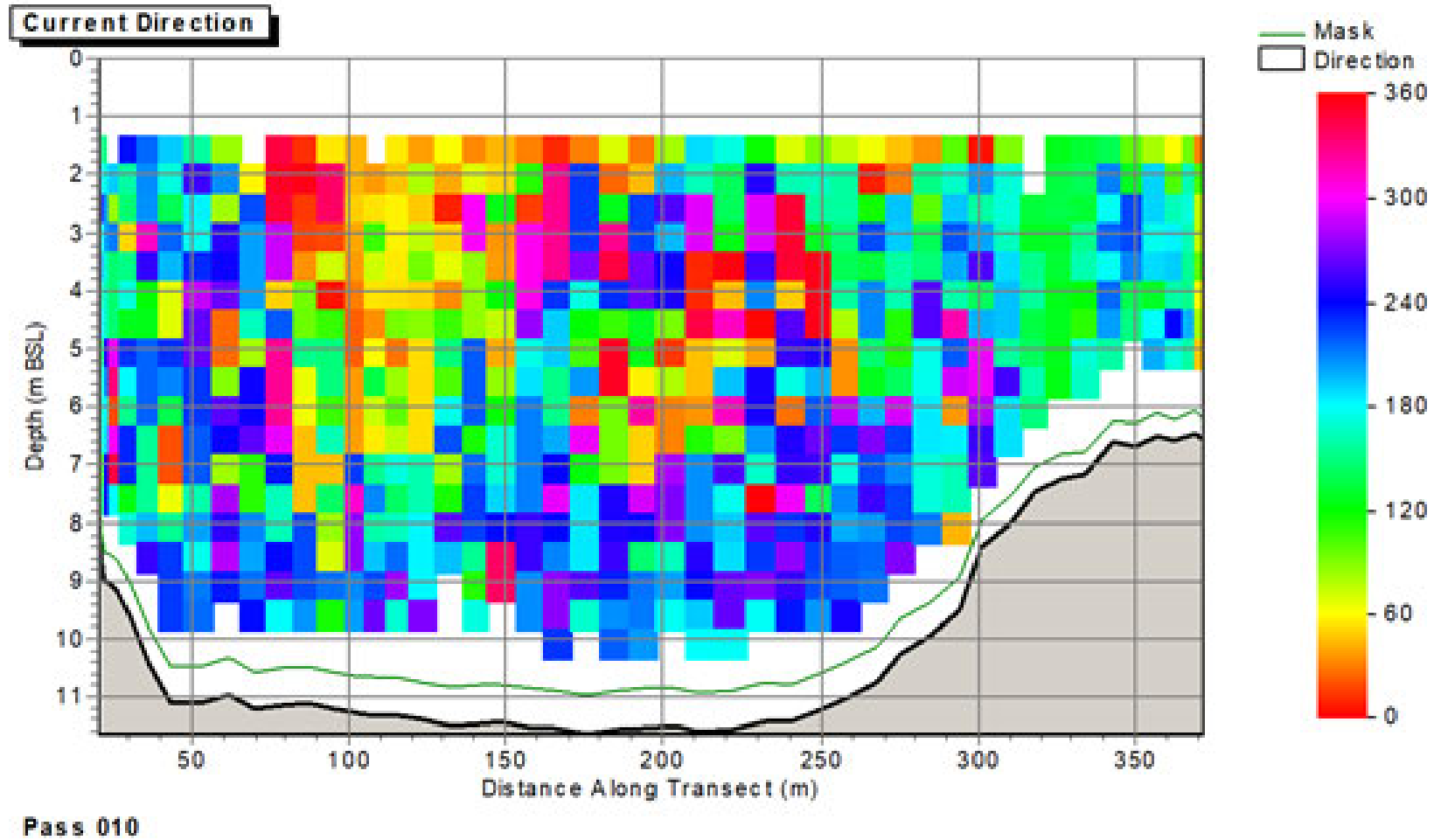


Figure provided by PD Teesport

Figure 52. Measured flow directions, Transect 1, Pass 1: Low water, cross section of speed with depth shown from west (left) to east (right)

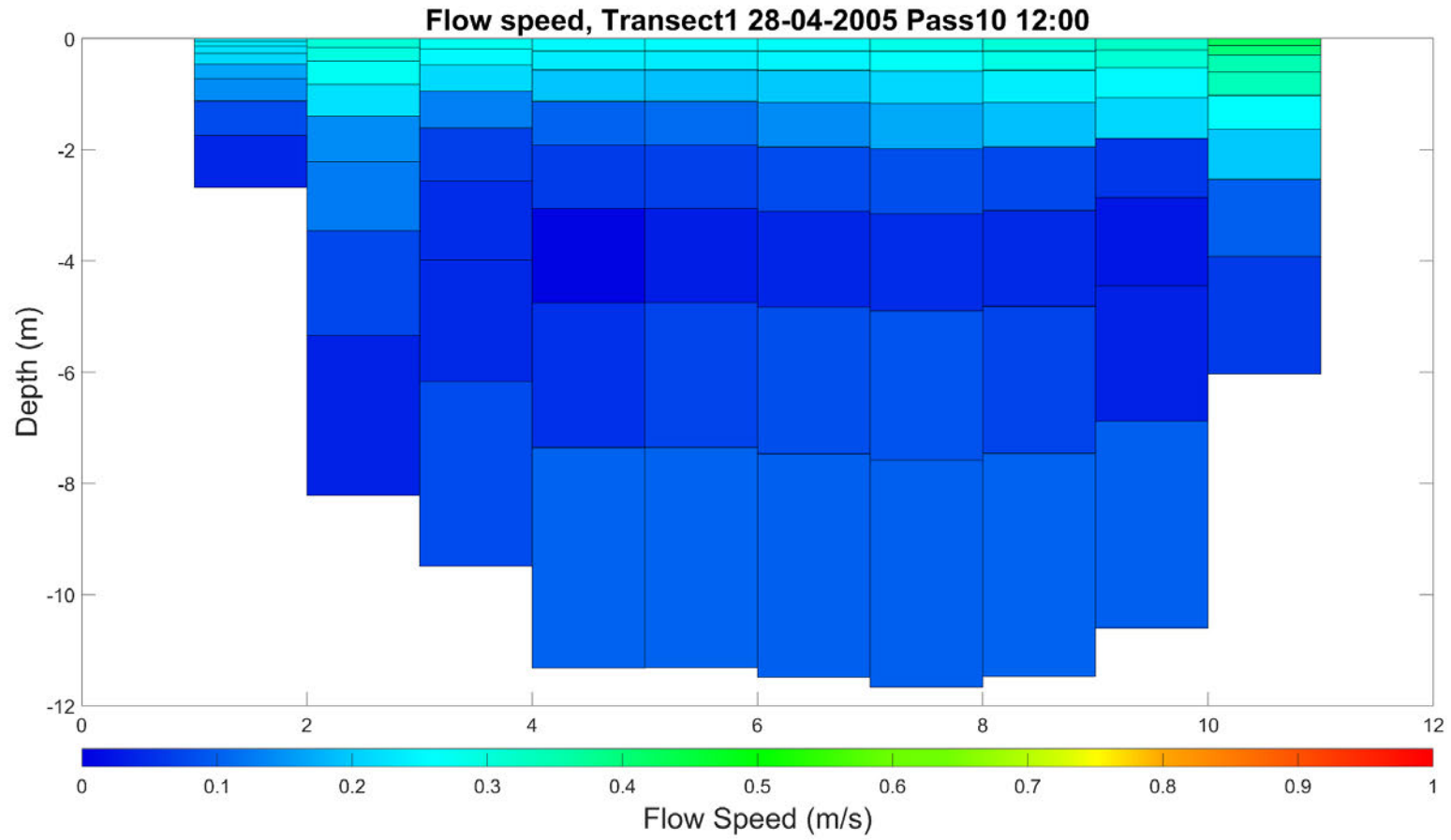


Figure 53. Modelled flow speed, Transect 1: Low tide, cross section of speed with depth shown from west (left) to east (right)

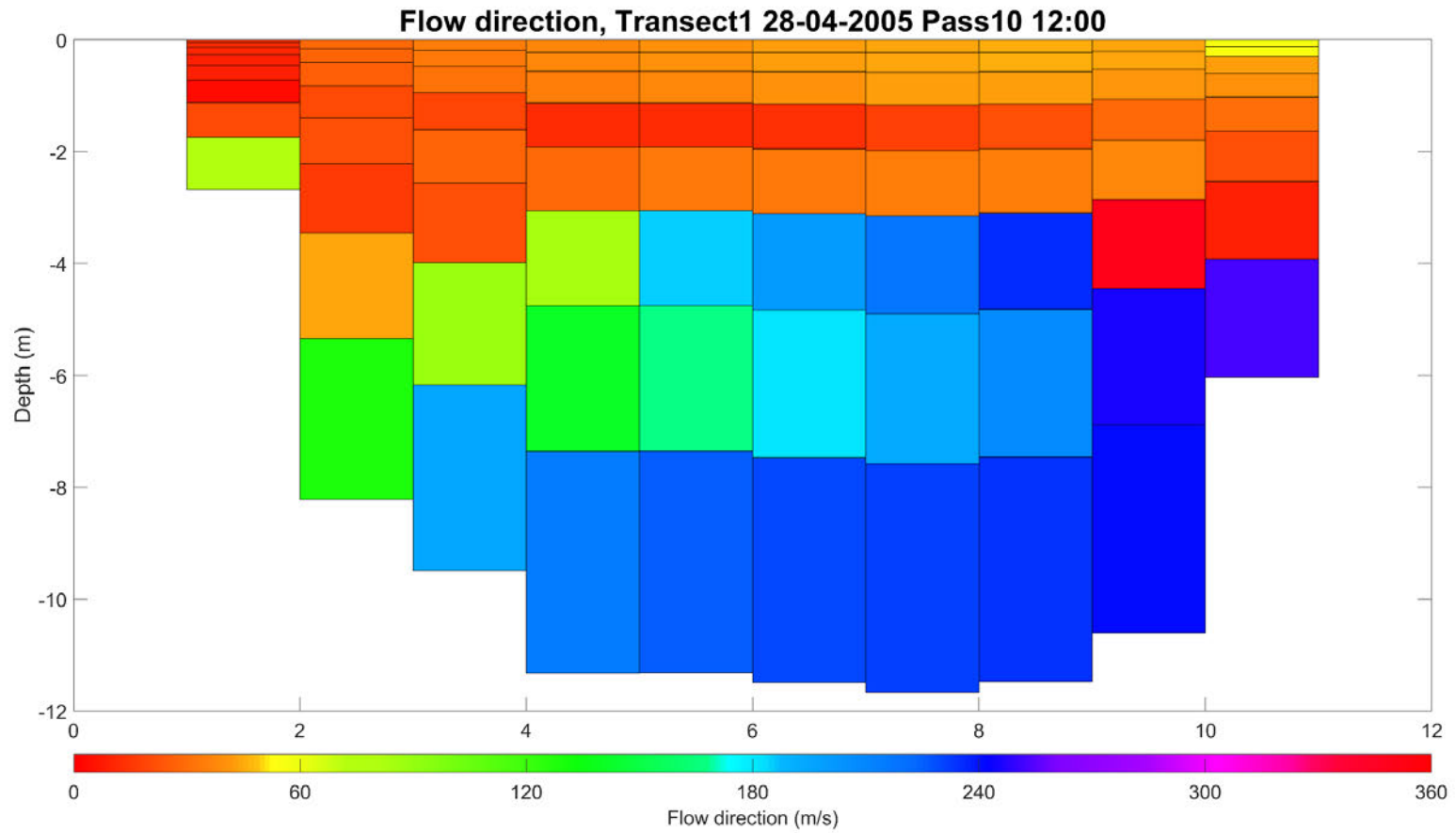


Figure 54. Modelled flow direction, Transect 1: Low tide, cross section of direction with depth shown from west (left) to east (right)

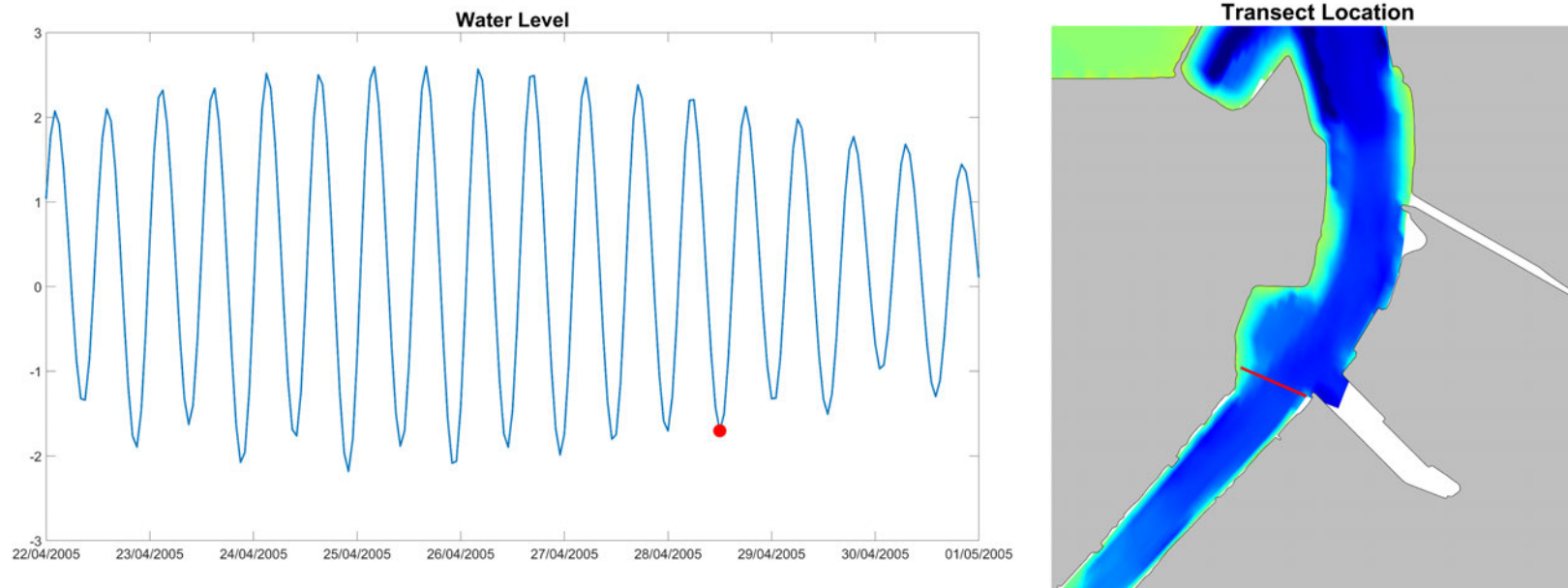


Figure 55. Tidal state and transect location extracted from the model for Transect 1 Pass 01: 28/04/2005

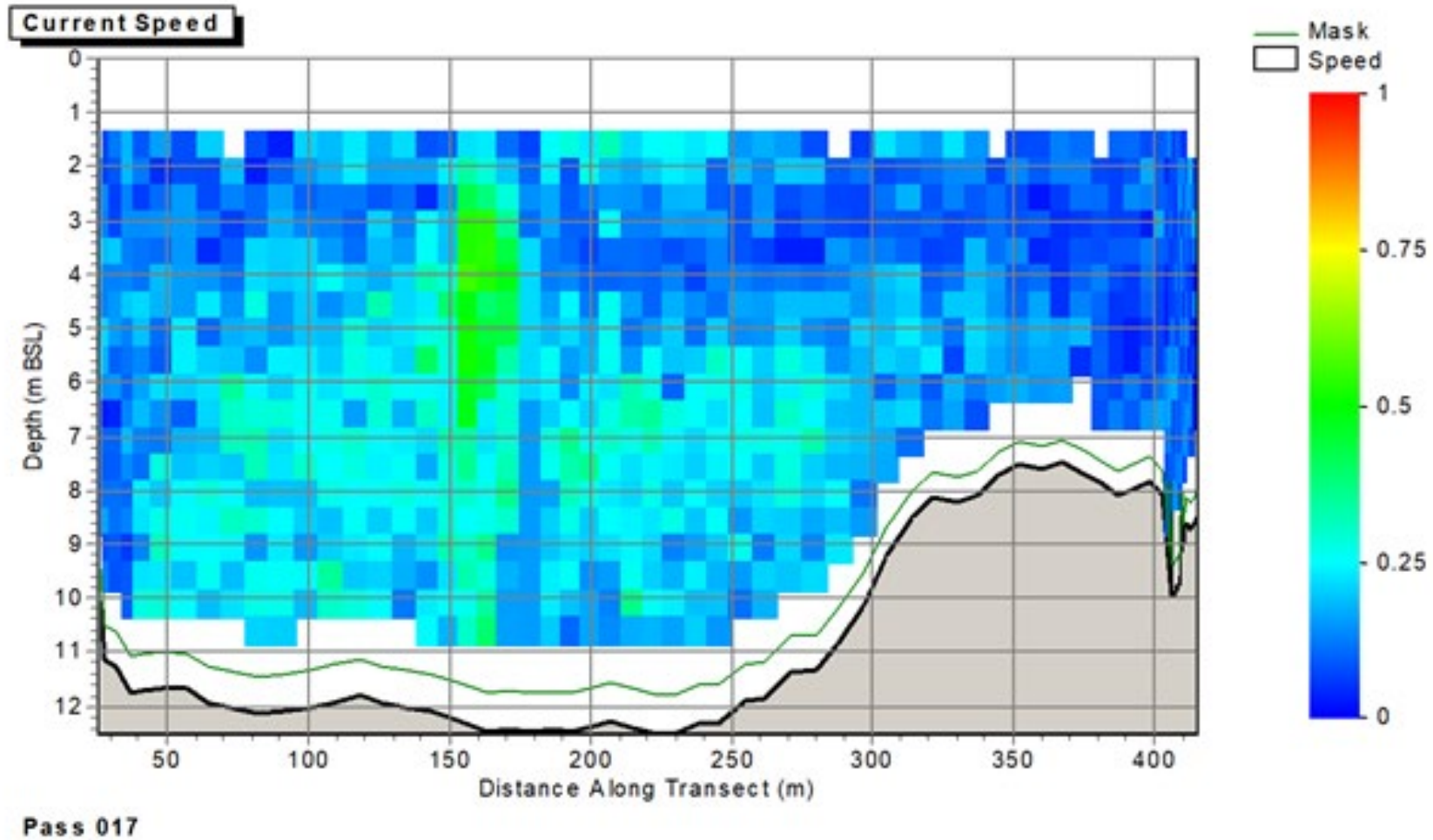


Figure provided by PD Teesport

Figure 56. Measured flow speeds, Transect 1, Pass 17: Flood tide, cross section of speed with depth shown from west (left) to east (right)

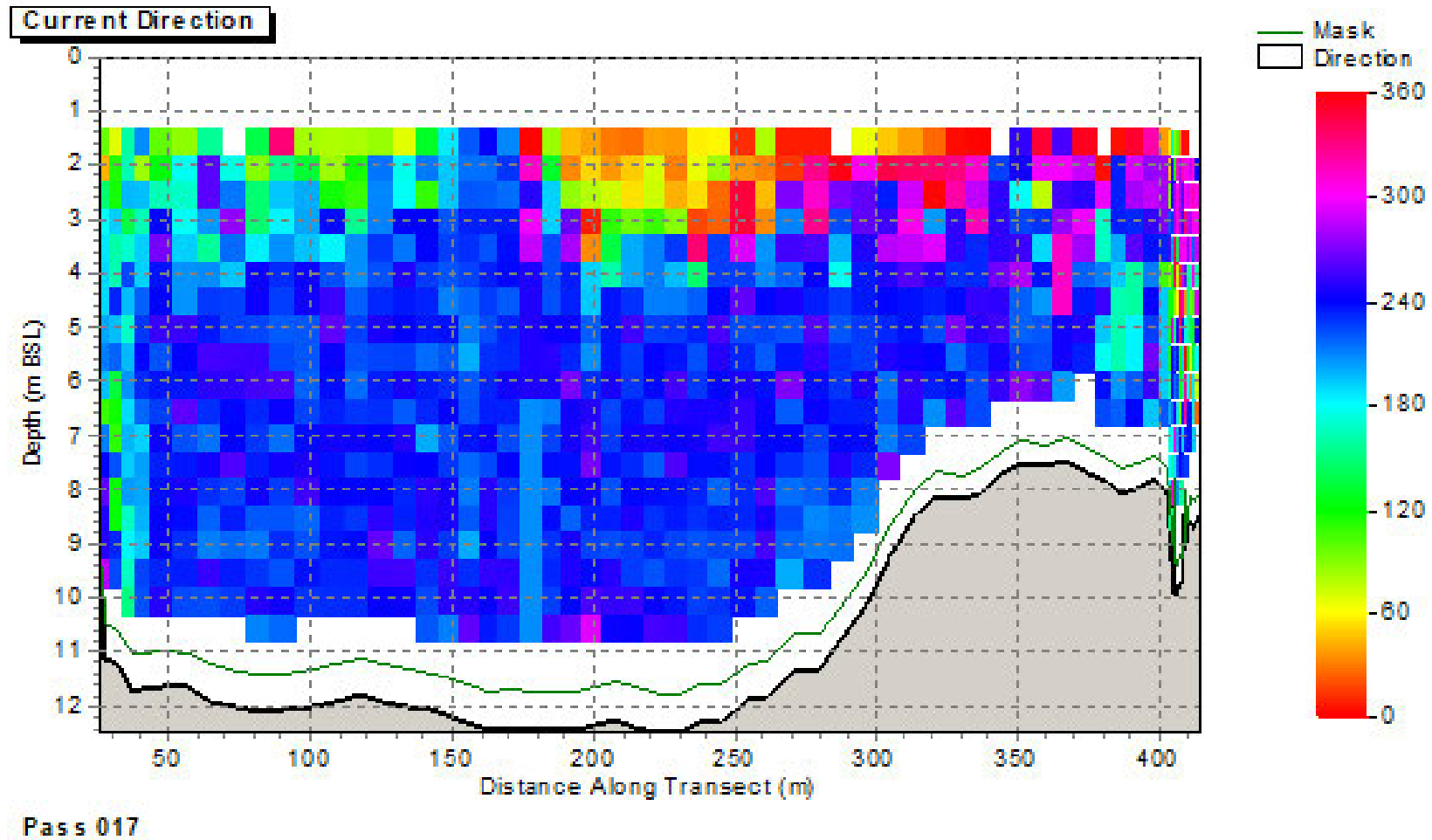


Figure provided by PD Teesport

Figure 57. Measured flow directions, Transect 1, Pass 17: Flood tide, cross section of speed with depth shown from west (left) to east (right)

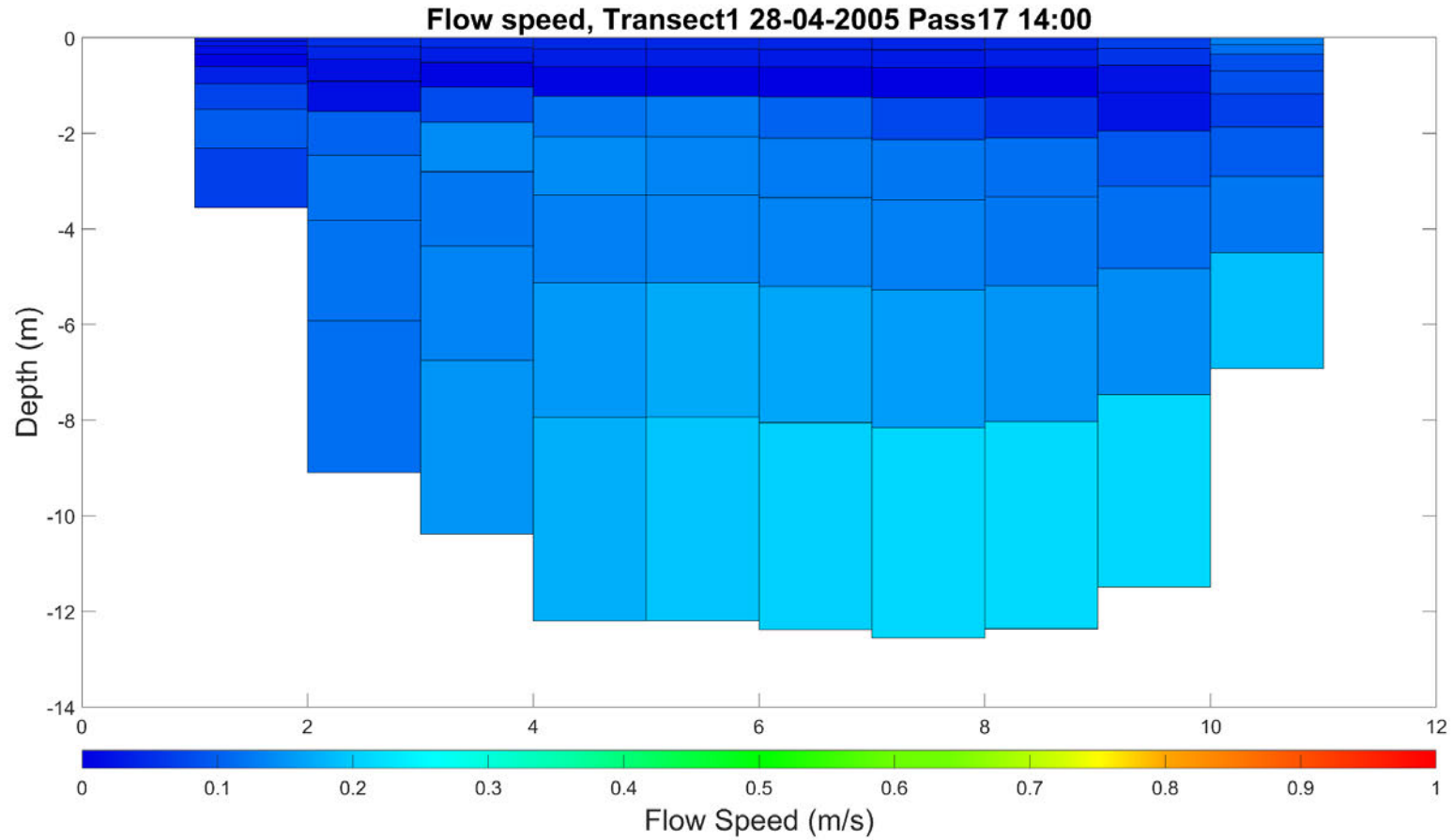


Figure 58. Modelled flow speed, Transect 1: Flood tide, cross section of speed with depth shown from west (left) to east (right)

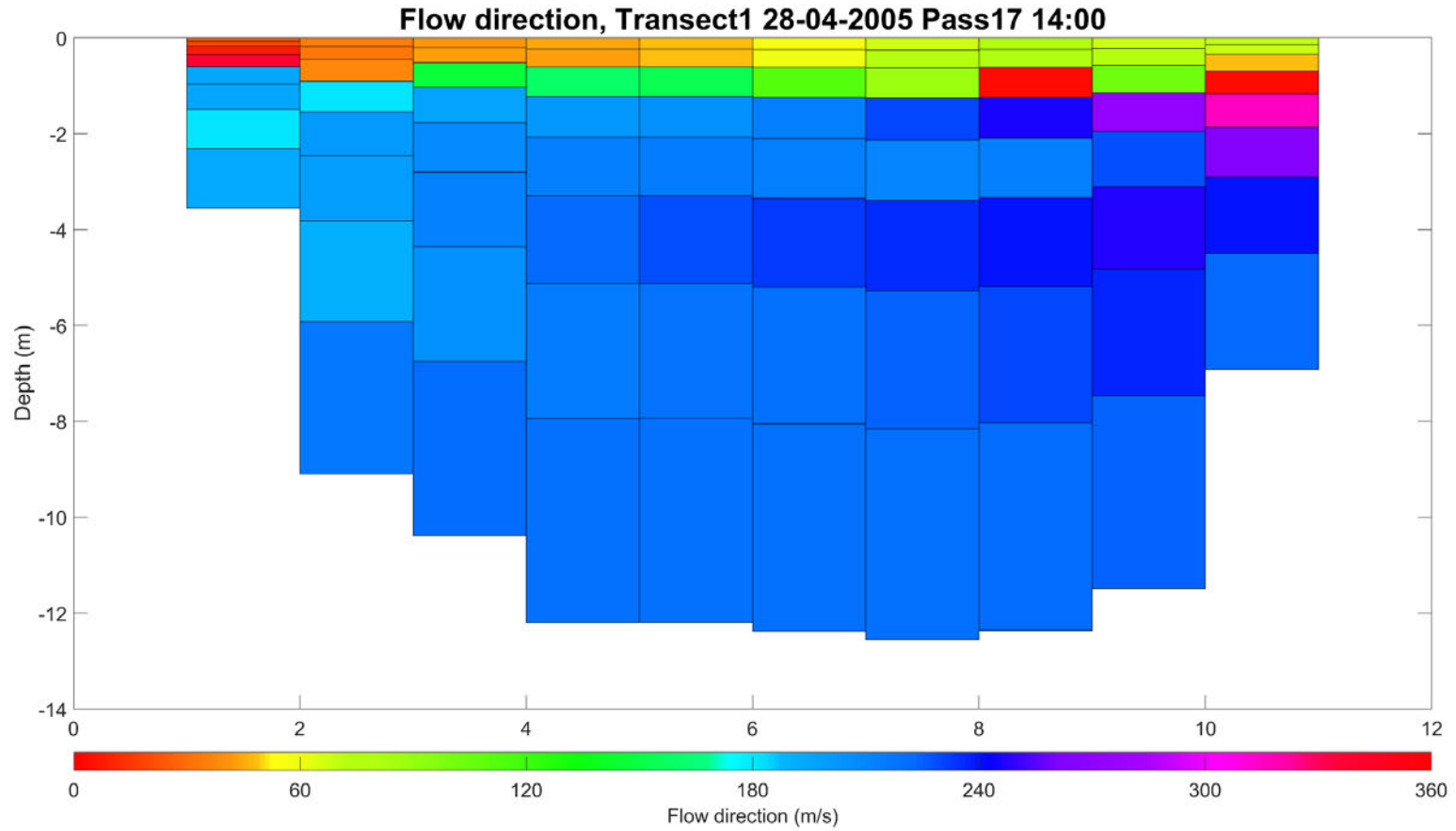


Figure 59. Modelled flow direction, Transect 1: Flood tide, cross section of direction with depth shown from west (left) to east (right)

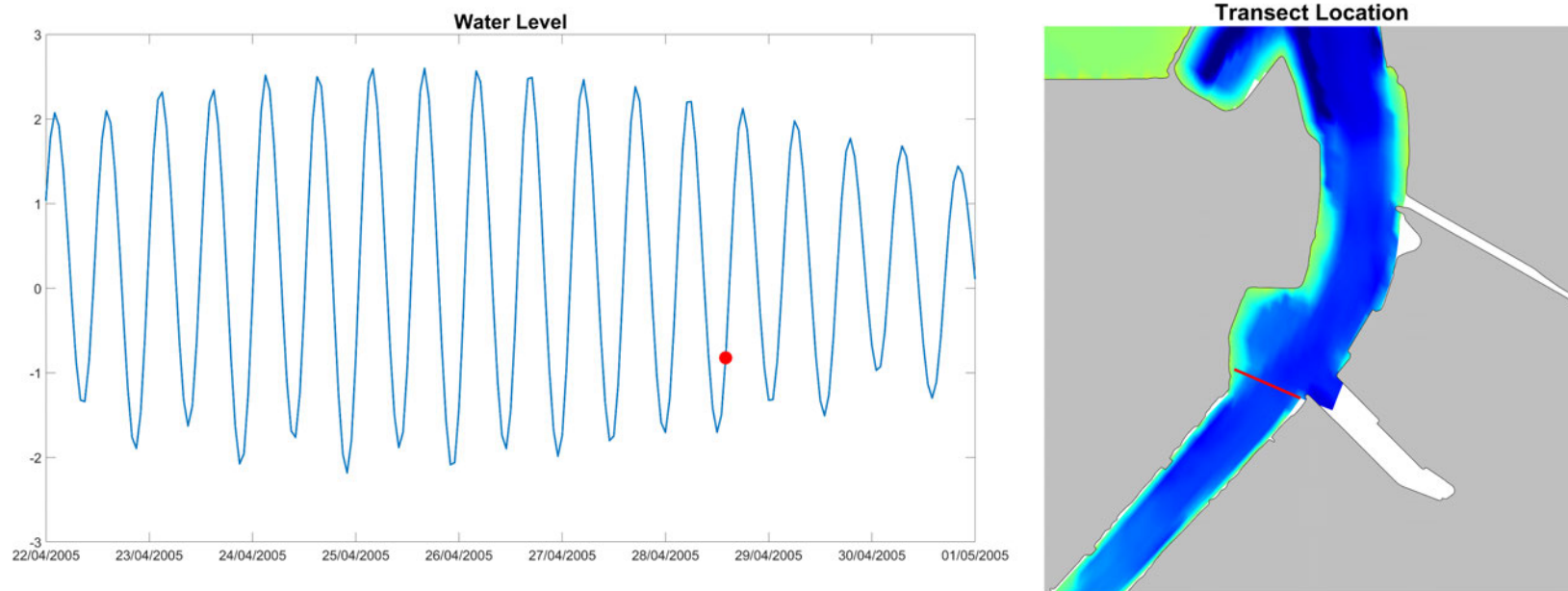


Figure 60. Tidal state and transect location extracted from the model for Transect 1 Pass 17: 28/04/2005

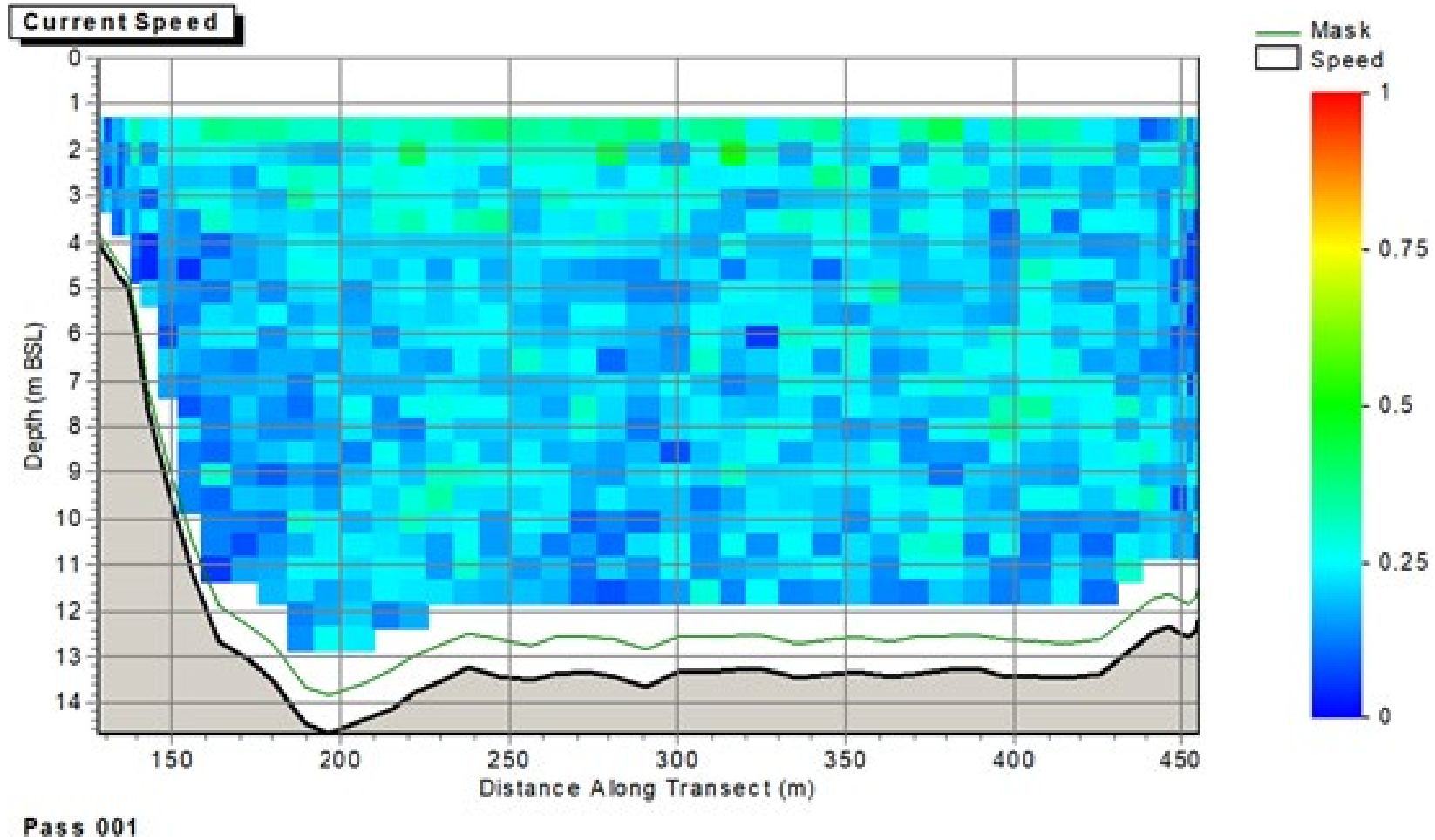


Figure provided by PD Teesport

Figure 61. Measured flow speed, Transect 7, Pass 1: Ebb tide, cross section of speed with depth shown from west (left) to east (right)

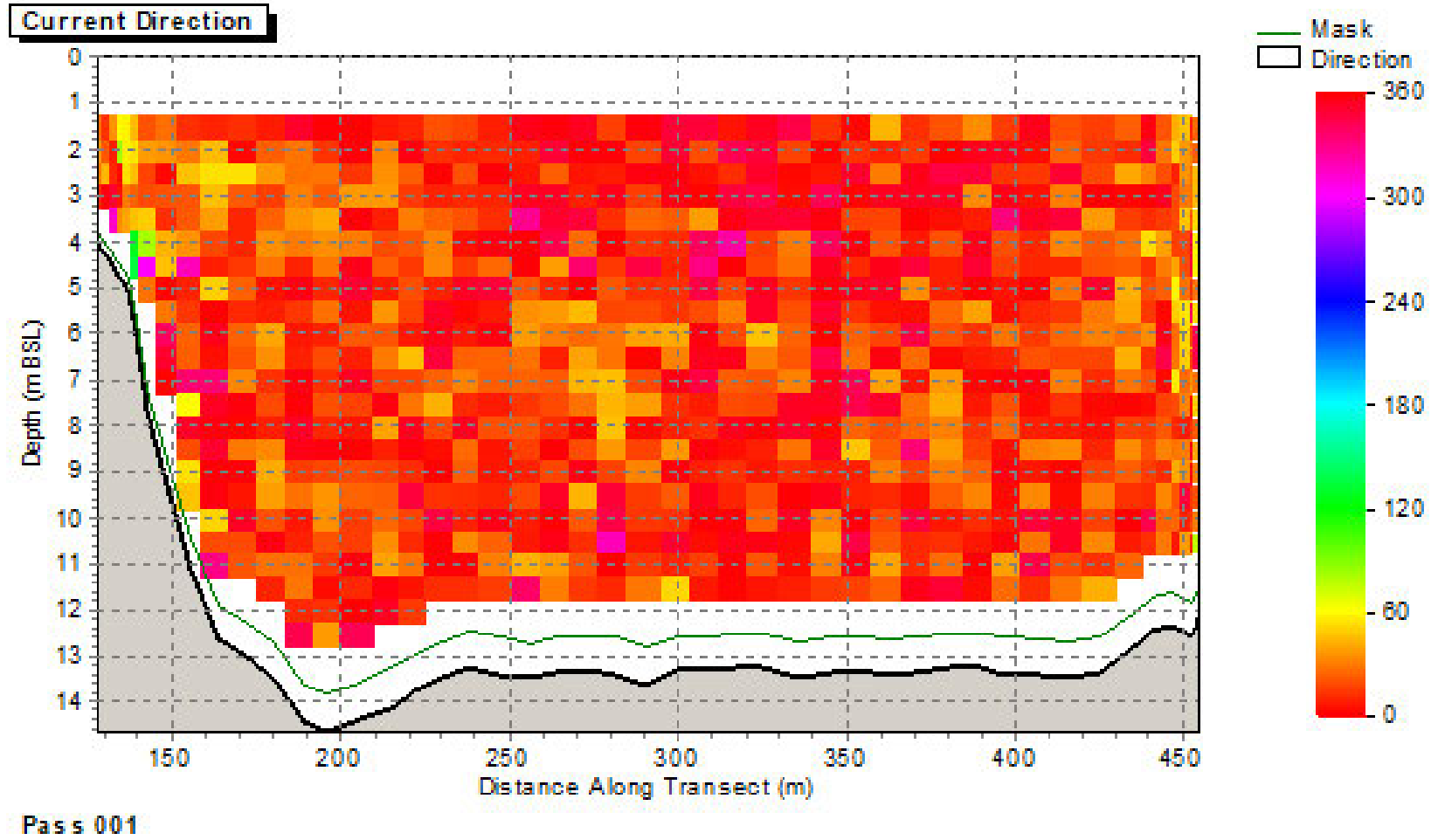


Figure provided by PD Teesport

Figure 62. Measured flow direction, Transect 7, Pass 1: Ebb tide, cross section of direction with depth shown from west (left) to east (right)

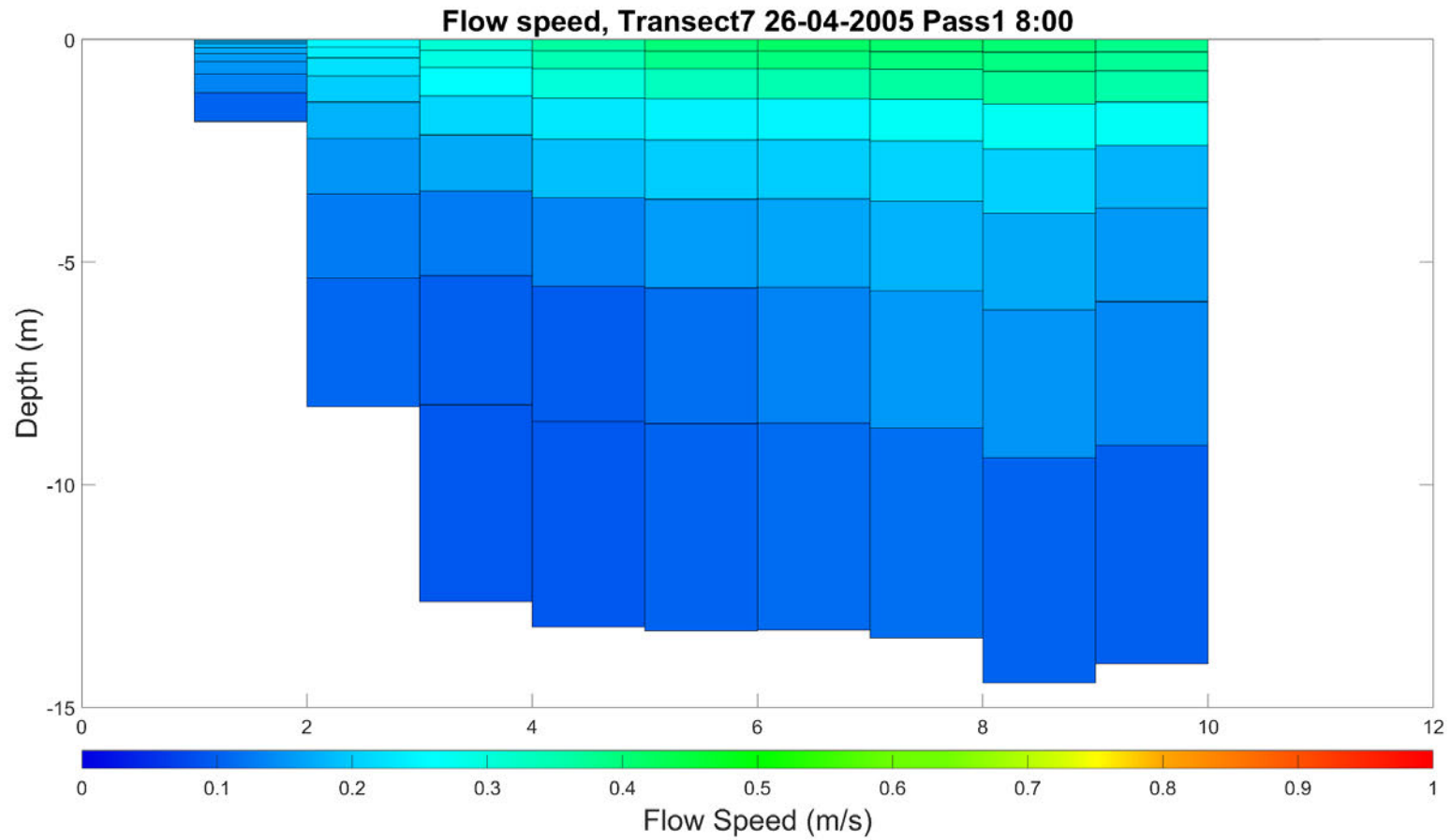


Figure 63. Modelled flow speed, Transect 7: Ebb tide, cross section of speed with depth shown from west (left) to east (right)

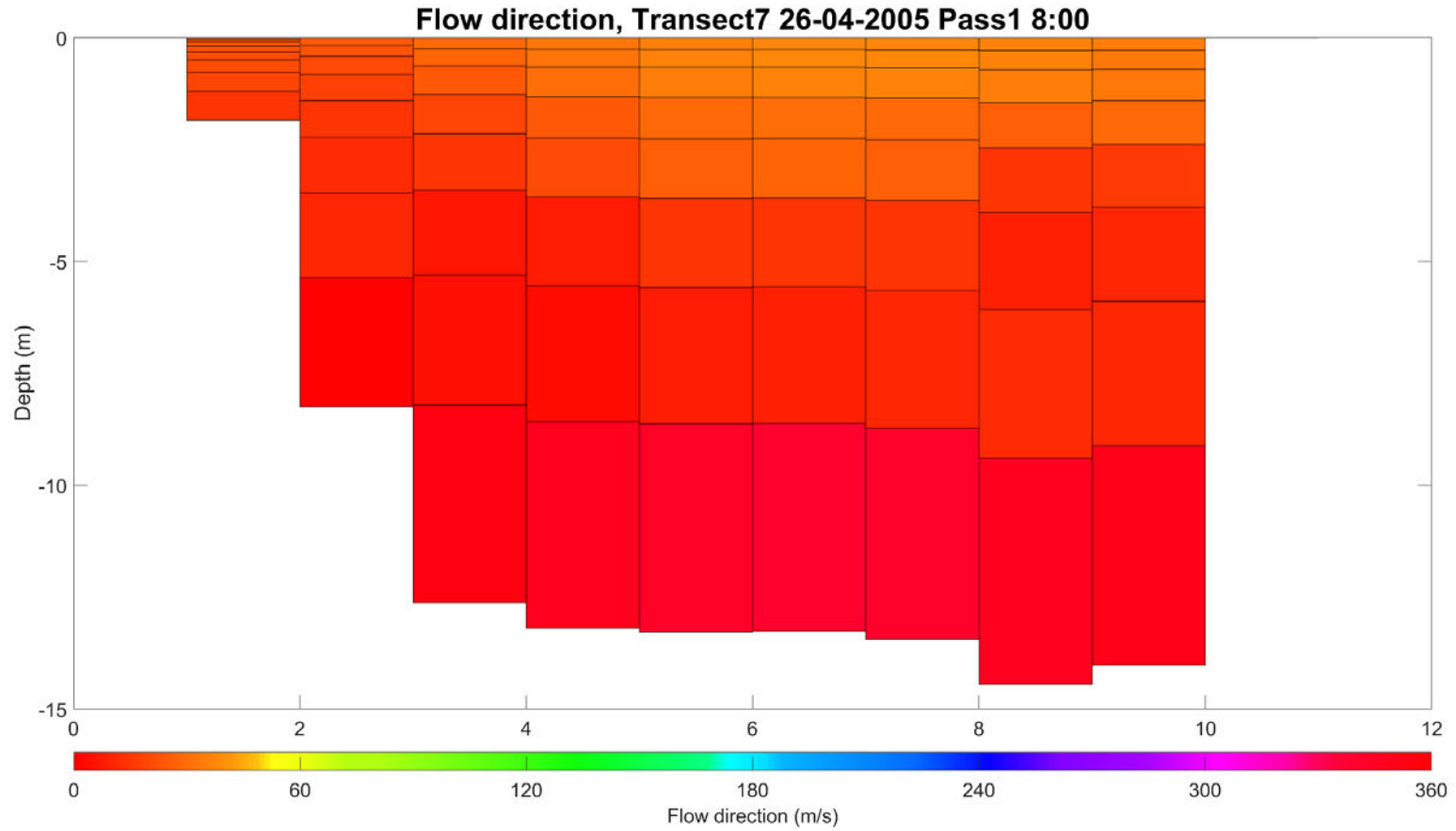


Figure 64. Modelled flow direction, Transect 7: Ebb tide, cross section of direction with depth shown from west (left) to east (right)

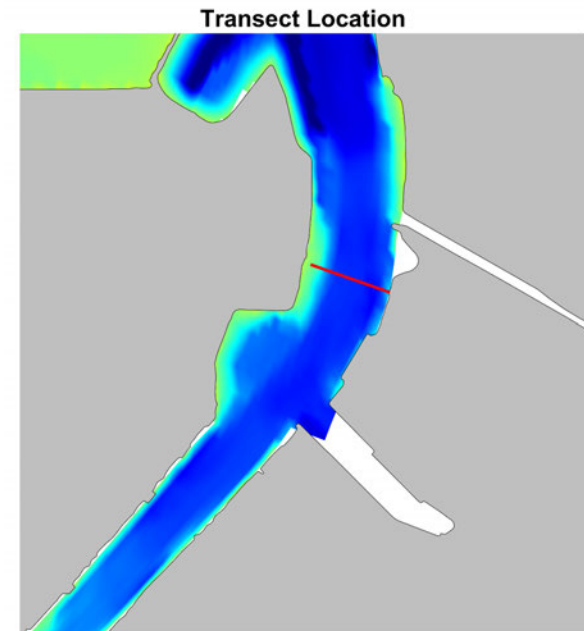
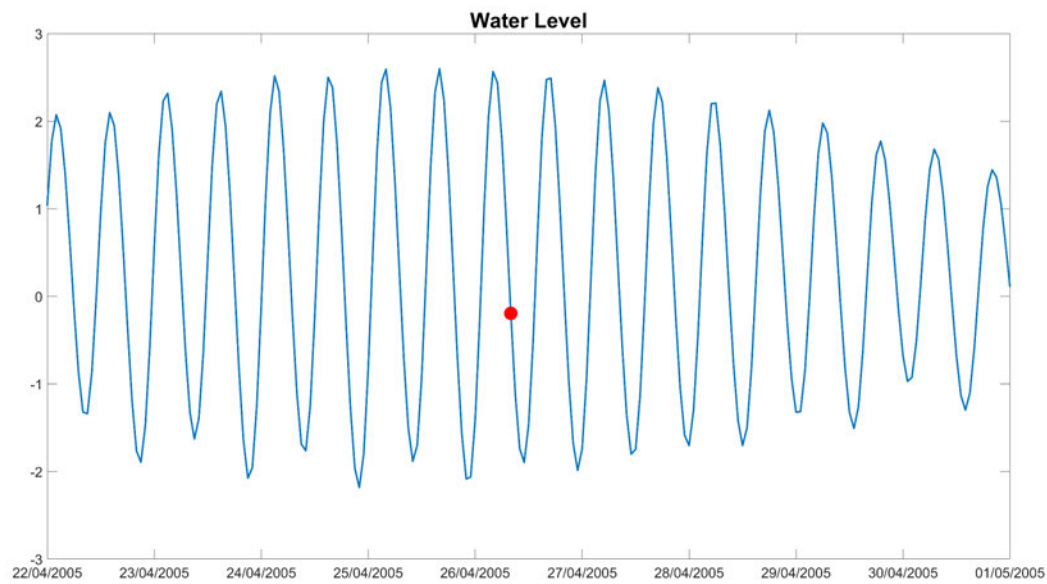


Figure 65. Tidal state and transect location extracted from the model for Transect 7 Pass 1: 26/04/2005

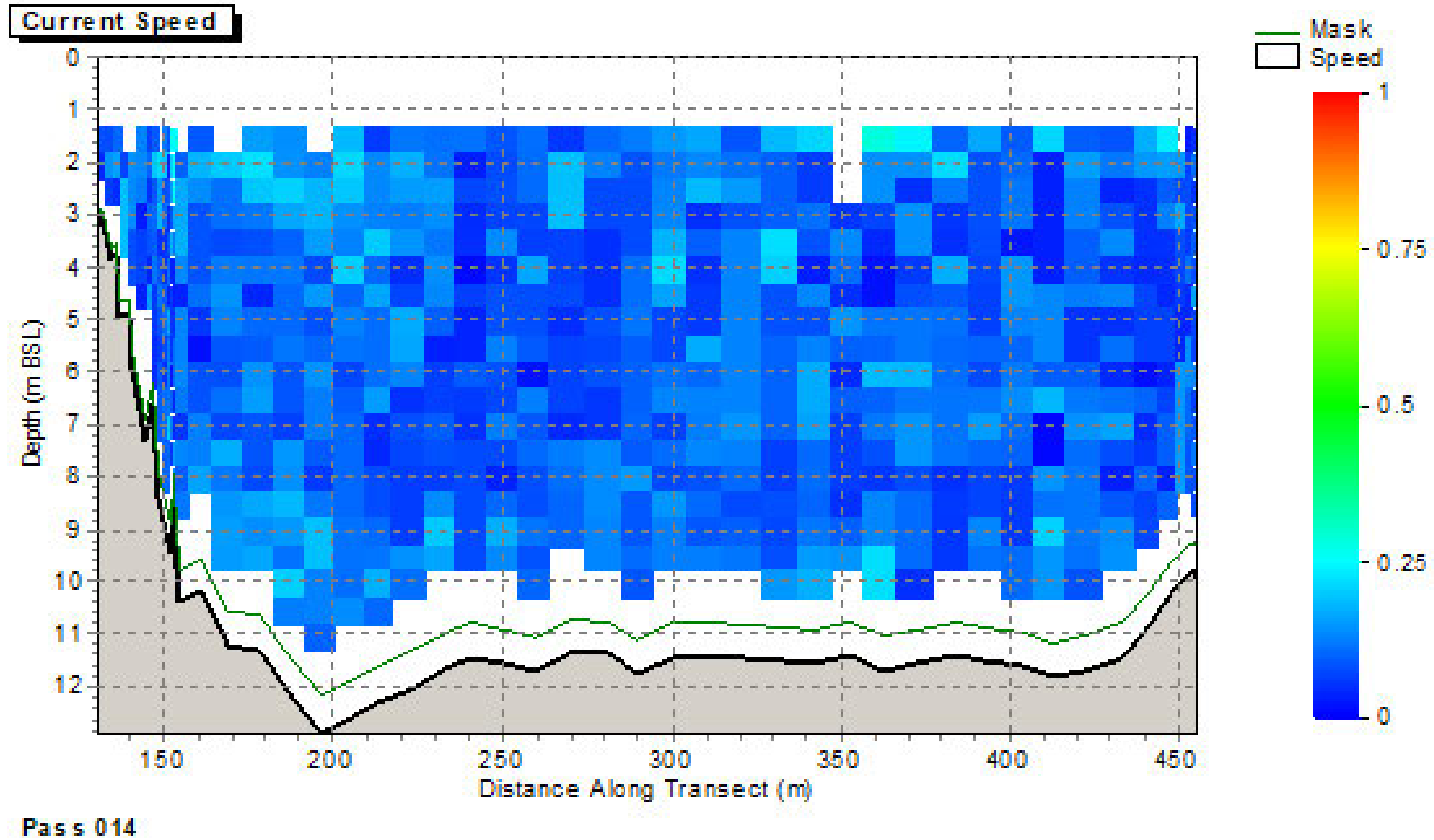


Figure provided by PD Teesport

Figure 66. Measured flow speed, Transect 7, Pass 14: Low water, cross section of speed with depth shown from west (left) to east (right)

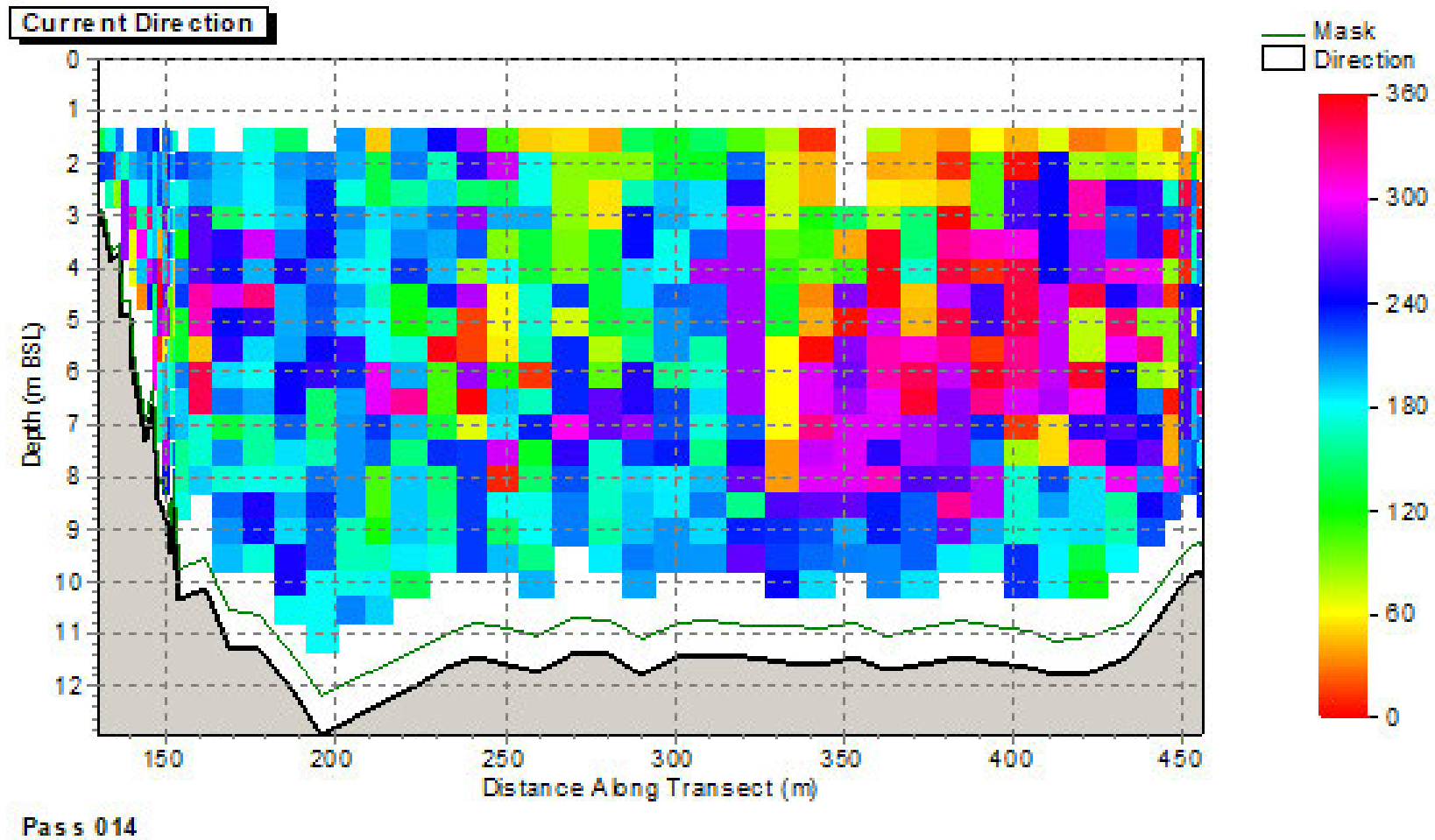


Figure provided by PD Teesport

Figure 67. Measured flow direction, Transect 7, Pass 14: Low water, cross section of direction with depth shown from west (left) to east (right)

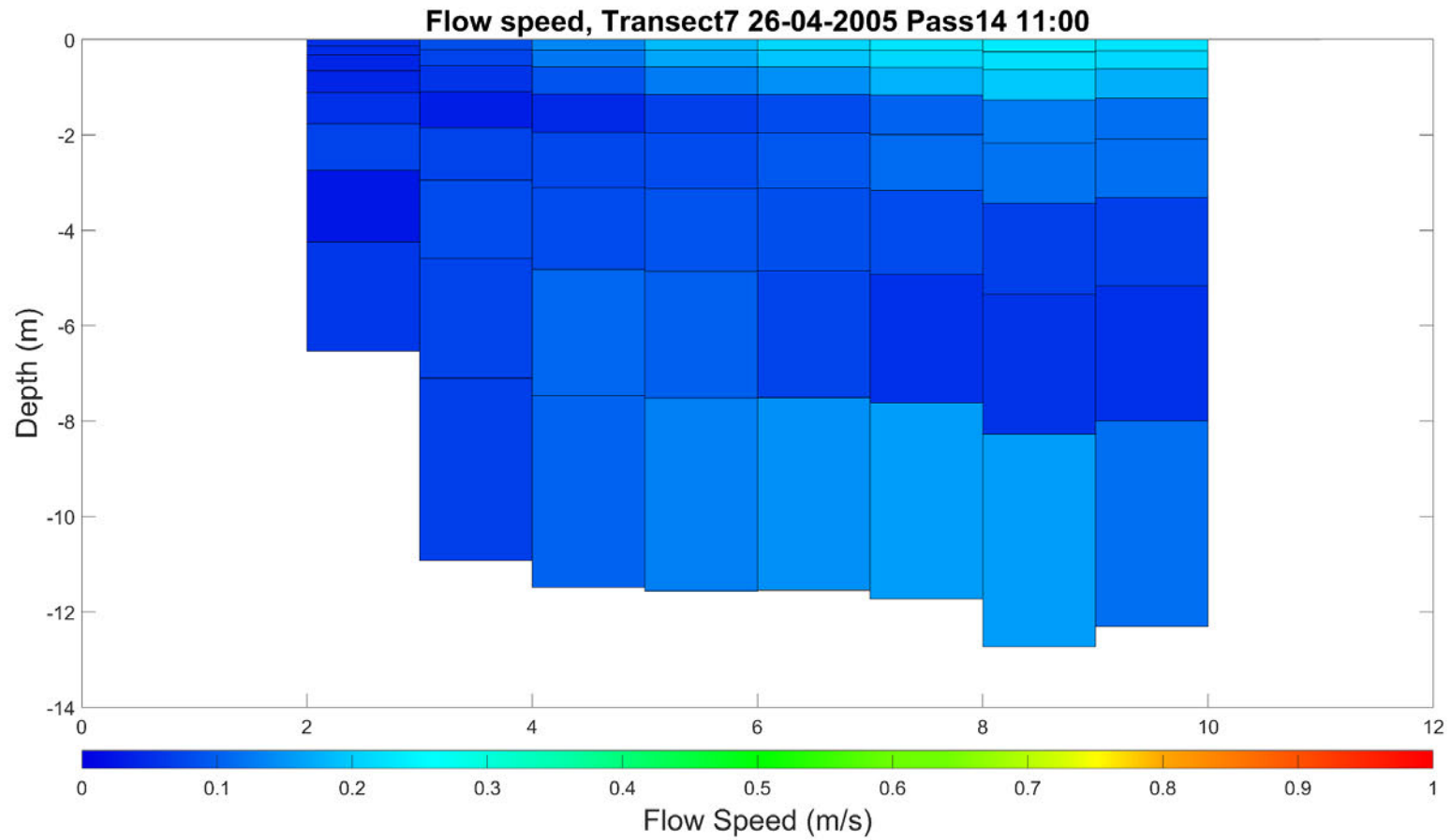


Figure 68. Modelled flow speed, Transect 7: Low water, cross section of speed with depth shown from west (left) to east (right)

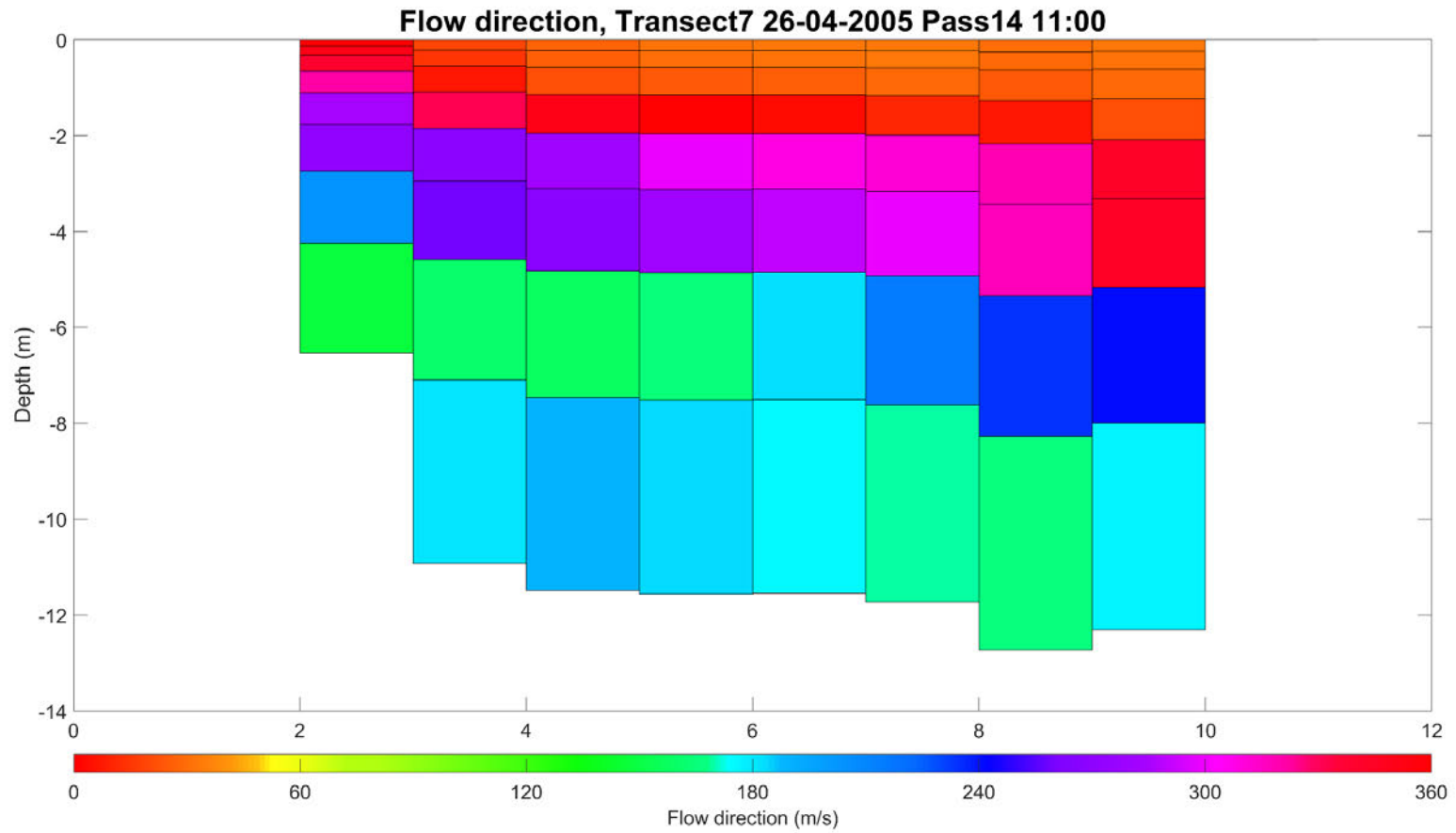


Figure 69. Modelled flow direction, Transect 7: Low water, cross section of direction with depth shown from west (left) to east (right)

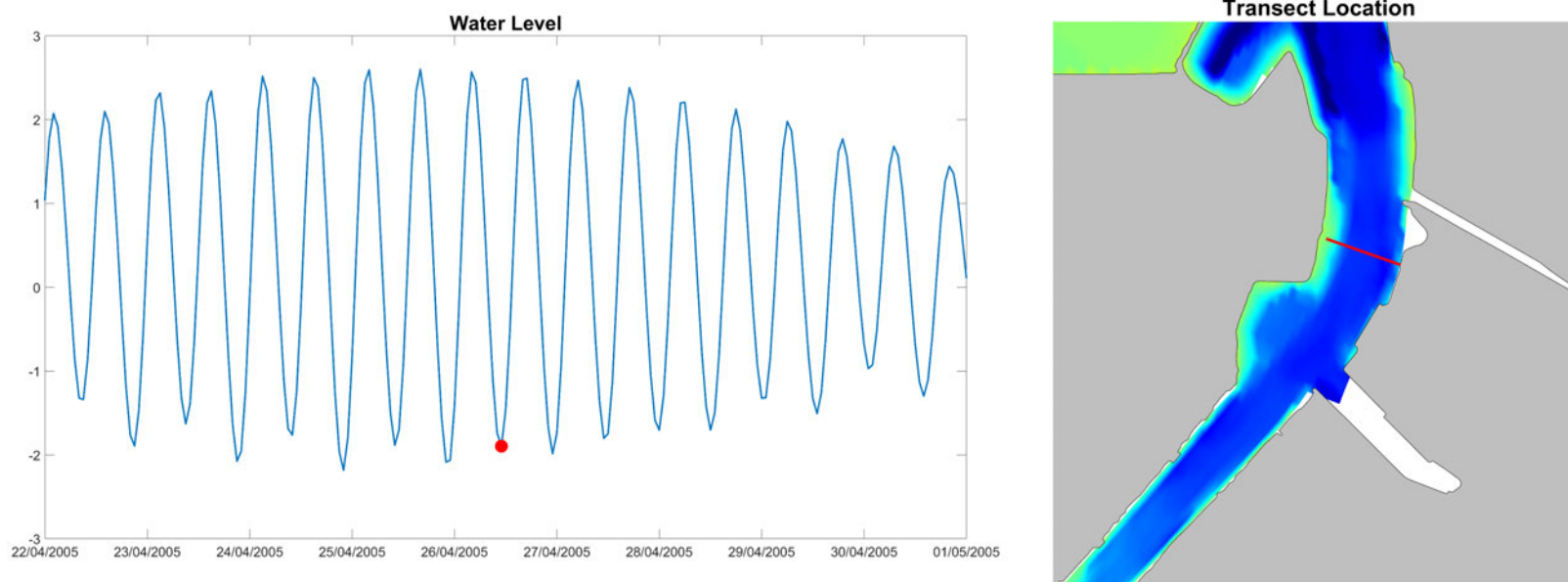


Figure 70. Tidal state and transect location extracted from the model for Transect 7 Pass 14: 26/04/2005

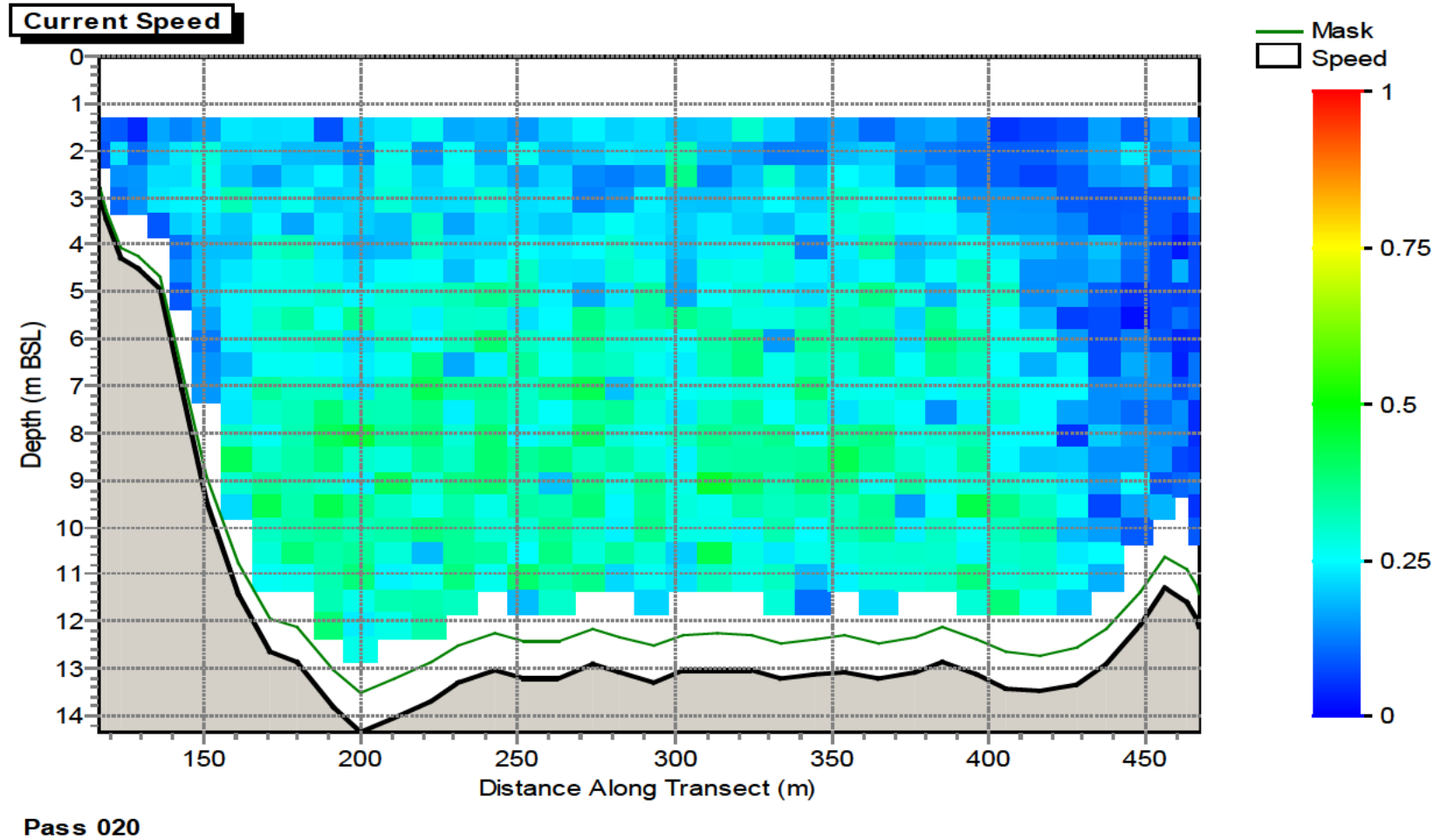


Figure provided by PD Teesport

Figure 71. Measured flow speed, Transect 7, Pass 20: Flood tide, cross section of speed with depth shown from west (left) to east (right)

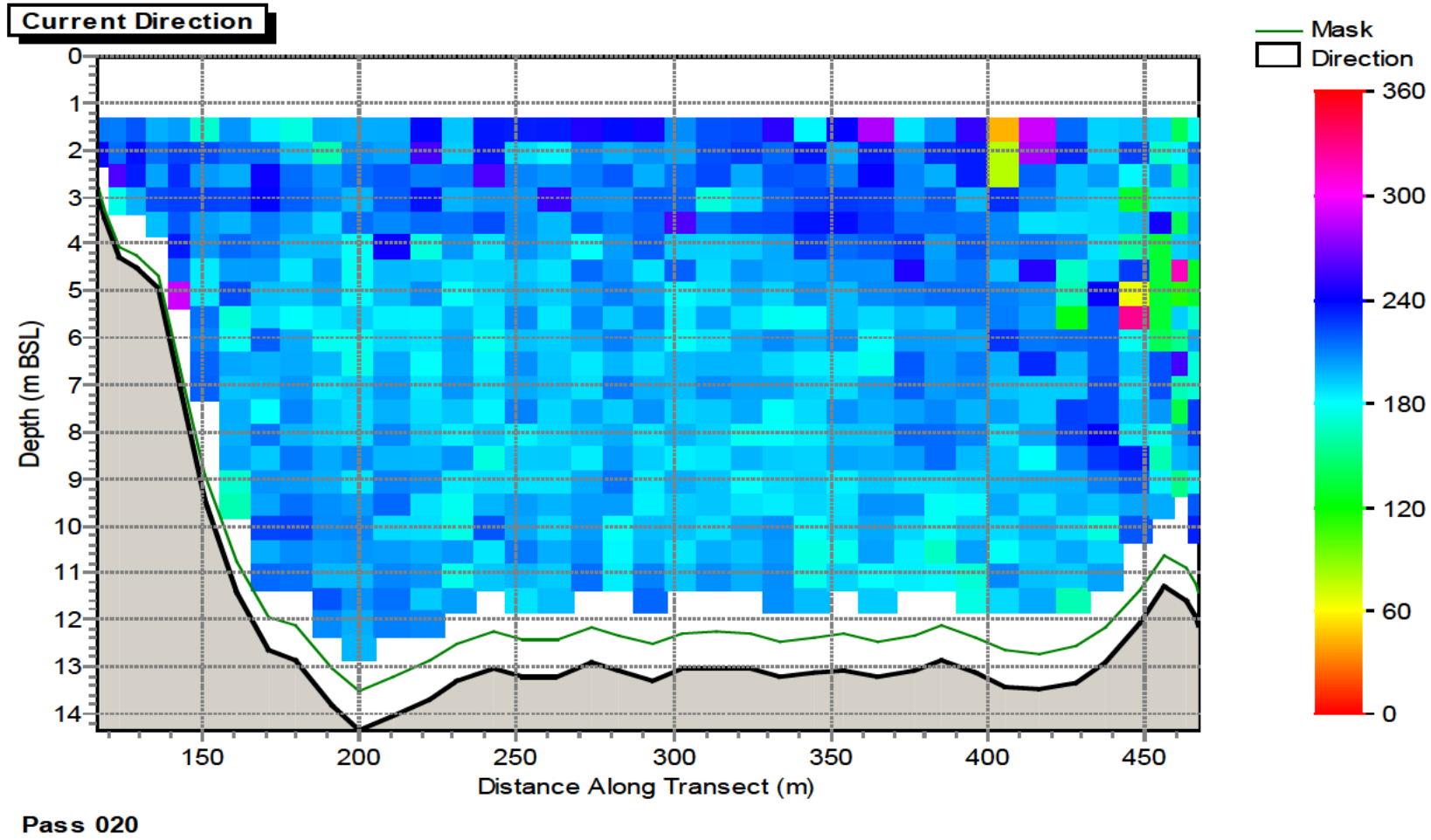


Figure provided by PD Teesport

Figure 72. Measured flow direction, Transect 7, Pass 20: Flood tide, cross section of direction with depth shown from west (left) to east (right)

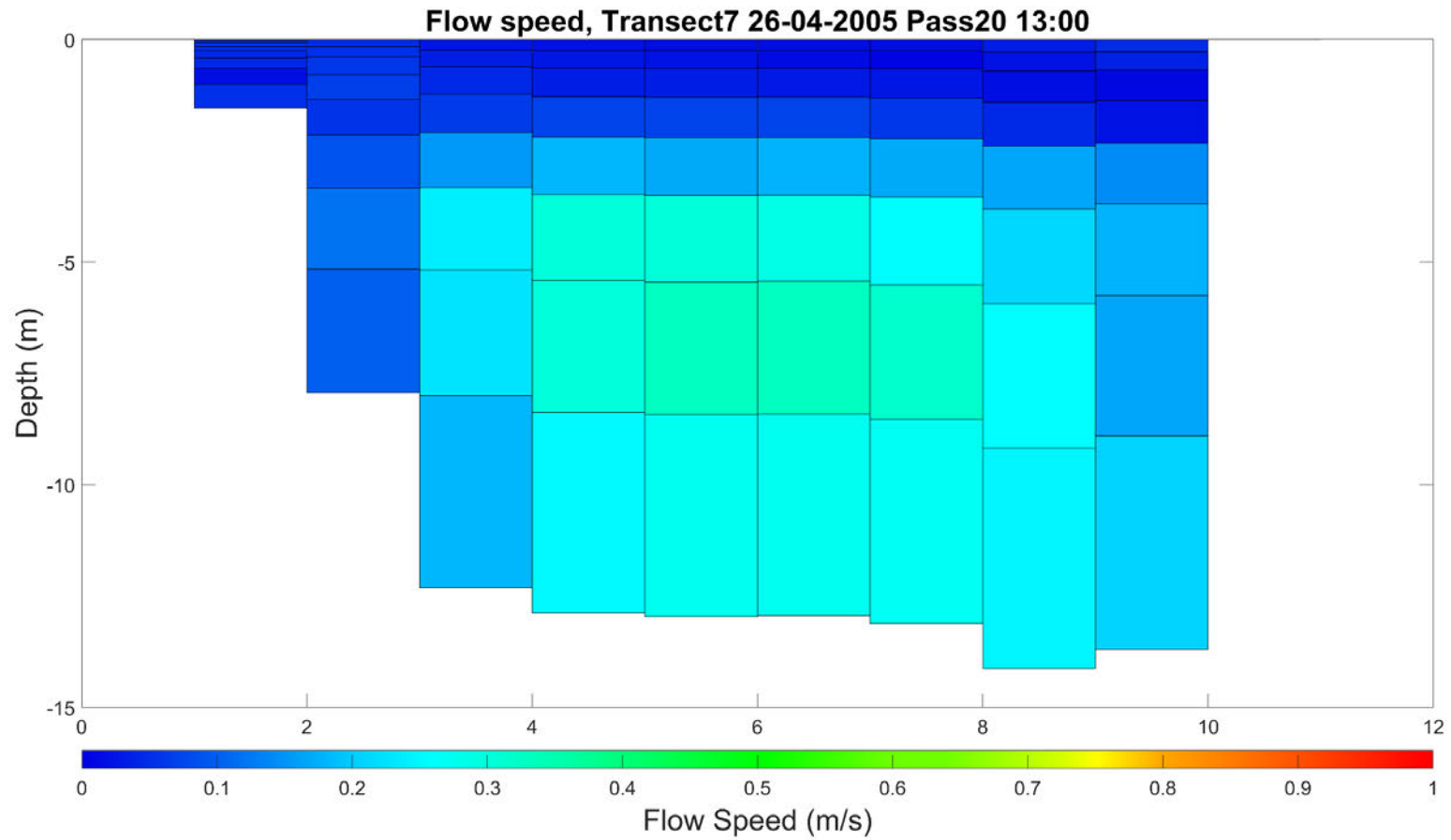


Figure 73. Modelled flow speed, Transect 7: Flood tide, cross section of speed with depth shown from west (left) to east (right)

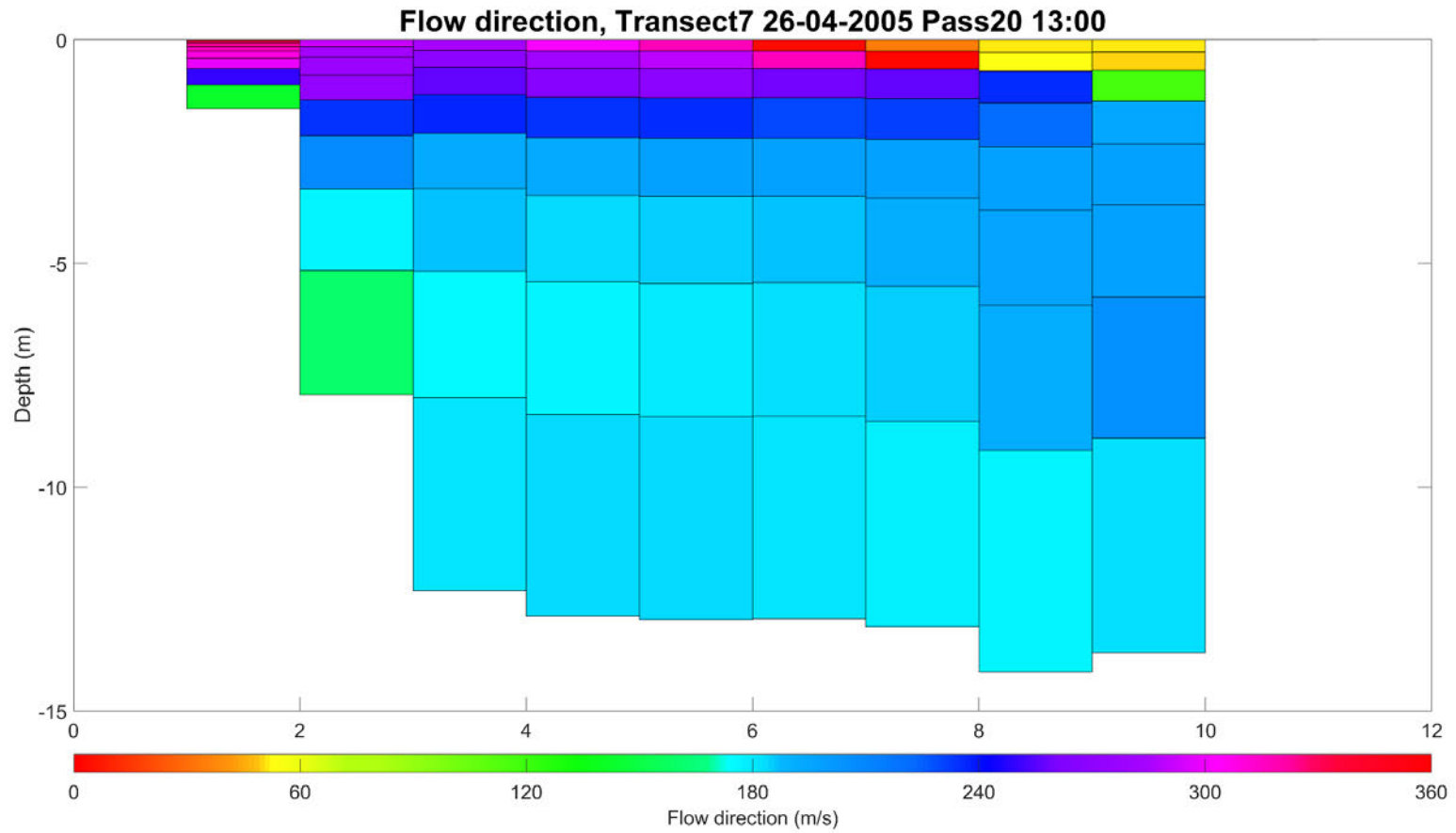


Figure 74. Modelled flow direction, Transect 7: Flood tide, cross section of direction with depth shown from west (left) to east (right)

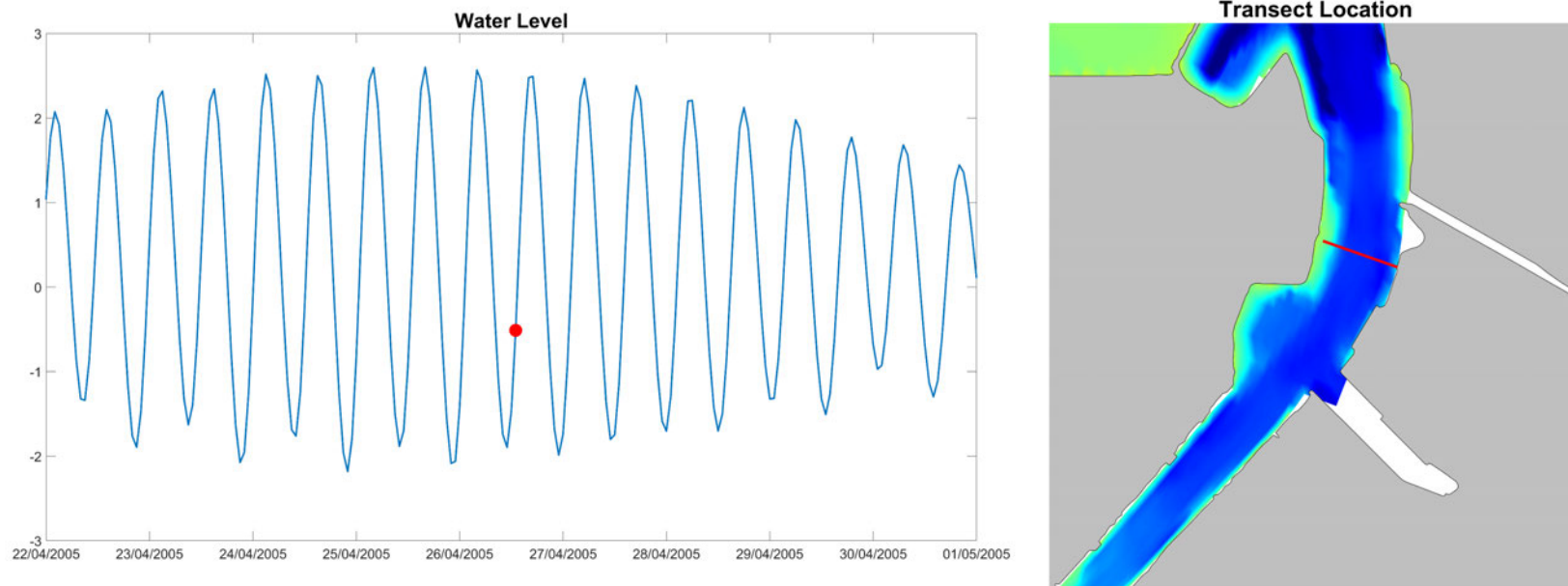


Figure 75. Tidal state and transect location extracted from the model for Transect 7 Pass 20: 26/04/2005

Timeseries flow data

Tees and Hartlepool Port Authority (THPA) previously provided measured flow speed and direction data from fixed current meter observations at a central location in the Tees Estuary. The location of the fixed current meter is data is shown in Figure 76 with the label Buoy 10. These data were processed in the previous study and assessed to identify spring and neap data periods of comparable magnitude to the model run period. The processed data for selected spring and neap tidal periods, have been utilised in this study to produce an equivalent comparison of measured and modelled data using the new modelled outputs. As an initial sense check, the modelled data were also compared against the previous modelled results.

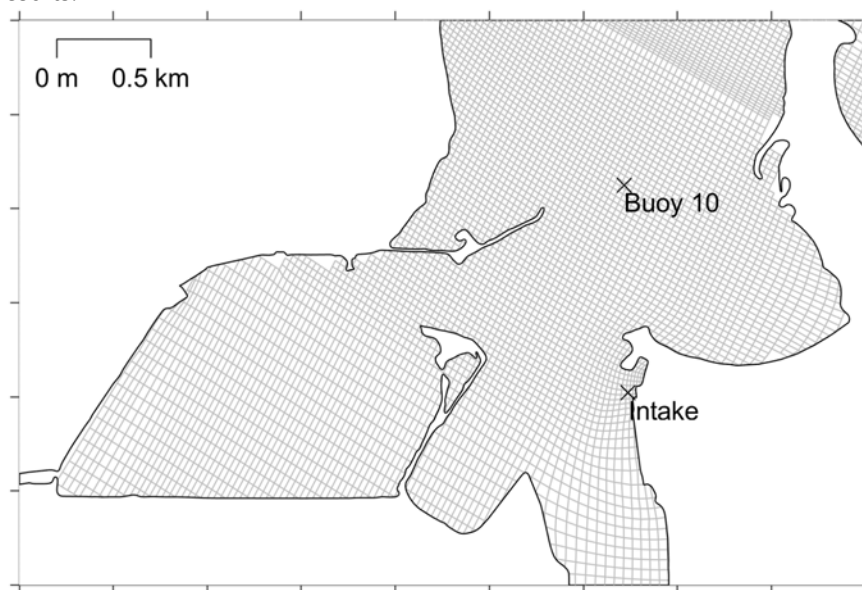


Figure 76. Fixed current meter location: Buoy 10

Comparison of the modelled and measured datasets are shown in Figure 77 for spring tides and Figure 78 for a neap condition. It should be remembered when examining the comparisons that:

- The layers in the model may not correspond exactly to the elevation of the instrument deployed in the field and none of the measurements would have been made for the exact tidal conditions, bathymetry and location being modelled. Hence a perfect calibration would not be expected.;
- The time period of the observations and model output is different. Comparison is between two data sets which have similar tidal ranges only. Due to this difference in data periods, as well as the small amount of measured data available, it has not been possible to carry out a statistical analysis.
- Field observations are represented by a poor temporal resolution of data points within the period of measurement. Hence variation within this period may have occurred which is not shown in the data.
- Freshwater regime during the collection period may be different from that specified in the model, which itself represents mean conditions.
- Time between the field observations and the present means that there could be differences in local bathymetry at and around the measured site compared to that modelled.

Comparisons were made at three layers within the water column: surface, middle and bed. There is generally good agreement between the phasing and magnitude in the datasets.

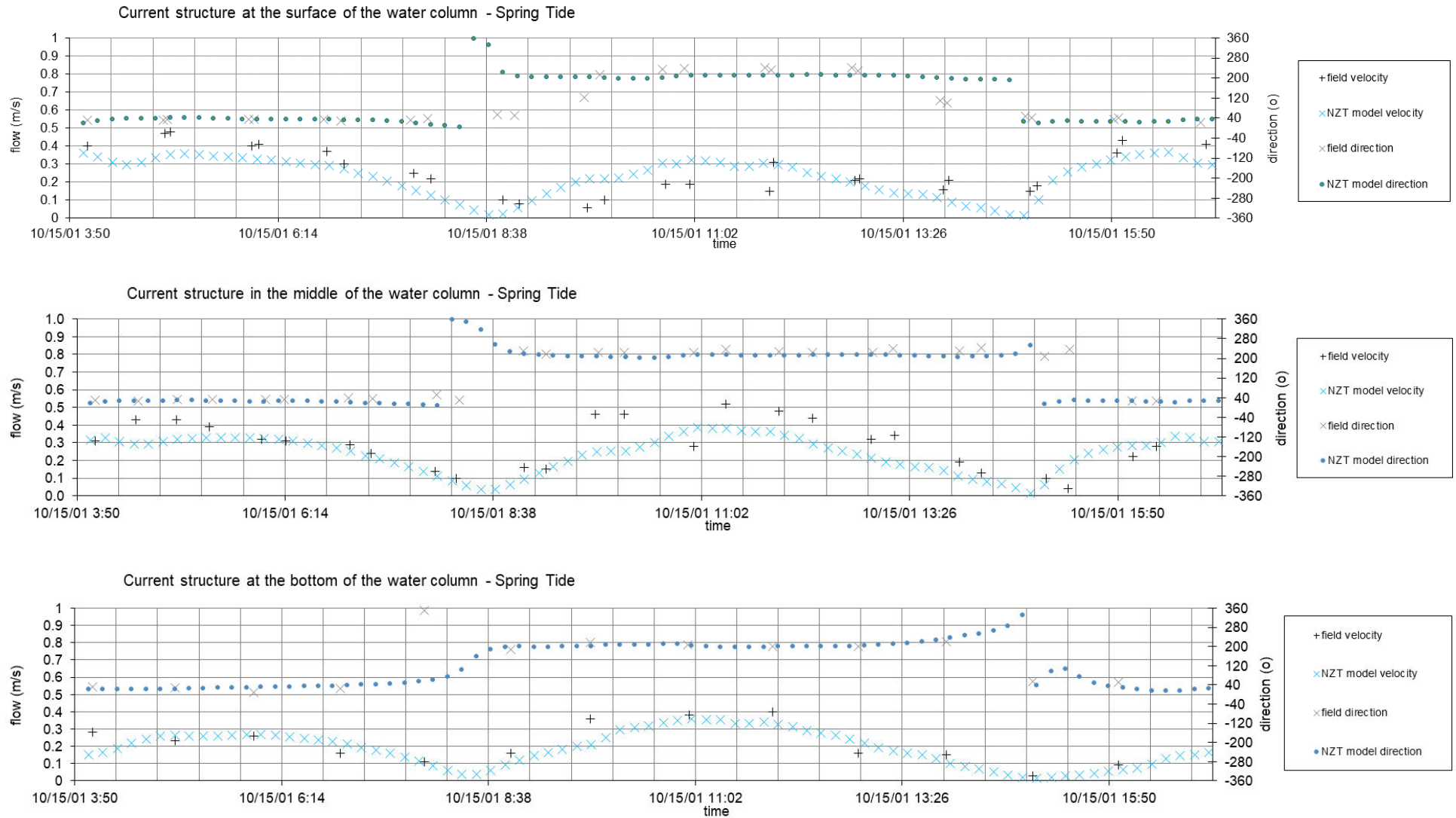


Figure 77. Measured and modelled flow speed and direction comparison at the top, middle and bottom of the water column. Buoy 10 – Spring tide

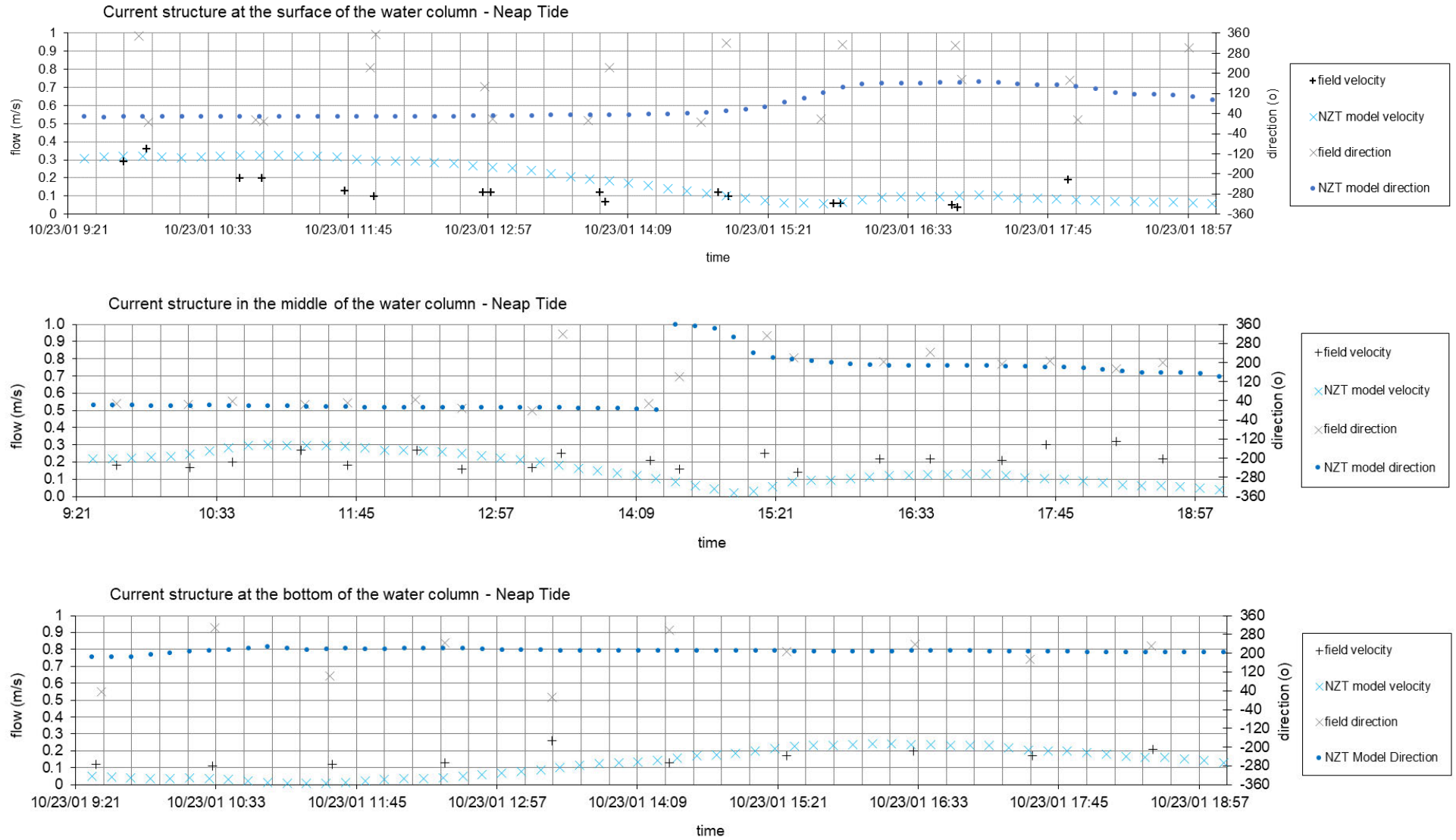


Figure 78. Measured and modelled flow speed and direction comparison at the top, middle and bottom of the water column. Buoy 10 – Neap tide

Offshore flow conditions

The above sections compare the model outputs against conditions within the Tees Estuary. There is limited measured data within the offshore coastal region, so comparison of the modelled flows has been undertaken against predicted tides using the UKHO Admiralty tide tables.

Modelled flow speeds and directions, over a mean spring tide, are compared in Table 18 which show the model is generally in good agreement with the variation in speed and direction across the flood and ebb tidal phases.

Table 18. Modelled and predicted flows speeds and directions within the offshore coastal region.

	Model		TT	
	Direction (°)	Speed (m/s)	Direction (°)	Speed (m/s)
HW-6	309	0.46	291	0.62
HW-5	305	0.46	296	0.57
HW-4	304	0.40	303	0.41
HW-3	307	0.28	303	0.21
HW-2	333	0.10		0
HW-1	96	0.17	111	0.41
HW	112	0.38	112	0.67
HW+1	115	0.47	109	0.57
HW+2	116	0.43	107	0.46
HW+3	116	0.28	110	0.36
HW+4	118	0.12	97	0.1
HW+5	274	0.04	278	0.1
HW+6	287	0.16	288	0.36

CTD data

AECOM have provided measurements of temperature and salinity from individual CTD (Conductivity, Temperature, Depth) casts deployed across the ADCP transects during the PD Teesport survey, conducted between 21/04/2005 to 30/04/2005.

All available CTD measured profiles have been plotted and compared against the model data available from the nearest model grid cell and coincident time. Sensitivity testing during the model build demonstrated that the salinity structure of the water column is sensitive to the starting salinity and to the discharge volume through the Tees Barrage. Three variations of the model have therefore been run for this data comparison to represent three alternative barrage discharges: Annual mean, summer and winter (as described in Table 15). The starting salinity of the model controls the resulting salinity of the bulk of the water column. The nature of the model setup (i.e. reasonably short duration with averaged discharge values across the barrage) means that the model will not reach a naturally stable point representative of a particular point in history: this would require a longer model duration and time varying discharges over a longer period, not felt necessary for the present study. Instead, it represents the conditions over a period of time rather than matching to specific day. The most appropriate starting value for the model salinity has been selected as 33.9 ppt based on values provided by AECOM from the Wood Draft Report (Wood, 2020) for seawater properties. This provides consistency throughout all modelled simulations (hydrodynamic and near-field thermal plume).

Figure 79 to Figure 81 present selected comparisons of CTD measurements and modelled profiles which are generally representative of the full set of profile comparisons.

It can be seen that the winter simulation (with higher freshwater flow discharges) creates the greatest variation in vertical structure, with the surface layer being significantly fresher for most states of the tide. This pattern is most consistent with the structure seen in the measured data. The salinity of the model tends to be fresher than the measurements for the bulk of the water column for all time periods and locations assessed, which tend to be closer to 35 ppt in most of the measured profiles. However, the measured salinity for this particular short period is more saline than other sources suggest for 'typical' conditions in the Tees Estuary, such as the Wood Draft Report (Wood, 2020), which documents 29.3 ppt for the Tees at Redcar Jetty and the Gares, and 32.8 ppt in the 'River Water'.

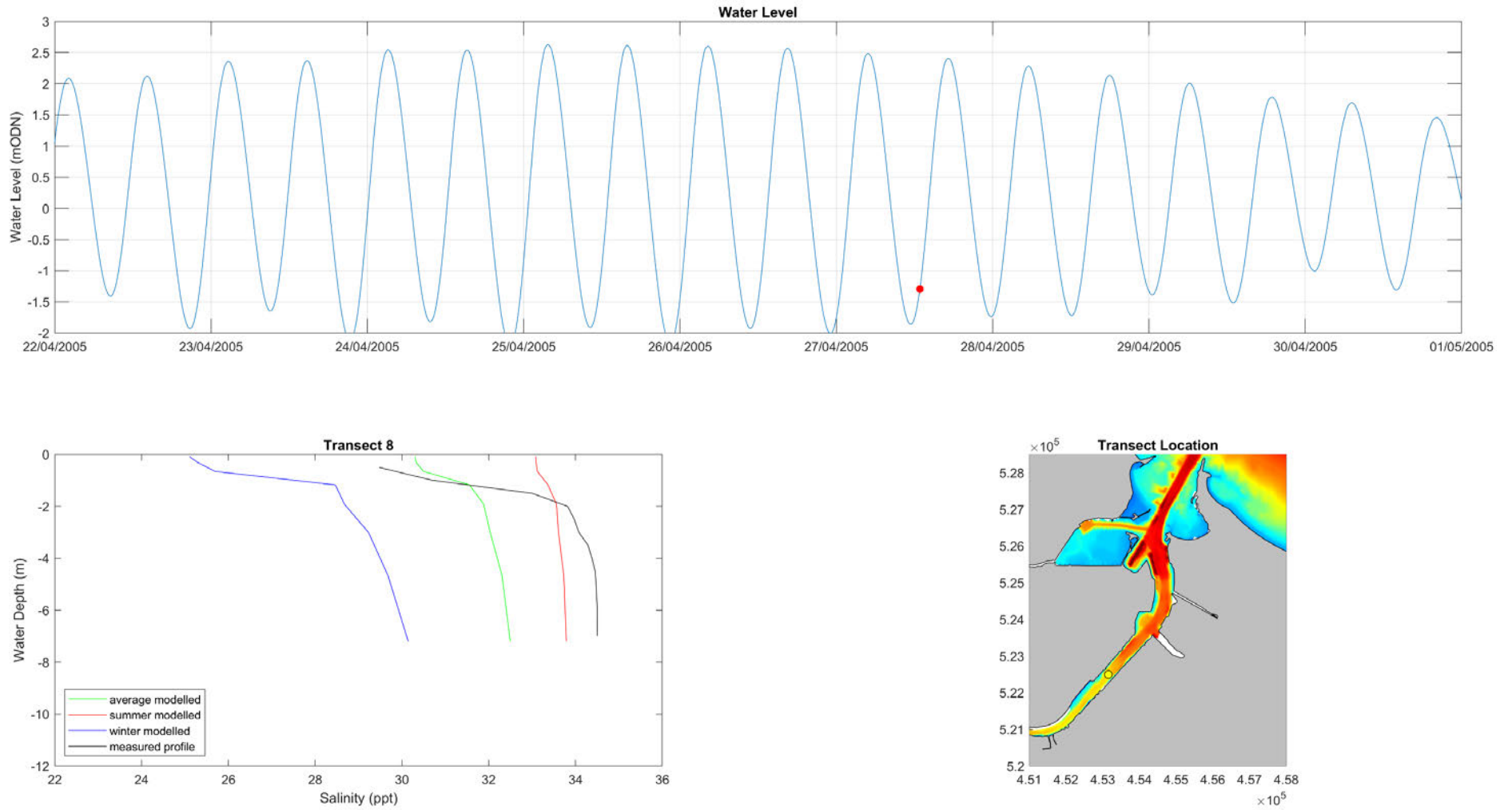


Figure 79. Comparison of measured and modelled salinity with depth: Transect 8 (red dot on top water level plot indicates point of the tide).

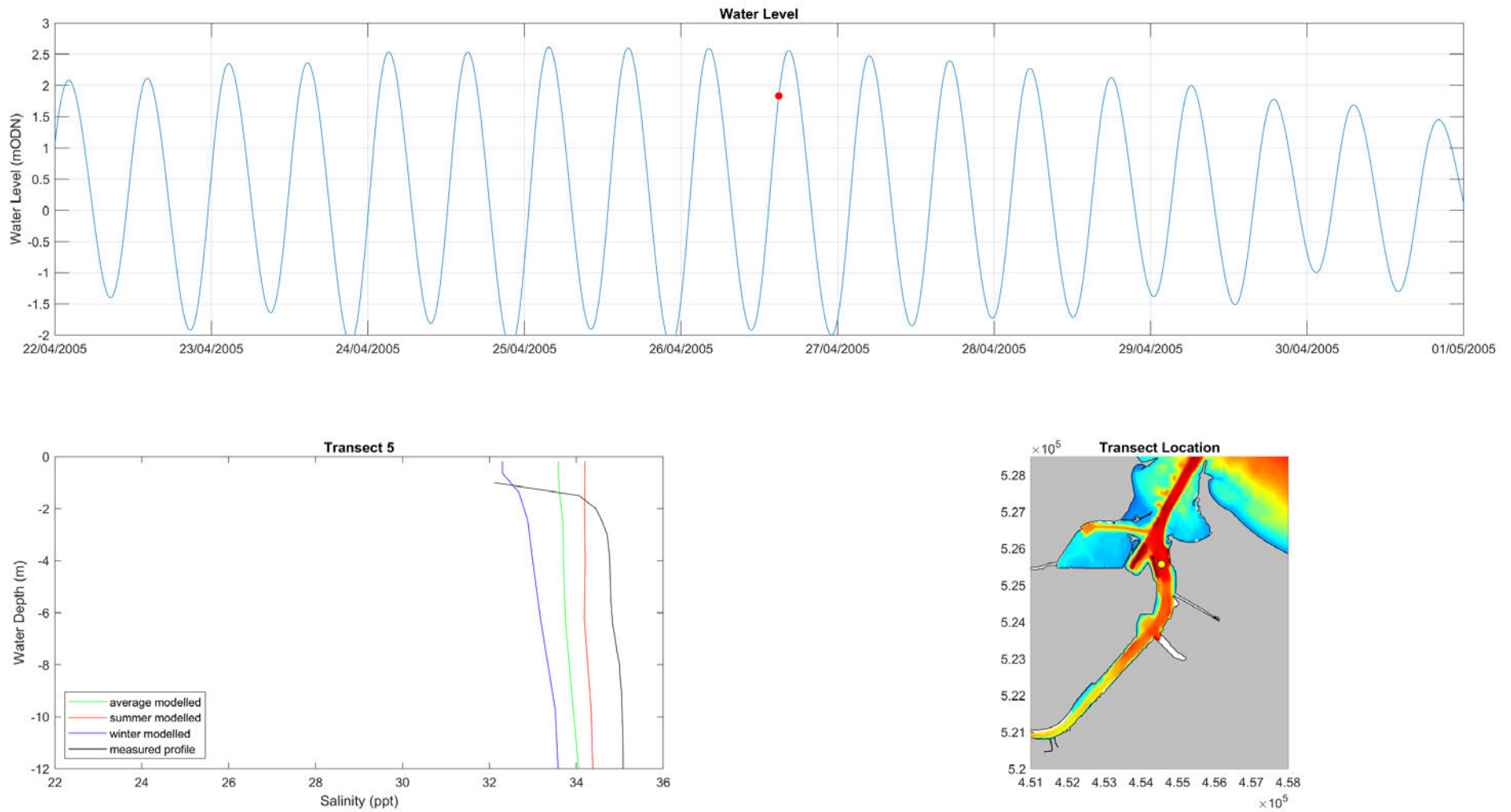


Figure 80. Comparison of measured and modelled salinity with depth: Transect 5, closest transect location to the cofferdam (red dot on top water level plot indicates point of the tide).

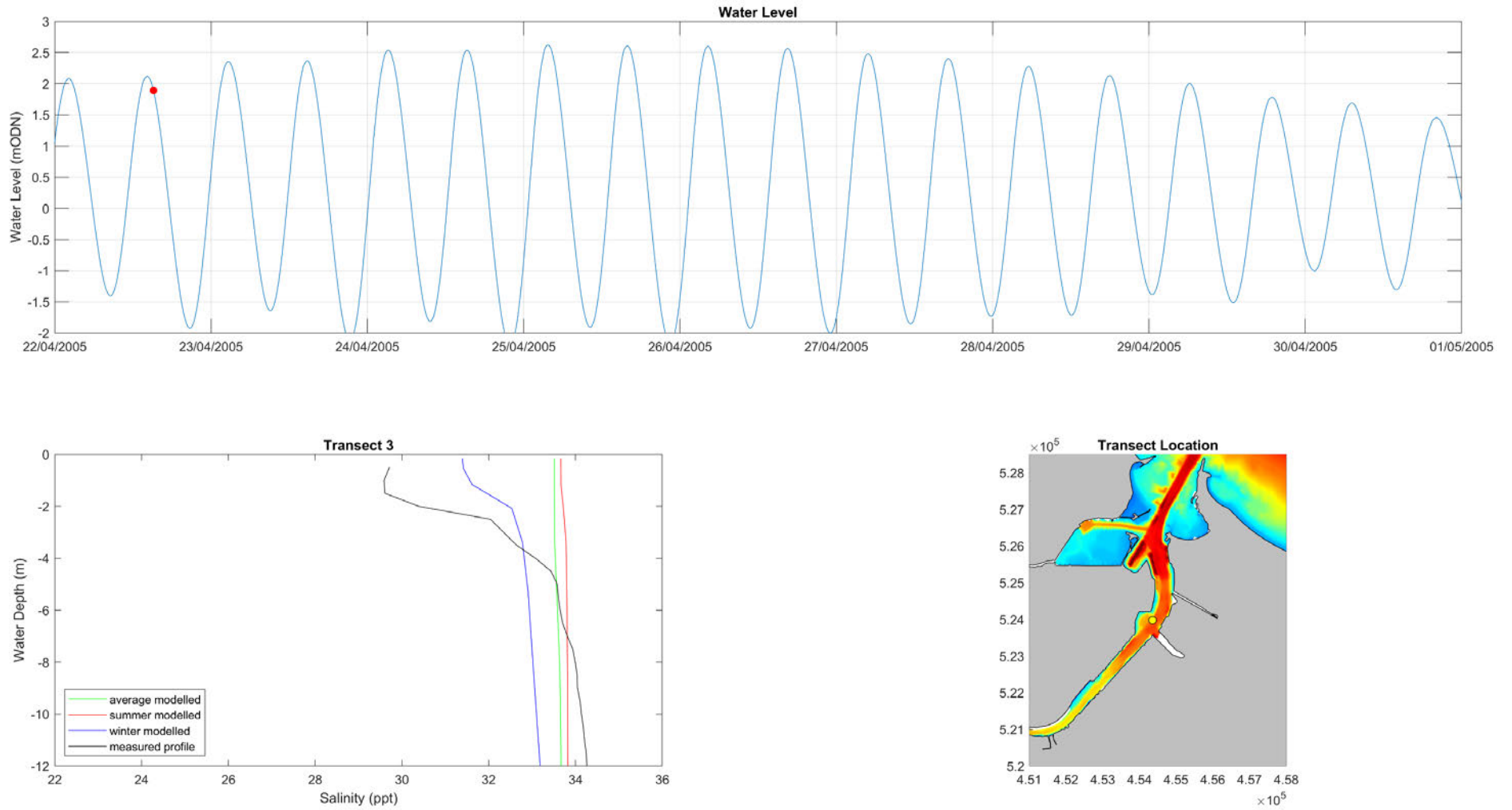


Figure 81. Comparison of measured and modelled salinity with depth: Transect 3 (red dot on top water level plot indicates point of the tide)

C CORMIX Extreme discharge event

During an extreme discharge event, the volume of effluent water that will be discharged through the outfall is estimated to be 5.75 m³/s. However, only a portion of the discharge (1.81 m³/s) will be heated and have an excess temperature, compared to the rest of the discharge and the ambient sea that it's being discharged into. In turn, this will result in the heated portion of the discharge mixing and diluting with the rest of the effluent prior to its discharge out of the outfall. To account for this, a percentage representation of the heated proportion of the discharge has been applied to the original excess temperature of 15°C. This has resulted in a combined excess temperature of 5°C being used to represent the discharge during an extreme event.

C.1 Flood Tide Variation

Figure 82 shows the downstream temperature excess of the resultant plume during a spring (run 26) and neap (run 27) flood tide under extreme discharge conditions, at Outfall 2. The neap tidal characteristics again result in a more extensive plume, reducing the excess temperature at a slower rate due to the slower tidal velocities compared to spring equivalent. This is highlighted by the offset of the 2 and 3°C flags which also indicate both flood states to have dispersed the excess temperature below 2°C by around 168 m downstream of the outfall.

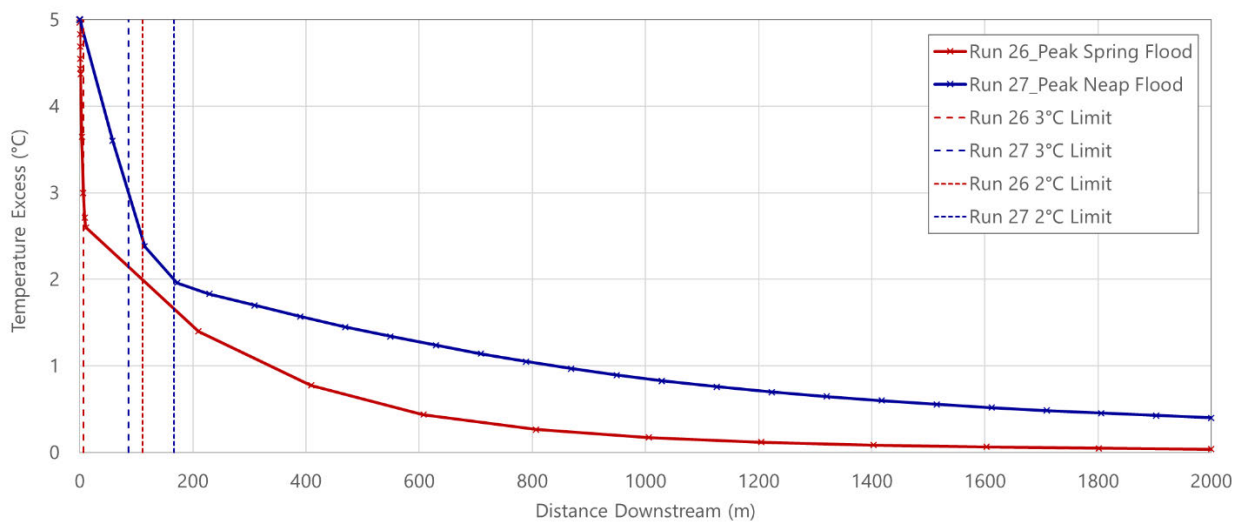


Figure 82. Spring and neap flood tide plume variations during extreme discharge events.

C.2 Ebb Tide Variation

Figure 83 shows the downstream temperature excess of the resultant plume during a spring (run 28) and neap (run 29) ebb tide under extreme discharge conditions, at Outfall 2. The ebb plume is shown to a larger extent under both spring and neap conditions due to the flood tidal velocities being slower for both spring and neap tides causing a slightly slower dispersion. Although the ebb tidal states exceed those on the flood, both ebb scenarios show for the excess temperature to be dispersed below 2°C excess by 235 m downstream of the outfall.

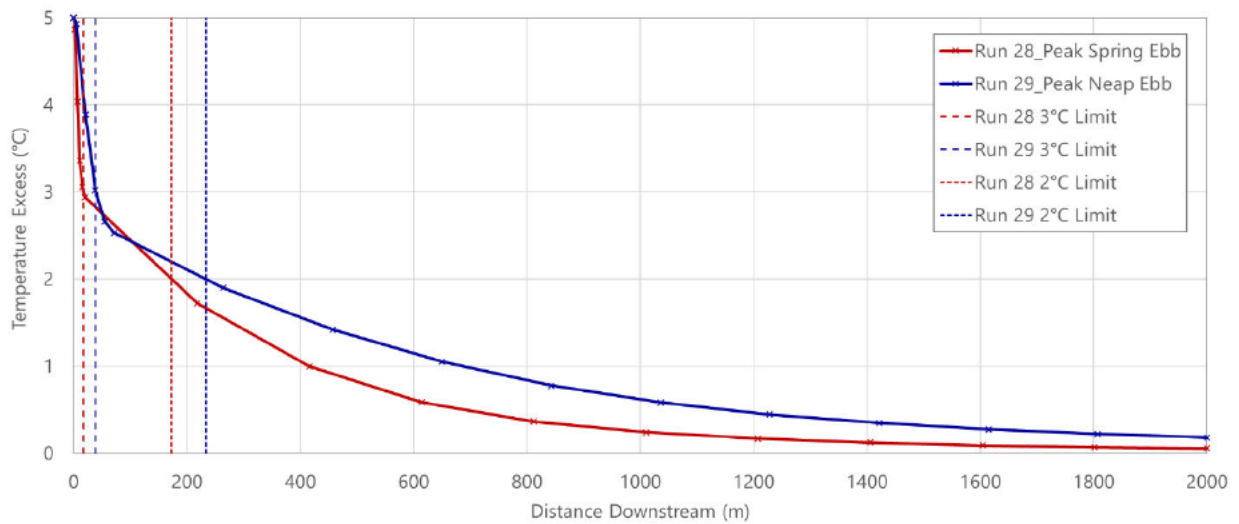


Figure 83. Spring and neap ebb tide plume variations during normal discharge events.

C.3 Temperature Excess Isolines

The extents of the 1-4 °C isolines for each scenario are outlined below in Table 19 summarising the excess temperatures for the 1-in-30-year event. Due to the reduced excess temperature used to represent the extreme event, there aren't any isolines representing an excess temperature of 5°C (as in the equivalent for the standard discharge event), as this is the input excess temperature which is instantly reduced upon dispersion into the sea.

Each of the isolines from the neap tidal states have been geo-referenced in Figure 84 as these extents exceed the corresponding extents during the spring tidal states. The plot highlights how the extreme discharge results in a greater plume with the excess temperatures being dispersed landward during the flood phase. It is to be noted that the 1°C contour has been clipped at the local coastline.

Table 19. Isoline extents for all tidal states under 1-in-30-year discharge conditions.

Excess Temperature Isoline (°C)	Spring Flood Tide (Run 26)	Spring Ebb Tide (Run 28)	Neap Flood Tide (Run 27)	Neap Ebb Tide (Run 29)
	Isoline Extent from Outfall (m)	Isoline Extent from Outfall (m)	Isoline Extent from Outfall (m)	Isoline Extent from Outfall (m)
1	338	416	839	685
2	111	173	167	234
3	6	18	86	38
4	3	7	42	19



Figure 84. Excess temperature isolines during a neap tide under 1-in-30-year discharge conditions.

The same trend as in the normal discharge conditions is also mirrored by the 1-in-30-year extreme discharge event. Since the tidal characteristics remain the same it follows that the same tidal states that produce the larger plumes under normal discharge events also produce the largest plumes during extreme discharge events. This is highlighted by the neap flood (run 27), with the flood tide plumes dominating in extent over the ebb phase.

Although the CORMIX output portrays the plume (neap flood – run 27) to potentially make landfall (using the low-water background image as guidance in Figure 84), it is again to be noted that the CORMIX model assumes full plume development under the given conditions and that the ambient flows (defined as constant in the model) will not persist long enough for a fully developed plume to form. In reality, the flows will reduce either side of the modelled peak conditions and turn with the tidal phase, further dissipating the excess thermal plume before it can fully develop to the state portrayed by the CORMIX outputs. Therefore, the CORMIX model results are to be only used to provide an insight to the relative differences between fully developed plumes under the range of constant ambient conditions modelled and that the far-field plume modelling using the Delft software is to be used as a more detailed insight into the influence of the varying tidal states on the excess temperature discharges.

Contact Us

ABPmer

Quayside Suite,

Medina Chambers

Town Quay, Southampton

SO14 2AQ

T

F

E enquiries@abpmer.co.uk

www.abpmer.co.uk

